Technical Report Documentation Page

1. Report No. FHWA/TX-07/0-4124-1	2. Government Accession No.	3. Recipient's Catalog No.
4. Title and Subtitle Strengthening Existing Non-Composite Steel Bridge Girders Using Post-Installed Shear Connectors		5. Report Date July 2007 6. Performing Organization Code
7. Author(s) Gunup Kwon, Brent Hungerford, Hulya Kayir, Brad Schaap, Young Kyu Ju, Richard Klingner, and Michael Engelhardt		8. Performing Organization Report No. 0-4124-1
9. Performing Organization Name and Address Center for Transportation Research The University of Texas at Austin 3208 Red River, Suite 200 Austin, TX 78705-2650		10. Work Unit No. (TRAIS) 11. Contract or Grant No. 0-4124
12. Sponsoring Agency Name and Address Texas Department of Transportation Research and Technology Implementation Office P.O. Box 5080 Austin, TX 78763-5080		13. Type of Report and Period Covered Technical Report (9/02 – 12/06) 14. Sponsoring Agency Code

15. Supplementary Notes
Project performed in cooperation with the Texas Department of Transportation and the Federal Highway Administration.

16. Abstract

This study investigated methods to strengthen existing non-composite steel bridge girders by the development of composite action between the steel girder and concrete slab. More specifically, the objective of this study was to identify structurally efficient and practical ways to post-install shear connectors in existing bridges. Various types of post-installed shear connection methods were tested under static, high-cycle fatigue, and low-cycle fatigue loads using a direct-shear test setup. Based on the results of single-shear connector tests, full-scale beam tests were performed under static load to evaluate system performance of the beams retrofitted for partial composite action with post-installed shear connectors.

The results of this study clearly demonstrate that the strength and stiffness of existing non-composite steel bridge girders can be increased significantly by post-installing shear connectors. Development of composite action between the existing steel girder and concrete slab through the installation of post-installed shear connectors appears to be a structurally efficient and cost-effective approach to retrofit existing bridges. The addition of post-installed shear connectors can increase the load capacity of existing steel girders on the order of 40 to 50%. Preliminary guidelines are provided.

17. Key Words strengthening, steel girders, retrofit, partial composite, shear studs		18. Distribution Statement No restrictions. This document is available to the public through the National Technical Information Service, Springfield, Virginia 22161; www.ntis.gov.	
19. Security Classif. (of report) Unclassified	20. Security Classif. (of this page) Unclassified	21. No. of pages 126	22. Price

Form DOT F 1700.7 (8-72) Reproduction of completed page authorized

Strengthening Existing Non-Composite Steel Bridge Girders Using Post-Installed Shear Connectors

Gunup Kwon
Brent Hungerford
Hulya Kayir
Brad Schaap
Young Kyu Ju
Richard Klingner
Michael Engelhardt

CTR Technical Report:	0-4124-1
Report Date:	July 2007
Project:	0-4124
Project Title:	Methods to Develop Composite Action in Non-Composite Bridge Floor Systems
Sponsoring Agency:	Texas Department of Transportation
Performing Agency:	Center for Transportation Research at The University of Texas at Austin

Project performed in cooperation with the Texas Department of Transportation and the Federal Highway Administration.

Center for Transportation Research
The University of Texas at Austin
3208 Red River
Austin, TX 78705

www.utexas.edu/research/ctr

Disclaimers

Author's Disclaimer: The contents of this report reflect the views of the authors, who are responsible for the facts and the accuracy of the data presented herein. The contents do not necessarily reflect the official view or policies of the Federal Highway Administration or the Texas Department of Transportation (TxDOT). This report does not constitute a standard, specification, or regulation.

Patent Disclaimer: There was no invention or discovery conceived or first actually reduced to practice in the course of or under this contract, including any art, method, process, machine manufacture, design or composition of matter, or any new useful improvement thereof, or any variety of plant, which is or may be patentable under the patent laws of the United States of America or any foreign country.

Notice: The United States Government and the State of Texas do not endorse products or manufacturers. If trade or manufacturers' names appear herein, it is solely because they are considered essential to the object of this report.

Engineering Disclaimer

NOT INTENDED FOR CONSTRUCTION, BIDDING, OR PERMIT PURPOSES.

Michael D. Engelhardt, Texas P.E. # 88934
Richard E. Klingner, Texas P.E. # 65541
Research Supervisors

Acknowledgments

The authors gratefully acknowledge the financial support provided for this project by the Texas Department of Transportation. The authors extend a special thanks to Jon Kilgore and Clara Carbajal of the Texas Department of Transportation for their support, assistance, and advice throughout the entire course of this project.

Products

Product P1, *Recommended methods and design procedures for adding composite action to existing non-composite bridge floor systems*, is included in Chapter 6 of this report.

Table of Contents

List of Figures

List of Tables

Chapter 1. Introduction

1.1 General

Of the nearly 49,200 bridges in Texas, almost 3,000 are considered structurally deficient by the National Bridge Inventory (National Bridge Inventory 2006). With a replacement cost estimated at over $15 billion, alternative economically feasible methods of rehabilitating these structurally inadequate bridges are highly desirable. For steel girder bridges, one way of doing this is by making their concrete decks act compositely with their underlying steel girders.

Composite construction has been used in bridges and buildings since the 1930s. It implies connecting one or more components of a structure so that they resist loads as a single unit, with a load-carrying capacity greater than what could be achieved if the components acted separately. In bridge construction, a steel girder and a concrete slab can be made to act together in flexure by welding shear connectors to the top flange of the steel girder and then casting the slab on top.

In Texas, approximately two out of every five bridges are made of steel girders topped with concrete slabs (National Bridge Inventory 2006). A significant number of older bridges with steel girders were not designed for composite action, and hence have no shear connectors. Connecting the steel girders and the concrete slab using shear connectors can increase the flexural capacity of the girders by 50% or more. Figure 1.1 shows a typical bridge that is a candidate for strengthening by creating composite action. This bridge was not designed for composite behavior and was not provided with shear connectors.

For such non-composite bridges, composite action can be achieved by using post-installed shear connectors. While such connectors are not common, they can be a potentially cost-effective alternative to replacement of the bridge. This study focuses on finding cost-effective, straightforward, and practical ways to create composite action in bridges originally designed as non-composite.

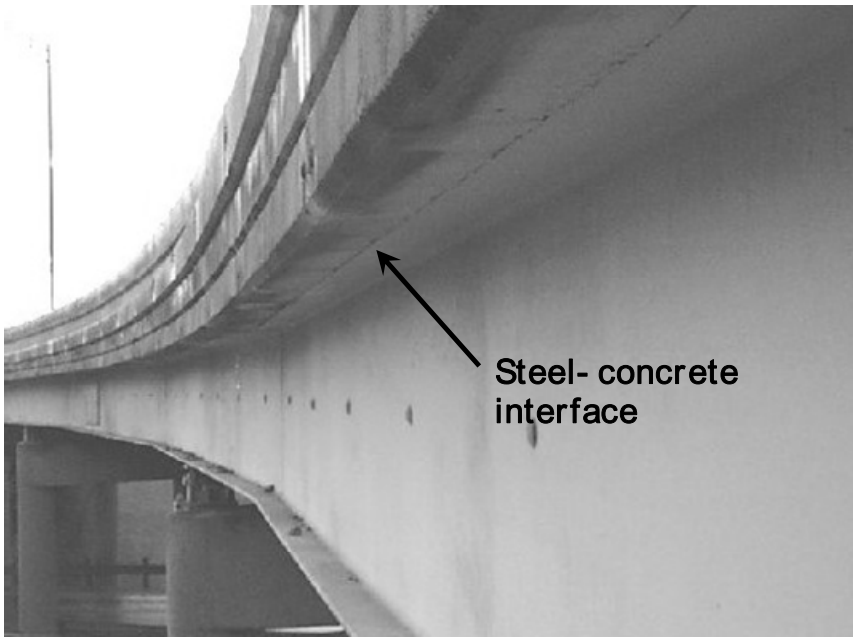

Figure 1.1: Typical candidate bridge for strengthening

1.2 Objective of TxDOT Project 0-4124

Texas Department of Transportation (TxDOT) Project 0-4124 aims to investigate structurally efficient, cost-effective, and practical ways to post-install shear connectors to increase the load carrying capacity of bridges originally designed as non-composite. The project included the following major tasks:

- Review the available technical literature on composite beam design, shear connector behavior, and American Association of State Highway and Transportation Officials (AASHTO) composite design provisions.
- Survey typical non-composite steel girder bridges to become familiar with typical member sizes, deck details, and condition of the bridges and to develop a prototype bridge for the modeling of experiments.
- Select possible post-installed shear connectors to be tested based on structural effectiveness, constructability, and cost.
- Test single-shear connectors under static loading: Identify shear connectors that display strength and stiffness comparable to those of a typical cast-in-place welded stud shear connector. Select post-installed shear connectors for further evaluation.
- Test the selected shear connectors under fatigue loading: Select shear connectors to be further evaluated under full-scale composite beam testing.
- Test full-scale composite beams to obtain information on load-deformation response, ultimate strength, and constructability.
- Make design recommendations for using post-installed shear connectors in steel bridges originally designed as non-composite.

1.3 Scope of Report

This report consists of six chapters. Chapter 2 provides background information necessary to assess the performance of shear connectors and composite beams. A summary of AASHTO specifications on the design of shear connectors in composite bridges is also included in Chapter 2. Chapter 3 summarizes single-shear connector tests under static loading. The static load-slip behavior of post-installed shear connectors and the criteria used to recommend particular shear connectors for further research are described. In Chapter 4, single-shear connector behavior under high-cycle fatigue and low-cycle fatigue is described; more static test results are provided; and preliminary design equations for post-installed shear connectors are provided. Chapter 5 summarizes full-scale beam tests of partially composite beams retrofitted with post-installed shear connectors. Behavior of the retrofitted beams is compared with non-composite beams. Chapter 6 includes a summary, conclusion, and recommendations for further research.

This report provides a summary of the activities and findings for TxDOT Research Project 0-4124. More detailed documentation of this research is provided in three MS theses (Hungerford 2004, Kayir 2006, Schaap 2004) and a PhD dissertation (Kwon 2008) completed in the Department of Civil, Architectural, and Environmental Engineering at The University of Texas at Austin. The reader is referred to these theses and dissertation for in-depth documentation of this research.

Chapter 2. Background: Behavior and Design of Composite Beams

2.1 Introduction

The American Association of State Highway and Transportation Officials (AASHTO) provides guidelines for the design of bridges in the U.S. Until recently, only allowable stress design (ASD) and load factor design (LFD) were used in AASHTO provisions and made available through the publication: *AASHTO Standard Specifications for Highway Bridges*. Since 1994, *AASHTO LRFD Bridge Design Specifications* has also been published utilizing load and resistance factor design (LRFD). The *AASHTO Standard Specifications for Highway Bridges* (2002) will be referred to as *AASHTO ASD* or *AASHTO LFD* in this report, depending on the type of design method discussed. *AASHTO LRFD Bridge Design Specifications* (2005) will be referred to as *AASHTO LRFD*.

The purpose of this study is to develop efficient and practical ways to increase load carrying capacity of existing non-composite bridge girders by post-installing shear connectors. This chapter starts with a general discussion of terms related to composite beams followed by various research results on welded stud shear connectors (shear studs) under static and fatigue loading. Welded stud shear connectors are the most common shear connector for new composite beam construction. Understanding the behavior of the shear studs and composite action are necessary to select structurally adequate post-installed shear connectors. Next, AASHTO design procedure for composite bridge girders is summarized, including the requirements of the *AASHTO LRFD* and of the *AASHTO Standard Specifications*. This chapter concludes with a discussion of partially composite design. Stiffness and strength of the partially composite beams are compared with non-composite steel girder system.

2.2 Composite Action

2.2.1 Composite Ratio (Degree of Shear Connection)

In general, composite action occurs when two or more components, such as a concrete bridge deck and a steel girder, act as a single structural element (see Figure 2.1). This composite action results in an increase in strength and stiffness of the bridge girders compared to non-composite beams. In the specific context of steel and concrete elements, a composite member may be defined as fully composite or partially composite.

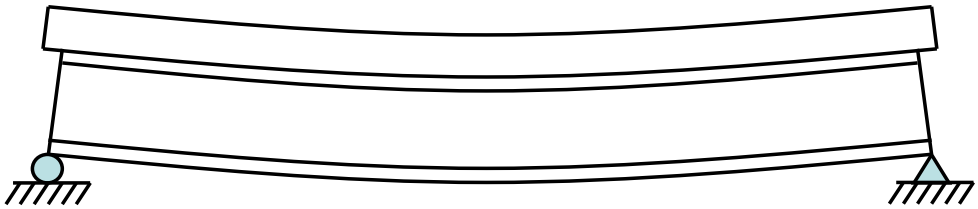

a) Non-composite action

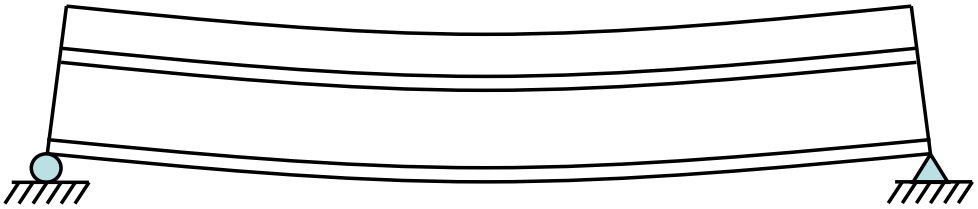

b) Composite action

Figure 2.1: Composite action

A girder is defined to be "fully composite" when sufficient shear connectors are provided to develop the full flexural strength of the given cross-section. That is, the flexural strength of the member is governed by the strength of the steel girder and the concrete slab; girder strength is not governed by the strength of the shear connectors. The number of shear studs required to develop fully composite strength, N_f, is the number of shear connectors that allows the composite girder to achieve its full ultimate strength and is obtained by calculating the force required to be transferred at the steel-concrete interface at the ultimate load state (Faella, Martinelli, and Nigro 2003). A simple procedure is provided in the *AASHTO ASD, LFD and LRFD Specifications* to determine N_f. The same procedure is also provided in the *Specification for Structural Steel Buildings* published by the American Institute of Steel Construction (AISC 2005). This procedure computes the force at the steel concrete interface when the fully composite cross-section reaches its plastic capacity. The plastic capacity of the fully composite cross-section occurs when the slab reaches its full compression capacity or when the steel girder is fully yielded.

A girder is defined to be "partially composite" when the flexural strength of its girder is governed by the strength of the shear connectors. The ultimate strength of a partially composite girder is less than that of a fully composite girder because the concrete cannot achieve its full plastic limit state, as the force in the slab is limited by the strength of the connectors. The decrease in flexural strength can be related to the degree of shear connection N / N_f (or η). The shear connectors must have the slip capacity required to achieve the desired load capacity (Johnson and Molenstra 1991). Further discussions on the maximum slip required by a bridge girder, as well as the slip capacity of a stud shear connector, are given later in this chapter.

For both fully composite and partially composite girders, some slip occurs at the steel-concrete interface, because shear connectors are not stiff enough to prevent it (Faella, Martinelli, and Nigro 2003). This slip primarily affects the stiffness of the composite member. In typical design practice, the elastic stiffness of a fully composite girder for checking service load deflections ignores slip at the steel-concrete interface, and the moment of inertia of the composite girder is computed based on a transformed cross-section. On the other hand, the calculation of elastic stiffness of a partially composite girder normally accounts for slip at the

steel-concrete interface, recognizing that slip will have a significant impact on stiffness even at service load levels.

2.2.2 Achieving Composite Action

Composite action is achieved by connecting the steel girder to the concrete slab to permit transfer of horizontal shear force at the steel-concrete interface. For new construction, the standard welded headed shear studs are used to transfer the horizontal shear, while the head prevents uplift of the slab (Matus and Jullien 1996). The stud shear connectors are normally welded to the girder flange using a stud welding process, although fillet welds can also be used. After welding the stud shear connectors, the concrete slab is cast and composite action between the steel girder and concrete slab is achieved.

The concept of strengthening existing non-composite steel girder bridges by creating composite action is not new. The 50-year-old Spruce Street Bridge in Scranton, Pennsylvania is an early example, strengthened in 1945. Its weight limit was almost doubled, to 30,000 pounds, by removing the concrete deck, installing spiral shear connectors, and casting a new deck (Cook 1977). The goal of the project discussed in this report, however, is to avoid the costly removal and replacement of the concrete deck by connecting the existing concrete and steel members.

2.2.3 Possible Shear Transfer Mechanisms

As described in the previous section, shear connectors must be capable of transferring the horizontal shear at the steel-concrete interface. Three basic methods of transferring the shear are bearing, friction, and adhesion.

Bearing is the most common mechanism for transferring the shear at the steel-concrete interface in composite girders. The shear stud, the most common shear connector used in practice, transfers the shear from the top flange of the steel girder through a weld, and then to the slab by the connector bearing on the concrete. Using friction to transfer the shear force provides a shear connection with high stiffness. This mechanism requires tension in the connector to create a normal compressive force at the steel-concrete interface. Shear is transferred completely by friction as long as it is less than the product of the coefficient of friction and the normal force. Friction is an ideal mechanism for fatigue loading, since stress fluctuations in the connector are small. Finally, adhesion at the steel-concrete interface can also be used to transfer shear. In a retrofit situation, this could potentially be accomplished by the use of structural adhesives at the steel concrete interface.

2.3 Behavior of Stud Shear Connectors

2.3.1 Push-out Test Setup

The types of tests that have typically been used to investigate the performance of shear connectors are beam tests and push-out tests. Starting with the tests of Ollgaard et al. (1971), stud shear connectors have traditionally been evaluated using push-out tests and their results are the basis for current *AASHTO Specifications*. Although beam tests more accurately represent actual conditions on a bridge, the behavior of individual shear connectors is not easy to measure. Further, beam tests are more costly than push-out tests. Push-out tests, on the other hand, can be constructed faster and closer examination of the behavior of individual shear studs is possible (Slutter and Fisher 1966).

In a push-out specimen, two concrete slabs are typically attached to the flanges of a steel beam with shear connectors. Figure 2.2 shows the standard push-out test setup included in the Eurocode (ENV 1994-1-1, 1992). Typically four shear connectors are installed on each side of a steel beam. Load is applied to the steel beam monotonically or cyclically until the shear connectors fail.

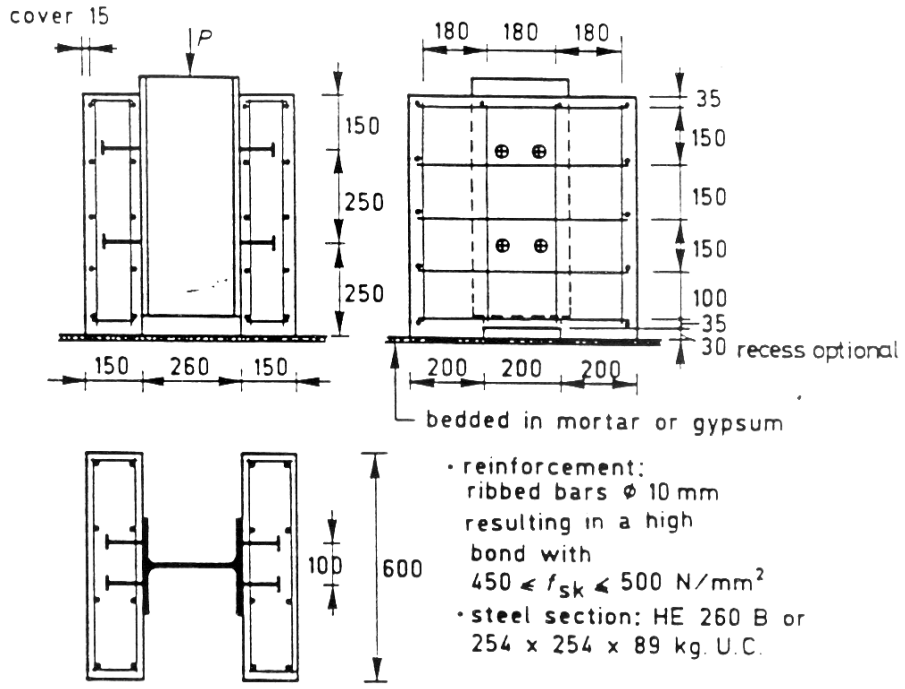

Figure 2.2: Push-out test setup according to the Eurocode (SI units)

2.3.2 Behavior of Stud Shear Connectors under Static Loading

Although many researchers have investigated the static strength of the stud shear connectors since the 1950s, perhaps the most extensive research on the static behavior of the headed stud was performed by Ollgaard, Slutter, and Fisher (1971). They looked at the effect of the compressive and tensile strength, density, aggregate type, and modulus of elasticity of the concrete, the diameter of the stud, and the number of connectors per slab in a standard push-out test. Johnson and Molenstra (1991) investigated the effect of the strength and modulus of elasticity of stud material on the static capacity of the shear connector and found it to be influential.

2.3.2.1 Strength of Shear Connectors

Many design equations have been developed to estimate the ultimate static strength of the stud shear connectors. Different researchers have found different variables to be influential on the static strength. Ollgaard, Slutter, and Fisher (1971) created an equation based on concrete properties and on the ultimate tensile strength of stud shear connector. They report that the concrete exhibits substantial inelastic deformation before failure. Ollgaard, Slutter, and Fisher

(1971) conclude that the concrete is the controlling medium, based on the observed behavior at ultimate load. They produced Equation 2.1:

$$Q_u = 1.106 \times A_s \times f'_c{}^{0.3} \times E_c{}^{0.44} \leq A_s \times f_u \qquad \textit{(Eq. 2.1)}$$

Where: Q_u = ultimate strength of connector (kips)
A_s = cross-sectional area of headed stud (in.^{2})
f'_c = specified compressive strength of concrete (ksi)
E_c = elastic modulus of concrete (ksi)
f_u = ultimate tensile strength of the stud material

The AISC LRFD Specification for Structural Steel Buildings (2005) and AASHTO specifications adopted a simplified equation, using the same variables:

$$Q_u = 0.5 \times A_s \times \sqrt{f'_c \times E_c} \leq A_s \times f_u \qquad (\textit{Eq. 2.2})$$

Ollgaard, Slutter and Fisher (1971) conclude from a plot of Q_u / A_s versus $\sqrt{f_c \times E_c}$ used to derive the equation that an upper bound to the connector strength is approached when $\sqrt{f_c \times E_c}$ is about 130, as the test data tend to plot along a horizontal line. Since this corresponds to a value of Q_u / A_s of about 65 ksi, they conclude that the cap is related to the ultimate tensile strength of the connector.

Equation 2.1 and Equation 2.2 are functions of only the concrete properties and the diameter of the stud (except for the cap in strength defined by $A_s F_u$). Oehlers and Johnson (1987) propose a simple expression for mean connector strength that also accounts for the constitutive properties of the steel:

$$Q_u = 5.0 \times A_s \times f_u \left(\frac{E_c}{E_s} \right)^{0.4} \times \left(\frac{f_{cu}'}{f_u} \right)^{0.35} \qquad (\textit{Eq. 2.3})$$

Where: E_s = modulus of elasticity of steel stud; and
f_{cu}' = specified cube compressive strength of concrete.
Consistent units must be used.

Design equations for the nominal shear strength of cast-in-place studs and post-installed anchors are also provided in Appendix D of ACI 318-05. The commentary to ACI 318-05 states that the shear strength of cast-in-place and post-installed anchors far from the edge of concrete are usually governed by either the pryout strength of concrete or the shear strength of the anchor. Since no pryout failure was observed during static tests in this study (described in Chapters 5 and 6), failure should therefore be governed by the strength of the anchor steel. ACI 318-05 provides two separate equations for the shear strength of cast-in-place studs and post-installed anchors. The equation for cast-in-place studs is the same equation for the ultimate tensile strength of steel as shown in Equation 2.4. The ultimate tensile strength is used instead of ultimate shear strength

because the area of the weld pool is greater than the nominal cross-sectional area of the connector.

$$Q_n = A_s f_u \qquad \textit{(Eq. 2.4)}$$

An equation predicting the ultimate shear strength of post-installed connectors exists only in ACI 318-05, and is based on the ultimate shear strength of steel. This equation is shown here as Equation 2.5.

$$Q_n = 0.6\, A_s f_u \qquad \textit{(Eq. 2.5)}$$

2.3.2.2 Load-Slip Curve

Ollgaard, Slutter, and Fisher (1971) also derived an empirical expression on the load-slip relationship for stud shear connectors:

$$Q = Q_u \times \left(1 - e^{-18\times\Delta}\right)^{2/5} \qquad \textit{(Eq. 2.6)}$$

Where: Q = applied shear (kips)

Q_u = ultimate strength of shear connector (kips)

Δ = slip of connector (in.)

This equation has a vertical slope at zero load. This was observed by Ollgaard, Slutter, and Fisher (1971) in the load-slip curves due to the bond between the concrete slab and the steel girder. For a slip equal to 0.2 in., the equation predicts loads of 99% of the ultimate load. However, bond at the steel-concrete interface may be lost in a bridge after being subjected to service loads for some period of time. Therefore, it is believed that Equation 2.6 overestimates the initial stiffness of the connector in an existing bridge. The stiffness at $0.5Q_u$ is proposed as initial stiffness of a shear stud by Oehlers and Bradford (1995).

Oehlers and Coughlan (1986) derived the stiffness of the stud shear connector under static and dynamic loads from 116 push-out test results. From the results of 42 push-out specimens with 19 mm and 22 mm diameter shear studs, a static load-slip curve was derived from linear regression analyses. Eq. 2.7 shows the load-slip relationship as the ratio of the slip to the shear connector diameter.

$$\Delta = \left(A + B \cdot f_{cu}'\right) \cdot d \qquad \textit{(Eq. 2.7)}$$

The coefficients A and B are listed in Table 2.1. f_{cu}' is measured in N/mm^2. Figure 2.3 shows load-slip relationships for a stud shear connector under static loading according to Equation 2.6 and Equation 2.7. Maximum strength of the stud shear connector is assumed to be 21.4 kips.

Table 2.1: Coefficients for static stiffness of a shear connector per Equation 2.7

Q/Q_u	A (10^{-3})	B (10^{-2})	Q/Q_u	A (10^{-3})	B (10^{-2})
0.1	22	20	0.85	138	72
0.2	40	37	0.9	156	70
0.3	52	48	0.95	223	119
0.4	63	55	0.99	319	170
0.5	80	73	1.0	371	208
0.6	102	96	1.0	406	251
0.7	120	102	0.99*	475	356
0.8	143	108	0.95*	453	178

*: reducing loads

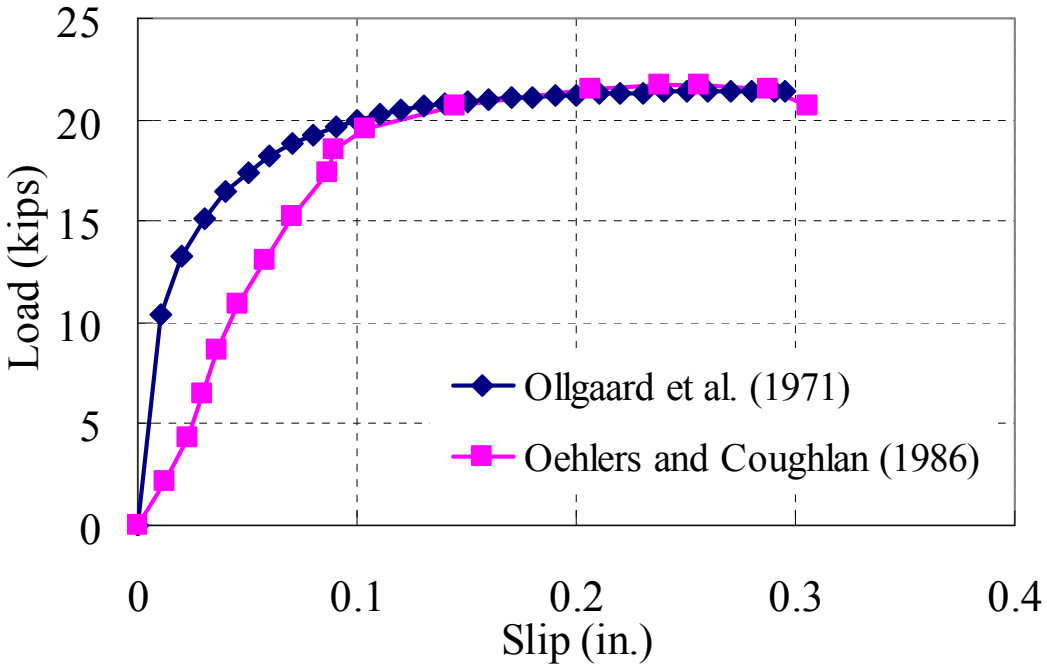

Figure 2.3: Load-slip relations for shear studs

2.3.2.3 Ultimate Slip Capacity

Oehlers and Sved (1995) show that fracture of the connector occurs at about $0.95\times Q_u$ on the descending branch of the load-slip curve. In the same paper, the authors show that the ultimate slip, s_u, can be estimated as (Oehlers and Sved 1995):

$$s_u = (0.45 - .0021 \times f'_c) \times d \qquad \textit{(Eq. 2.8)}$$

Where: s_u = ultimate slip capacity of connector.
SI units should be used for this equation.

The slip at maximum load, $s_{@Qu}$, is given by (in SI units):

$$s_{@Qu} = (0.41 - 0.0030 \times f'_c) \times d \qquad \textit{(Eq. 2.9)}$$

Where: $s_{@Qu}$ =connector slip at maximum load.

Johnson and Molenstra (1991) propose Equation 2.10 and Equation 2.11 based on pre-1985 data:

$$s_{@Qu} = (0.389 - 0.0023 \times f_{cu}') \times d \qquad \textit{(Eq. 2.10)}$$

$$s_u = (0.453 - 0.0018 \times f_{cu}') \times d \qquad \textit{(Eq. 2.11)}$$

Subsequent work has shown that slip at $0.95 \times Q_u$ on the descending branch is about 7.25-mm (0.29-in.) (Johnson and Molenstra 1991).

2.3.3 Behavior of Stud Shear Connectors under Fatigue Loading

2.3.3.1 High Cycle Fatigue

In AASHTO provisions prior the 1970s, fatigue did not govern the design of shear connectors in composite bridges. A composite member was designed to reach its ultimate flexural capacity before the shear connectors yielded. That is, shear connectors were designed for the interface shear computed based on elastic analysis of the transformed section, following the shear diagram for the member. Consequently, fatigue did not control shear connector design. The resulting design, however, was very conservative and required a large number of shear connectors to be placed along the span of a bridge (Slutter and Fisher 1966).

As design provisions proved to be uneconomical and inefficient, many researchers started focusing on ways to change the design of composite bridges so that the number of shear connectors could be reduced. This was accomplished by using plastic analysis to determine the interface shear at ultimate strength of the composite girder. This reduced the number of shear connectors needed for static ultimate loads on the bridge. However, this resulted in the need to consider the effect of fatigue loading on the shear connectors. Since the design provisions at the time relied solely on static strength tests, new research was required to assess the behavior of shear connectors under cyclic loading.

2.3.3.1.1 Factors Influencing Fatigue Life

A main objective of past research on fatigue of stud shear connectors was to determine the factors that influence the fatigue life. Lehman et al. (1965) conducted fatigue tests on 3/4-in. diameter stud shear connectors in lightweight concrete to compare results to those for regular concrete. Slutter and Fisher (1966) investigated the effect of stress range, minimum stress, and load reversal on the fatigue life of 3/4-in. and 7/8-in. diameter stud shear connectors. Similarly, Mainstone and Menzies (1967) looked into the effect of four different ratios of minimum to

maximum shear. Badie (2002) focused on the testing of larger diameter studs (7/8-in. and 1-1/4-in. diameter) and their response to fatigue loads.

Slutter and Fisher (1965) and Lehman et al. (1965) found that stress range is the most important variable affecting the fatigue life of a shear connector. Stress range is defined as the difference between the maximum and minimum stress acting on a connector, where the average stress is calculated based on the effective tensile stress area of a stud. Johnson (2000), citing the work of Oehlers (1990), states that the maximum load applied to a shear connector has a small influence below load levels that are about 60% of the connector's static shear strength. Loading frequency was reported to be insignificant to the fatigue life of shear connectors (Nakajima 2003).

Concrete strength was found to not have a significant effect on fatigue life (Slutter and Fisher 1966). The study by Lehman et al. (1965) shows no significant difference between the fatigue behavior of shear connectors (3/4-in. diameter) in lightweight and normal weight concrete.

Lehman et al. (1965) indicate that no direct relationship can be drawn between the slip and fatigue life of a shear connector, however, distinct slip characteristics can be observed under fatigue loading. They report an initial gradual increase in slip followed by leveling of the slip curve with little increase up to failure. A sudden increase in the rate of slip was observed as specimens reached failure, which they believe can be used as a failure criterion in both beam and push-out tests. Roberts and Dogan (1997) indicate that the sudden increase in slip occurs simultaneously with the propagation of fatigue cracks through a connector, which leads to a reduction in stiffness. For a constant stress range, Mainstone and Menzies (1967) observed reduction in the range of slip with increasing load ratio (increasing mean load).

Early beam tests suggested that no direct relationship exists between the static and fatigue strength of shear connectors (King et al. 1965, Toprac 1965). This was later observed also by Slutter and Fisher (1966) and became the basis for *AASHTO Specifications*, where the static strength of a connector is treated separately from its fatigue strength. This concept was later challenged by Mainstone and Menzies (1971), Oehlers and Foley (1985), and Oehlers (1990) who found that the ultimate strength of a connector decreases once fatigue loads are applied.

2.3.3.1.2 S-N Plot for High Cycle Fatigue Tests

The result of high-cycle fatigue test can be displayed in a plot of stress range (S) versus the number of cycles to failure (N). S-N curve data reported by Thurlimann (1959), Slutter and Fisher (1966), Lehman et al. (1967), Mainstone and Menzies (1967), Badie (2002), and Ryu et al. (2003) are presented in Figure 2.4. This figure only includes data from uni-directional push-out tests conducted for high-cycle fatigue on 3/4-in. and 7/8-in. diameter shear studs. Data from push-out tests are typically used to evaluate fatigue performance of shear connectors, and have been shown to be more conservative compared to beam tests (King et al. 1962, Slutter and Fisher 1966). Both stud diameters are presented due to their similar behavior as suggested by Slutter and Fisher (1966). Stress ranges used by these researchers ranged between 8 ksi and 25 ksi with fatigue lives ranging from 6000 to over 10 million cycles. Specimens that did not experience fatigue failure are shown as runout tests with arrows adjacent to the corresponding data points. This S-N plot was used as a benchmark for high-cycle tests performed as a part of this study.

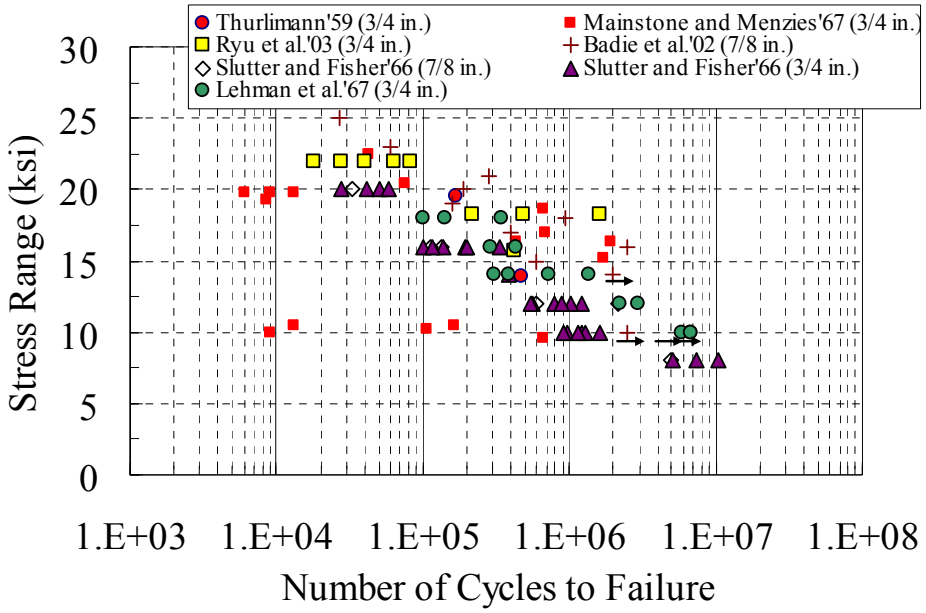

Figure 2.4: S-N data for shear studs from push-out tests

As a result of push-out tests conducted by Slutter and Fisher (1966) the relationship between the number of fatigue cycles to failure and the stress range is presented as Equation 2.12. This equation conservatively ignores data obtained from reversed load tests.

$$LogN = 8.072 - 0.1753 S_r \qquad \textit{(Eq. 2. 12)}$$

Where: N = number of fatigue cycles to failure
S_r = range of shear stress (ksi)

Based on the fact that push-out tests underestimate results from beam tests, Slutter and Fisher (1966) used push-out test results to derive a conservative design equation for shear connectors. The derived equation is the basis for current *AASHTO Specifications* for small diameter shear connectors (less than or equal to 7/8-in.).

The design recommendations made by Slutter and Fisher (1966) enabled the uniform spacing of shear connectors along the length of a bridge. This was followed by a significant reduction in the number of shear connectors used in design and reduction in construction costs.

While most research focused on the fatigue endurance of shear connectors, some researchers such as Oehlers and Foley (1985) and Oehlers (1990) focused on the strength of shear connectors after application of fatigue loads. Contradicting the earlier belief of researchers such as Slutter and Fisher (1966), they believe that the fatigue and static behavior of shear connectors are related. The analytical work of Oehlers and Foley (1985) and the experimental work of Oehlers (1990) show that the static strength of a shear connector decreases as soon as fatigue loads are applied. They propose changing the design of shear connectors in bridges to account for the reduction in static strength due to fatigue.

2.3.3.2 Low Cycle Fatigue

Factors that influence the fatigue life of shear connectors have been widely studied in the past several decades. Research suggests that the fatigue life of shear connectors depends mostly on the stress range applied to them. However, most research has focused on loading cases in which shear connectors deform within their elastic range. In recent years, studies have also considered cases where connectors are loaded into their inelastic range. These studies show loading shear connectors into their inelastic range results in a low number of cycles to reach failure; a phenomenon called low-cycle fatigue. Although a composite bridge would typically undergo high-cycle fatigue under service loads, shear connectors could experience low-cycle fatigue due to recurring overloads; especially in the case of partially composite design. Oehlers and Foley (1985) suggest that "the peak load or an occasional overload does not affect the rate of fatigue crack propagation, but it does affect the endurance [of a stud shear connector] by limiting the amount of fatigue cracking that can occur before the stud fractures."

Oehlers and Seracino (1998) indicate that with the application of fatigue loads, the stiffness of a shear connector decreases, eventually reducing the state of the bridge to partial composite interaction. Therefore, they believe that the research by Gattesco et al. (1997) does not only apply to bridges with partially composite design, but also to bridges with fully composite design.

Gattesco et al. (1997) suggested that inelastic behavior of shear connectors change the structural response of a bridge in two ways:

1) Reduction in load amplitude: As the number of loading cycles increase the load amplitude experienced by shear connectors reduces with time (Fig. 2.5(b)).

2) Load reversal: This usually occurs when connectors, typically at beam supports, yield while the rest of the beam behaves elastically. Load reversal is experienced if the recovered slip required by the beam is greater than the slip a yielded connector can recover by unloading (Figures 2.5(c) and 2.6).

Due to the difficulty in capturing the effects of load redistribution between shear connectors, researchers believe high-cycle and low-cycle fatigue should differ in the way they are studied. While high-cycle fatigue is usually studied using load control, low-cycle fatigue is typically studied using a displacement control approach. With displacement controlled tests the "slip-history" of a shear connector gains importance (Gattesco et al. 1997).

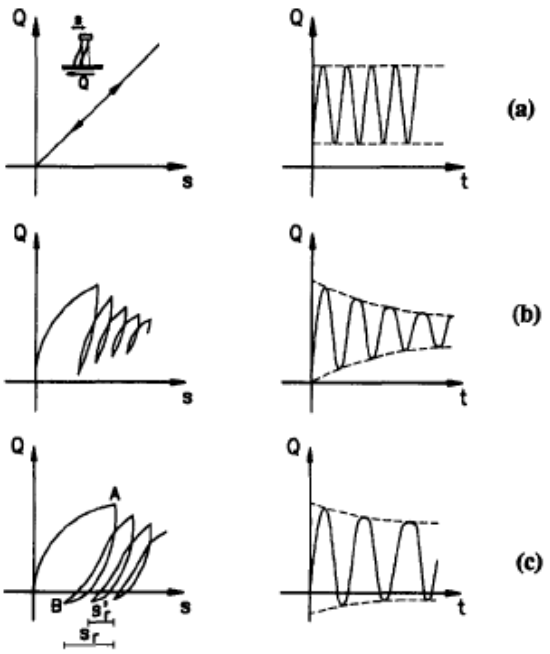

Figure 2.5: Load (Q)-Slip (s) and Load (Q)-Time (t) curves of a shear connector in a structure: (a) Elastic behavior; (b) Inelastic behavior; (c) Inelastic behavior with reversed loading (Gattesco et al. 1997)

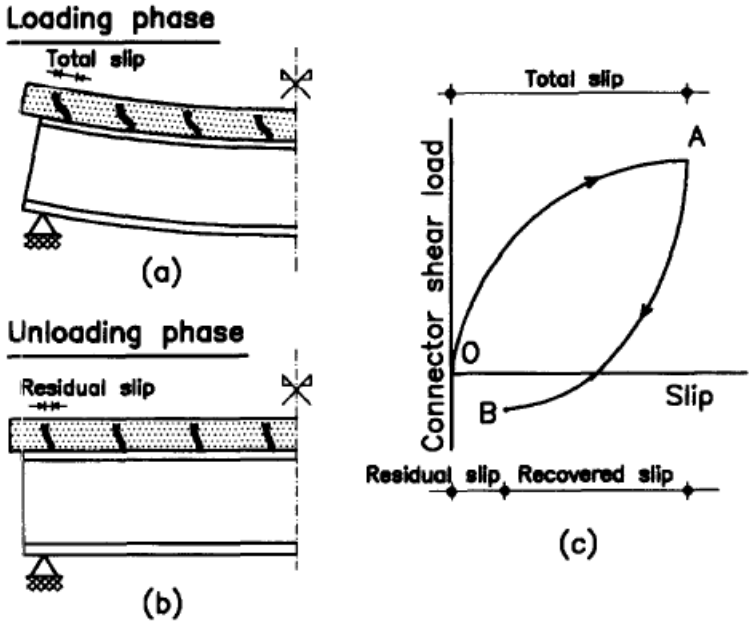

Figure 2.6: Connector load-slip relationship (Gattesco and Giuriani 1996)

2.3.3.2.1 Research by Gattesco and Giuriani

The main goal of the tests performed by Gattesco and Giuriani (1996) was to investigate the behavior of shear connectors under reversed shear loading. Tests were performed by applying blocks of loading cycles with varying ranges of shear. Load cycles were applied at a rate of 500 N/s and the accumulated damage was monitored after each loading cycle. Each block of cycles ended when the slip increment, Δs, reached either a null or a constant value. For unidirectional tests, Δs was found to increase during initial cycles and later tend to a constant value. On the other hand, for reversed load tests, a more rapid deterioration was reported of the stud shank and the concrete in front of the stud. In this case, Δs was observed to grow with each loading cycle.

Over 300 cycles, the authors reported a 15 to 25% reduction in the slope of the unloading branch of the load-slip curve. This suggests that the recovered slip increases with each cycle. This is expected due to the accumulation of damage and loss of stiffness of the connector and concrete after each loading cycle (Gattesco and Giuriani 1996).

2.3.3.2.2 Research by Gattesco et al.

The purpose of experiments by Gattesco et al. (1997) was to assess the performance of shear connectors under low-cycle fatigue. The authors believe that especially for long-span composite beams with partial composite interaction, slip at the steel-concrete interface can reach values that would force shear connectors into inelastic deformations. This would cause some shear connectors in the composite beam to fail after only a small number of cycles.

To determine the low-cycle fatigue endurance of shear connectors, the authors used a displacement control approach where they determined the fatigue life of a connector with a given slip history. The slip history used for the connectors was determined analytically in a previous study by Gattesco and Giuriani (1990). The authors believe the amount of deformation a shear connector experiences beyond its elastic range depends on the amount the entire beam deforms, which reaches a constant value after a certain number of cycles. The numerical analysis by Gattesco and Giuriani (1990) showed that the ratio of maximum to minimum slip was found to be 0.5.

Gattesco et al. (1997) conducted eight direct shear tests with 3/4-in. diameter shear studs under low-cycle fatigue. The maximum induced slip values and corresponding number of cycles to failure are shown in Table 2.2.

Table 2.2: Maximum slip used for each specimen and corresponding number of cycles to failure (Gattesco et al. 1997)

Specimen Number	Maximum slip (mm)	Number of cycles
1	0.80	38,338
2	1.00	18,400
3	1.00	13,200
4	1.25	5,274
5	1.50	3,040
6	2.00	3,230
7	2.00	1,440
8	3.00	432

The authors found that as the maximum slip value exceeded 1mm, the fatigue life of the connectors were lower than 10,000 cycles. The corresponding shear load at every displacement cycle was also found to reduce at the beginning of each test due to concrete damage around the shear connector. Fatigue failure was observed through the stud shank (Gattesco et al. 1997).

2.4 AASHTO Provisions for Shear Connectors in Composite Bridges

2.4.1 Shear Connector Provisions in AASHTO Standard Specifications for Highway Bridges

Design requirements for shear connectors in AASHTO are the same for both ASD and LFD. Section 10.38 of *AASHTO ASD* deals with the design of composite girders and it is also referenced in Section 10.50 of *AASHTO LFD*. In Section 10.38 shear connectors are required to satisfy fatigue load and static load criteria separately. Shear connectors are typically first designed for fatigue loads and then checked for ultimate strength.

The design for shear connectors starts with an initial selection of the number of shear connectors needed in a bridge cross section. Next, the allowable range of horizontal shear force on a single welded stud (with a height-to-diameter ratio greater than or equal to 4), is calculated using Equation 2.13 (*AASHTO ASD 10.38.5.1.1*).

$$Z_r = \alpha d^2 \qquad \textit{(Eq. 2.13)}$$

Where: α = 3,000 for 100,000 fatigue cycles
10,600 for 500,000 fatigue cycles
7,850 for 2,000,000 fatigue cycles
5,500 for over 2,000,000 fatigue cycles

d = diameter of stud (in.)

As *AASHTO Standard Specifications* consider the effects of fatigue at service loads, the response of a composite bridge is calculated using elastic theory. This leads to the horizontal shear present per unit length of the beam, S_r, also known as shear flow, to be determined using Equation 2.14 (*AASHTO ASD 10.38.5.1.1*).

$$S_r = \frac{V_r Q}{I} \qquad \textit{(Eq. 2.14)}$$

Where: V_r = range of shear at cross section due to live and impact loads (kips)
Q = first moment of area of the transformed concrete section under compression, about the neutral axis of the composite section (in^3)
I = moment of inertia of the transformed composite section (in^4)

Once the shear strength of a welded stud and shear flow are determined, the spacing of shear connectors at a bridge cross section can be calculated with Equation 2.15 (*AASHTO ASD 10.38.5.1.1*).

$$s = \frac{\sum Z_r}{S_r} \leq 24\ in. \qquad \textit{(Eq. 2.15)}$$

Where: s = required spacing (center-to-center) of shear connectors (in.)
$\sum Z_r$ = the sum of the allowable range of horizontal shear on all connectors at cross-section (kips)

After the spacing of shear connectors are determined to satisfy fatigue requirements, this value must also be checked for ultimate strength requirements. These requirements utilize plastic theory. The force in the slab is taken as the smaller of either the ultimate strength of the steel in tension (Equation 2.16) or the ultimate strength of the concrete in compression (Equation 2.17) (*AASHTO ASD 10.38.5.1.2*).

$$P_1 = A_s F_y \qquad \textit{(Eq. 2.16)}$$

$$P_2 = 0.85 f_c' b t_c \qquad \textit{(Eq. 2.17)}$$

Where: P_1 = ultimate strength of steel (kips)
P_2 = ultimate strength of concrete in compression (kips)
A_s = area of steel including cover plates (in2)
F_y = specified minimum yield strength of steel (ksi)
f_c' = 28 day compressive strength of concrete (ksi)
b = effective flange width (in.)
t_c = thickness of concrete slab (in.)

To determine the number of shear connectors required, the ultimate strength of single connector, Q_u is needed and is given in Equation 2.18 (*AASHTO ASD 10.38.5.1.2*). This

equation was developed by Ollgaard et al. (1971) and suggests that the static strength of a shear connector depends on its diameter, the strength of concrete, the elastic modulus of concrete, and the tensile strength of the shear connector (assuming f_u of shear connector steel is 60,000 psi).

$$Q_u = 0.4d^2\sqrt{f_c' E_c} \le 60{,}000A_s \qquad \textit{(Eq. 2.18)}$$

Where: d = diameter of stud

f_c' = 28 day compressive strength of concrete (ksi)

A_s = area of shear connector (in^2)

E_c = modulus of elasticity of concrete (lb/in^2) given as in Equation 2.19:

$$E_c = w^{3/2}33\sqrt{f_c'} \qquad \textit{(Eq. 2.19)}$$

Where: w = unit weight of concrete (lb/ft3)

Finally, the minimum required number of shear connectors at a cross section is calculated using Equation 2.20 (*AASHTO ASD 10.38.5.1.2*).

$$N_1 = \frac{P}{\phi Q_u} \qquad \textit{(Eq. 2.20)}$$

Where: N_1 = minimum number of connectors between points of maximum positive moment and adjacent end supports

P = lesser of P_1 or P_2 (kips)

ϕ = reduction factor = 0.85

General requirements are also given in *AASHTO Standard Specifications* for shear connectors and are the same for both *ASD* and *LFD* design. Shear connectors are required to be mechanical anchors and "…shall be capable of resisting both horizontal and vertical movement between the concrete and the steel" (*AASHTO ASD 10.38.2.2*). A minimum embedment depth of 2 in. is specified for shear connectors, with a minimum clear cover requirement of 2 in. (*AASHTO ASD 10.38.2.3*). Edge distance and longitudinal spacing requirements are also given in Section 10.38.2.4. The edge to edge clear distance between the girder flange and the shear connectors must be greater than 1 in. Also, adjacent shear connectors must be at least 4 in. apart on center (*AASHTO ASD 10.38.2.4*).

The location of shear connectors is discussed in *AASHTO ASD Section 10.38.4.2*. Shear connectors are to be placed in either positive moment regions or throughout the entire length of a bridge. In the case of a continuous span bridge, shear connectors may be placed in the negative moment regions if the reinforcing steel in the concrete is considered as part of the composite section (*AASHTO ASD 10.38.4.2*).

2.4.2 Shear Connector Provisions in the AASHTO LRFD Bridge Design Specifications

AASHTO LRFD follows the same design procedures as *AASHTO ASD* and *LFD* for shear connectors. A number of shear connectors in a cross section is chosen and the spacing (pitch) is determined based on fatigue provisions. The selected number of shear connectors is then checked

for ultimate strength requirements. General provisions for shear connector design in *AASHTO LRFD* are the same as in *AASHTO ASD*.

AASHTO LRFD uses somewhat different equations for determining the strength of a shear stud under fatigue and static loads compared to *AASHTO ASD*. Equation 2.21 shows the shear resistance of a single connector, Z_r, for fatigue loading, given in *AASHTO LRFD Section 6.10.10.2*. This equation is same as Equation 2.13, except with a lower limit, below which the connector is not expected to fail. Z_r has units of ksi.

$$Z_r = \alpha d^2 \geq \frac{5.5d^2}{2} \qquad \textit{(Eq. 2.21)}$$

$$\alpha = 34.5 - 4.28 \log N \qquad \textit{(Eq. 2.22)}$$

Where: d = diameter of stud (in.)
N = number of fatigue load cycles specified in *AASHTO LRFD Section 6.6.1.2.5* for a bridge with a design life of 75 years.

The unfactored shear strength of a shear connector, Q_n, is given in *AASHTO LRFD Section 6.10.10.4.3* and is presented here as Equation 2.23.

$$Q_n = 0.5 A_{sc} \sqrt{f_c' E_c} \leq A_{sc} f_u \qquad \textit{(Eq. 2.23)}$$

Where: f_u = specified minimum tensile strength of a stud (ksi)

2.5 Design of Partially Composite Beams

Current *AASHTO Specifications* require composite beams to be designed as fully composite, and have no provisions for partially composite design. However, in retrofit situation, the installation of post-installed shear connectors is likely to be more costly and time consuming than welded stud shear connectors used in new construction. Because of the higher installation costs, it is preferable to use the minimum number of post-installed shear connectors needed to achieve a desired level of strengthening. This, in turn, suggests the need to design such systems for partially composite action.

2.5.1 Comparison with Non-Composite Steel Girder

Composite action between the steel beam and the concrete slab can be achieved by installing shear connectors. These shear connectors transfer longitudinal shear at the steel-concrete interface resulting in composite action. This composite action can lead to significant increases in stiffness and strength compared to non-composite beams. The following sections discuss the increases in stiffness and strength that can be achieved with composite action, and demonstrate the efficiency of partially composite design.

2.5.1.1 Stiffness under Service Load

The stiffness of a steel-concrete composite beam can be represented by the vertical deflection under service load. A mathematical expression of the load-deflection relationship for partially composite beams was derived by Viest et al. (1952). However, this closed form solution is very complex and impractical to use for the design purposes.

A more practical solution for predicting deflection of a composite beam considering slip at the steel-concrete interface was proposed by Johnson and May (1975). For a composite beam with a shear connection ratio of η, a convenient design equation was proposed by a linear interpolation approach. The equation is:

$$v_{part} = v_{full} + \alpha \cdot \left(v_{steel} - v_{full}\right) \cdot \left(1 - \eta\right) \qquad \textit{(Eq. 2.24)}$$

Where: v_{steel} = Deflection of bare steel beam

α = non-dimensional deflection parameter, 0.4 recommended (Ohelers 1995)

η = Shear connection ratio $\left(N / N_{full}\right)$

N = Number of shear connector in a shear span

N_{full} = Number of shear connector for full shear connection

This equation was compared with the results from theoretical composite beam analysis by McGarraugh and Baldwin (1971). This comparison showed that this equation provides a conservative prediction of deflections for partially composite beams.

The commentary of the *AISC LRFD Specification for Structural Steel Buildings* provides an equation for the effective moment of inertia to estimate deflections of partially composite beams in the elastic range of behavior. This equation results in the deflection of fully composite beams and bare beams, when $\eta = 1$ and $\eta = 0$, respectively. The equation is:

$$I_{eff} = I_s + \sqrt{\left(\sum Q_n / C_f\right)}\left(I_{tr} - I_s\right) \qquad \textit{(Eq. 2.25)}$$

Where: I_s = Moment of inertia for the steel beam

I_{tr} = Moment of inertia for the fully composite beam

$\sum Q_n$ = strength of shear connectors between the point of maximum positive moment and the point of zero moment to either side

C_f = Compression force in concrete slab for fully composite beam

Figure 2.7 shows the elastic stiffness of composite beams with different shear connection ratios derived from Equation 2.25.

As shown in Figure 2.7, partially composite beams show much higher stiffness than non-composite beams. This indicates that a significant decrease in deflection under service load is expected when even a small number of post-installed shear connectors are installed in an existing non-composite beam.

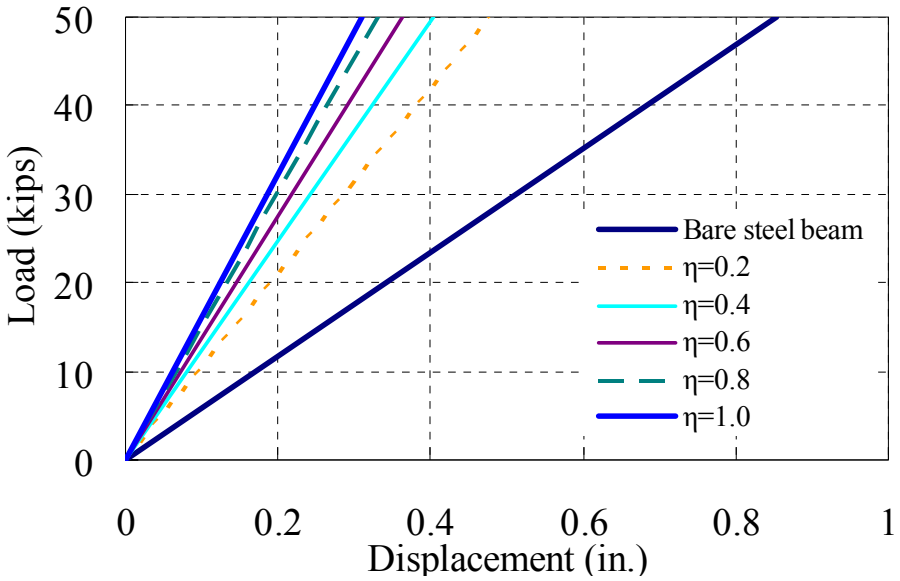

Figure 2.7: Initial stiffness of composite beams (AISC, 2005)

2.5.1.2 Ultimate Load Carrying Capacity

The flexural strength of fully and partially composite beams can be calculated by simple plastic cross-sectional analysis assuming full yielding in the steel beam and a rectangular stress block in the concrete slab (Viest 1997). The plastic stress distribution on the cross-section of a composite beam is shown in Figure 2.8. The contribution of the longitudinal reinforcement to the flexural strength of the cross-section is normally very small, and typically neglected in the analysis.

The compression force C in the concrete slab is the smallest value among the following three equations.

$$C_1 = A_s F_y \qquad \textit{(Eq. 2.26a)}$$

$$C_2 = 0.85 f_c' A_c \qquad \textit{(Eq. 2.26b)}$$

$$C_3 = \sum Q_n \qquad \textit{(Eq. 2.26c)}$$

Flexural capacity of the composite beam cross-section can then be calculated by computing the moment of the resultant forces in Figure 2.8. For partially composite beams, Equation 2.26c controls the compression force in the concrete slab. For design of composite beams according to current AASHTO provisions, Equation 2.26c is not permitted. Consequently, partially composite beams are implicitly prohibited by AASHTO.

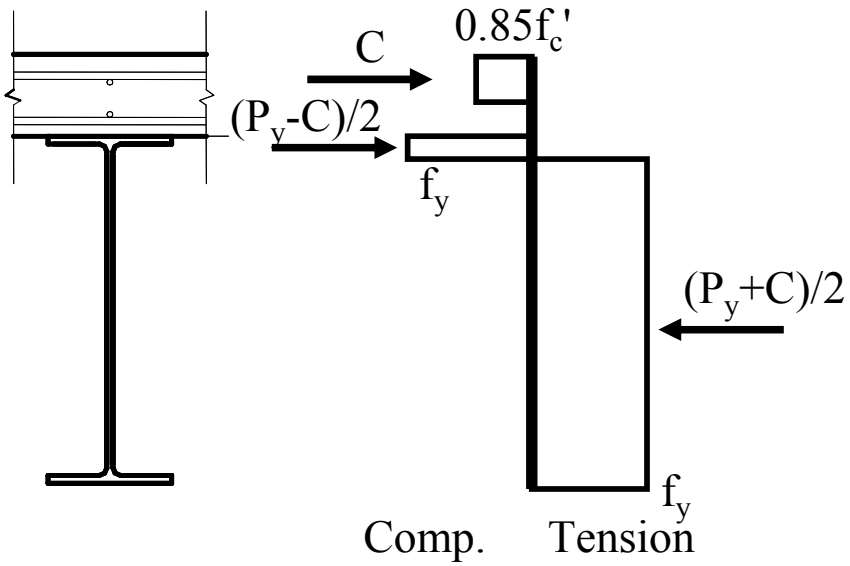

Figure 2.8: Plastic cross-section analysis for composite beams

An example of the ultimate load carrying capacity of a composite beam with different shear connection ratios is shown in Figure 2.9. Details of the composite beam are same as the full-scale beam test specimens described in Chapter 5. Observe that a partially composite beam with low shear connection ratios still shows much higher strength than the non-composite beam. For example, even with a shear connection ratio as low as 30%, a strength increase of about 50% is achieved.

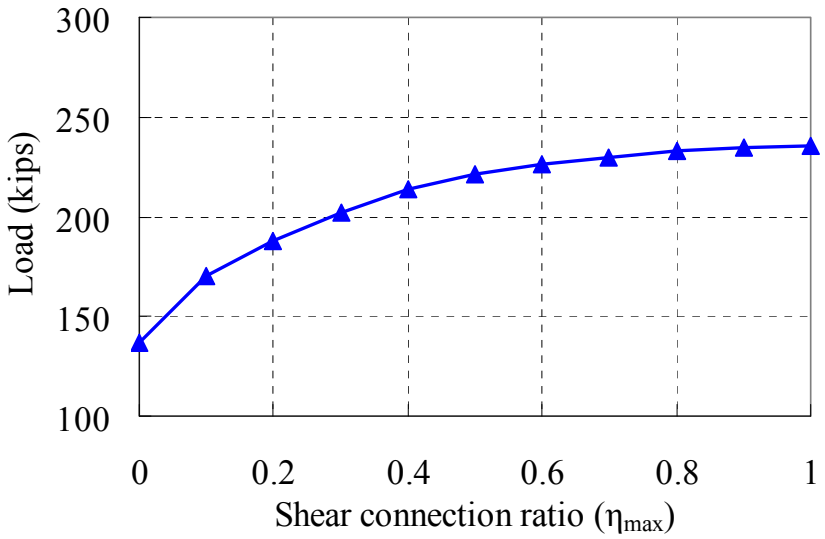

Figure 2.9: Ultimate load carrying capacity of a composite beam

2.6 Approaches for Design of Composite Bridge Girders with Post-Installed Shear Connectors

This chapter discussed design procedures for composite beams in the *AASHTO Specifications*. The AASHTO composite beam design provisions are intended for new construction using welded stud shear connectors, and are based on past research on these systems. Further, current *AASHTO Specifications* only recognize fully composite design, and do not include provisions for partially composite design. The absence of partially composite design provisions in AASHTO likely reflects the fact that fatigue design requirements for shear studs normally results in the need for a large number of shear connectors that will typically lead to a fully composite beam for static strength calculations. Thus, the use of partially composite design is not normally used for bridge girders. By contrast, partially composite design is used on a routine basis for composite beams in buildings, and the *AISC Specification for Structural Steel Buildings* has included detailed design provisions for partially composite beams for many years. The popularity of partially composite beams in buildings reflects the great efficiency of partially composite design for both strength and stiffness, as illustrated in Figures 2.7 and 2.9. The different approaches to composite beam design in buildings versus bridges (bridges normally use fully composite beams; buildings normally use partially composite beams) likely reflects the dominating influence of fatigue in design of the composite beams for bridges, and the absence of fatigue considerations in design of composite beams for buildings.

When considering the development of composite action in existing non-composite bridge beams, a number of changes from conventional bridge design practice are needed. The welded shear stud, commonly used in new construction, is not likely to be a practical alternative as a post-installed shear connector. Consequently, new types of shear connectors must be developed, and these connectors must be tested to determine their strength, stiffness, and deformation capacity under static loads. They must also be tested to determine their performance under both high-cycle and low-cycle fatigue loading. Thus, the current practice of using welded stud shear connectors must be changed to enable the use of unconventional shear connectors. While there is a long history of research and testing of welded stud shear connectors, there is little data on post-installed shear connectors. Consequently, much of this research project was aimed at developing concepts for post-installed shear connectors, and conducting tests to determine properties needed for design.

In addition to developing new types of shear connectors, economical strengthening of existing non-composite beams will almost certainly require adopting partially composite design. The cost of post-installed shear connectors for an existing bridge is likely to be far greater than the cost of welded studs for new construction. Fully-composite design will therefore likely be very costly for strengthening existing bridges. Thus, the economic viability of strengthening existing non-composite bridges by post-installing shear connectors is likely to depend largely on the ability to implement partially composite design.

The development and testing of post-installed shear connectors are described in the following chapters. Shear connectors were tested under static loading high-cycle fatigue loading and low-cycle fatigue loadings. The feasibility of partially composite design using post-installed shear connectors is then demonstrated in tests on large-scale composite beam specimens.

Chapter 3. Single-Shear Connector Tests: Phase I—Static Tests

3.1 Introduction

When choosing a post-installed shear connector for strengthening an existing bridge, both the structural performance of the connector as well as the difficulty of installation are important factors. In this chapter, various types of post-installed shear connectors considered in this study are first described. Next, a setup for testing single-shear connectors was developed and various types of shear connectors were tested to identify load-slip behavior under static monotonic loading. Based on the results of these tests and on considerations of constructability, the most promising post-installed shear connectors for bridge strengthening applications were identified. These post-installed shear connectors were then subjected to further testing, which is described in Chapter 4.

3.2 Investigated Types of Post-installed Shear Connectors

A total of 13 post-installed shear connection methods were considered in this project, of which 11 were tested under static loading. In this section, the 11 connection methods are introduced and their installation process in existing bridges is briefly described. Each method is provided with an abbreviated name, which will be used throughout the remainder of this report to refer to each shear connection method. Installation methods and tools used for these connection methods are discussed in greater detail in Hungerford (2004) and Schaap (2004). In addition to discussing the post-installed shear connection methods, the conventional cast-in-place welded stud is also included in the discussion. In the various tests conducted on post-installed shear connectors in this project, tests were also conducted on conventional cast-in-place welded studs, to provide baseline data from which to judge the performance of the post-installed connectors. Figure 3.1 shows the various post-installed shear connectors investigated in this chapter.

Figure 3.1: Post-installed shear connectors investigated under static loading

3.2.1 Cast-in-Place Welded Stud (CIPST)

The cast-in-place welded shear stud is the most common shear connector used in modern composite bridge construction. It is a headed round steel bar that is welded to the top flange of a steel girder with a stud welding gun. Once the studs are welded, the concrete slab is cast (see Figure 3.2). The cast-in-place shear stud was used as a benchmark in this study, with which all other post-installed connectors were compared.

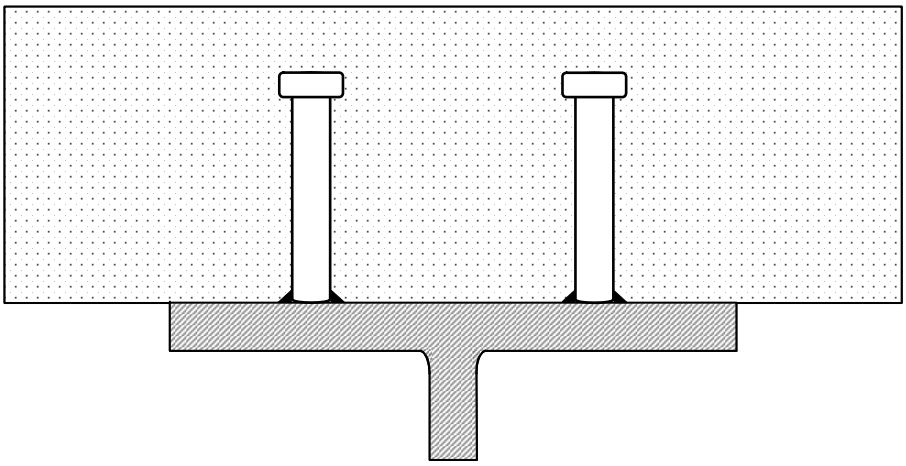

Figure 3.2: Cast-in-place welded stud

3.2.2 Post-Installed Welded Stud (POSST)

This method also uses the welded shear stud. However, the stud is installed after the concrete slab is in place. This requires coring a hole through the concrete slab to allow enough space for a shear stud and stud welding gun to fit. Once the hole is cored, the top flange of the girder is cleaned and the stud is welded. The hole is then filled with non-shrink grout (see Figure 3.3).

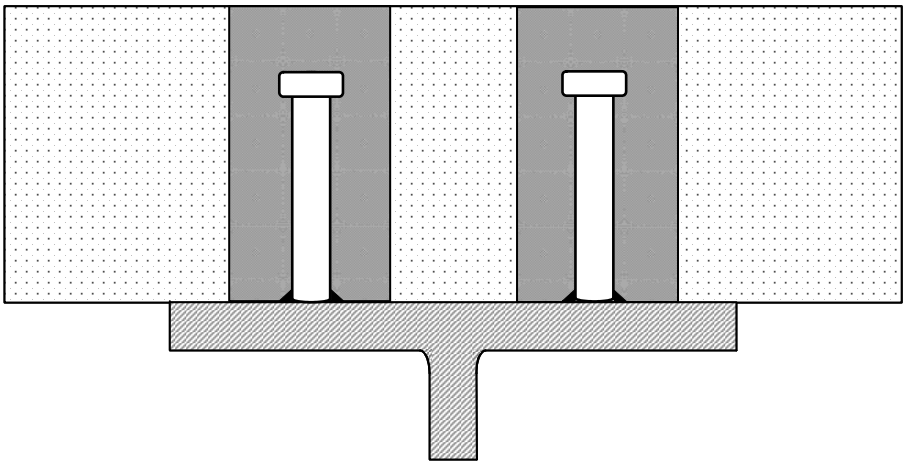

Figure 3.3: Post-installed welded stud

3.2.3 Stud Welded to Plate (STWPL)

This method is a variation on the POSST method, as shown in Figure 3.4. The stud in the STWPL method is welded to a separate plate that is then fillet welded onto the side of the girder. A smaller diameter hole is required in the slab than that for the POSST method, since the stud is shop-welded to a separate steel plate.

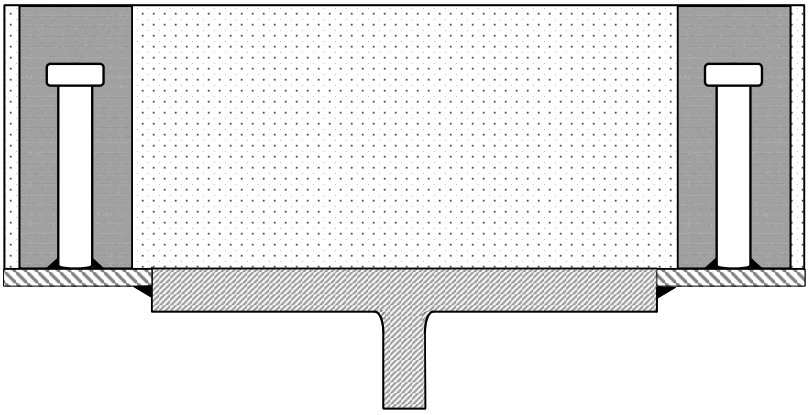

Figure 3.4: Stud welded to plate

3.2.4 Double-Nut Bolt (DBLNB)

The connector used in this method is a high strength ASTM A325 or A490 bolt. The installation of this connector requires drilling holes through both the concrete slab and the steel girder. The connector is then inserted in the hole and is held in place by two nuts. A bottom nut is placed and tightened while the two top nuts prevent rotation of the bolt. Once the connector is in place the hole is filled with non-shrink grout (see Figure 3.5).

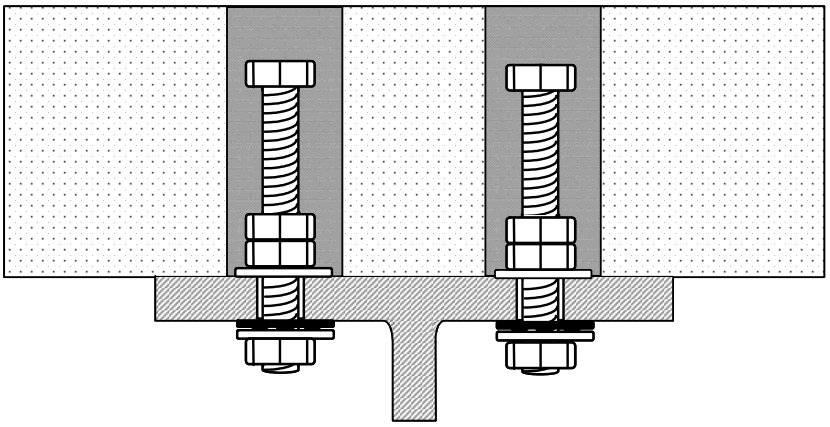

Figure 3.5: Double-nut bolt

3.2.5 High-Tension Friction Grip Bolt (HTFGB)

With this method, the concrete slab and the steel girder are clamped together with a high-strength A325 or A490 bolt. Shear force between the concrete and the steel is initially transferred through friction. Once friction is overcome, shear force is transferred through bearing between the bolt and the concrete.

To install this connector, two different size holes are drilled through the concrete slab. The bolt is inserted from the top of the slab and tightened from underneath up to the required pretension. The remaining hole at the surface of the slab is later filled with non-shrink grout (see Figure 3.6).

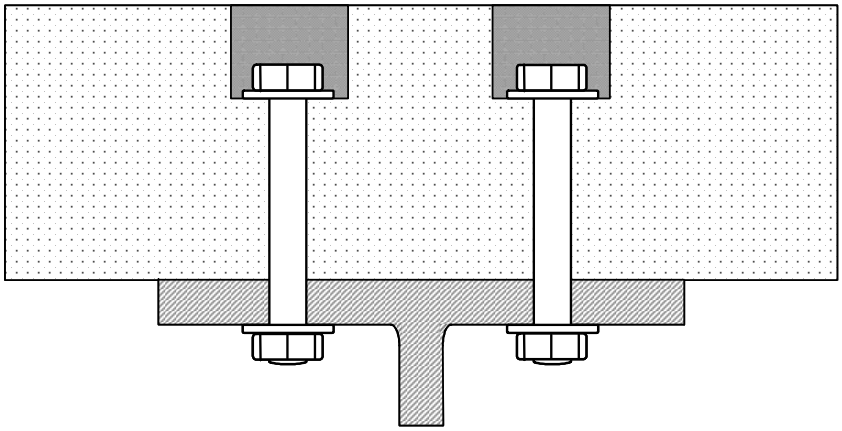

Figure 3.6: High-tension friction grip bolt

3.2.6 Expansion Anchor (KWIKB)

For this connector, holes are drilled through both the girder flange and the concrete slab from the bottom of the slab. The anchor is then tapped into the hole and tightened (see Figure 3.7). The expansion anchor is another connector that initially utilizes friction to transfer shear forces between the slab and the girder. Once friction at the steel-concrete interface is overcome with increasing load, the connector moves in the hole and transfers shear forces through bearing.

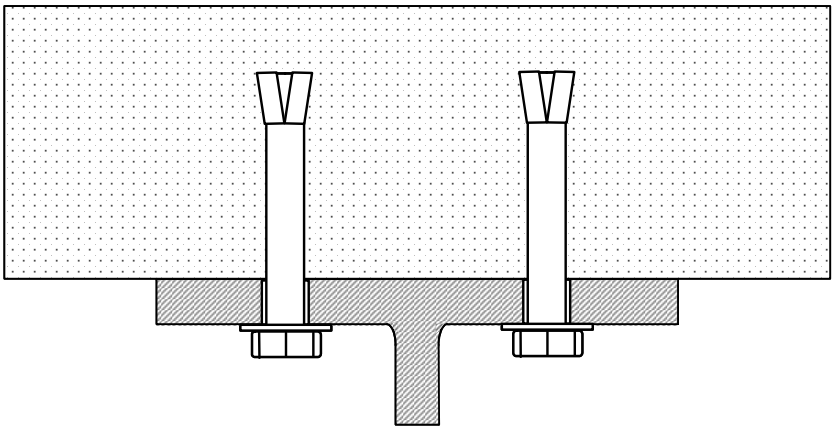

Figure 3.7: Expansion anchor

3.2.7 Undercut Anchor (MAXIB)

The undercut anchor, like the expansion anchor, transfers shear forces initially through friction followed by bearing. The connector is installed by first drilling holes through the girder and the slab from under the bridge. The hole in the slab is then undercut using a special undercutting drill. The connector is set with a special setting device and the nut is tightened until the required pretension is reached (see Figure 3.8).

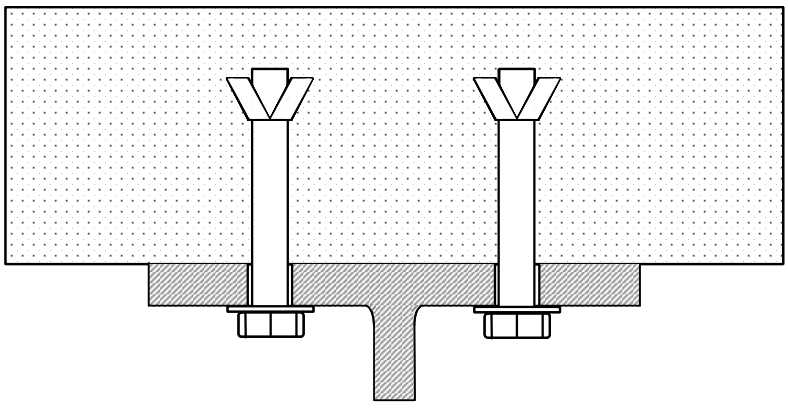

Figure 3.8: Undercut anchor

3.2.8 Welded Threaded Rod (POSTR)

As shown in Figure 3.9, this method is another variation on the POSST method. A hole is cored through the concrete slab and a fully threaded rod is welded onto the steel girder. Prior to grouting, a sheath is placed around the rod to prevent grout from filling the threads. The hole is grouted leaving room for a washer and a nut. The sheath is later removed and the nut is tightened. As a result, the rod transfers shear forces first by friction, and then by bearing once friction is overcome.

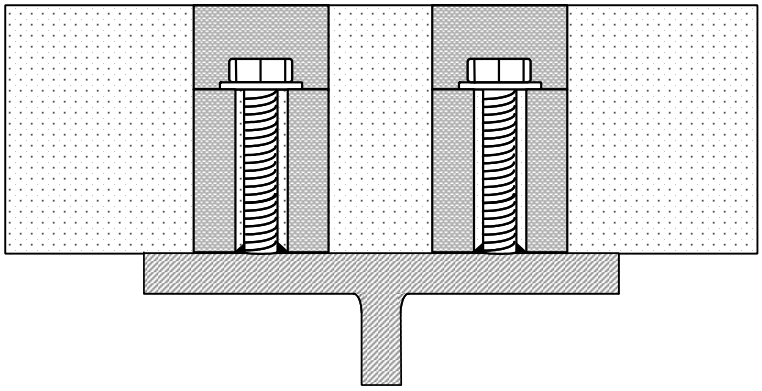

Figure 3.9: Welded threaded rod

3.2.9 HAS-E Adhesive Anchor (HASAA)

With this method, a hole is drilled from under the bridge, through the steel flange and into the concrete slab. Adhesive is injected overhead into the hole in the slab and then a threaded rod is inserted (Figure 3.10). Once the adhesive cures, the connector is tightened from under the bridge. In testing this method, an adhesive and threaded rods manufactured by Hilti Corp. were used. The Hilti adhesive was designated HY 150 and the threaded rod was designated as HAS-E.

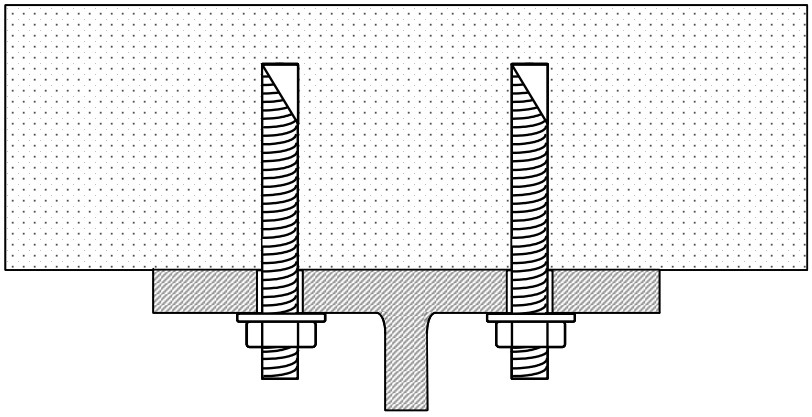

Figure 3.10: HAS-E adhesive anchor

3.2.10 HIT-TZ Adhesive Anchor (HITTZ)

Similar to the HAS-E anchor this anchor uses friction followed by bearing to transfer shear forces from the bridge girder to the slab. The difference between these two connectors is the way forces are transferred from the connector to the adhesive. The Hilti HAS-E anchor relies on the bond between its threads and the adhesive. The HIT-TZ anchor, on the other hand, transfers forces to the adhesive through wedging action due to its special threads (see Figure 3.11).

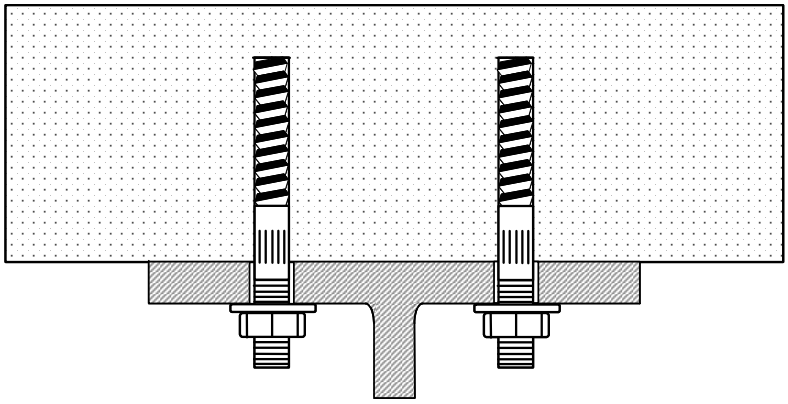

Figure 3.11: HIT-TZ adhesive anchor

3.2.11 Concrete Screw (WEDGB)

This connector requires a hole to be drilled through both the steel girder and the concrete slab from under the bridge. The concrete screw is then simply driven into the hole and screwed into place (see Figure 3.12). No adhesives or grout are required.

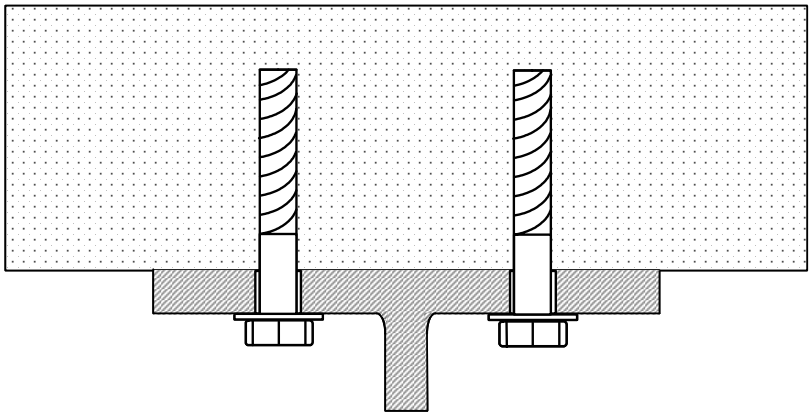

Figure 3.12: Wedge-bolt concrete screw

3.2.12 Epoxy Plate (3MEPX)

The Epoxy Plate (see Figure 3.13) is the only method that directly utilizes adhesion to transfer shear between the slab and the girder. A steel plate is welded to the edge of the top

girder flange. The perimeter of the plate is then sealed with epoxy. Epoxy is injected to fill the gap between the slab and the plate until epoxy ejects through predrilled exit holes.

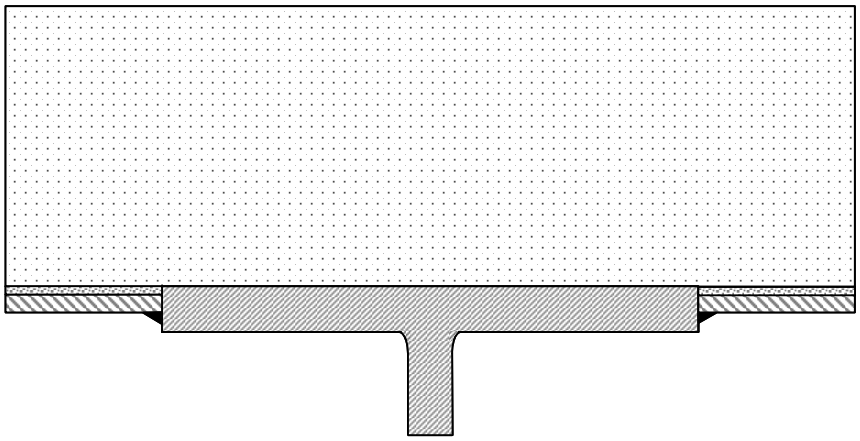

Figure 3.13: Epoxy plate

3.3 Development of Direct-Shear Single-Connector Test Specimens

The direct-shear, single-connector test specimens used in this study were developed based on the idealized prototype bridge developed from an investigation of typical details in existing non-composite steel girder bridges (Hungerford 2004). Field investigations revealed that for typical bridges that might be retrofitted in this manner, the slab was about 7 to 8-inches thick. Girders were rolled A36 wide-flange shapes with a flange width in the range of about 11 to 14-inches, and a flange thickness in the range of about 3/4-inch to 1-1/8-inch. A 36- x 6- x 1-in. steel test plate was selected for use in the test specimen because it represented approximately one-half of the top flange of a steel girder from the idealized prototype bridge as shown in Figure 3.14. Concrete blocks measuring 23-1/2 x 23-1/2 x 7-in. were cast to represent the concrete slab.

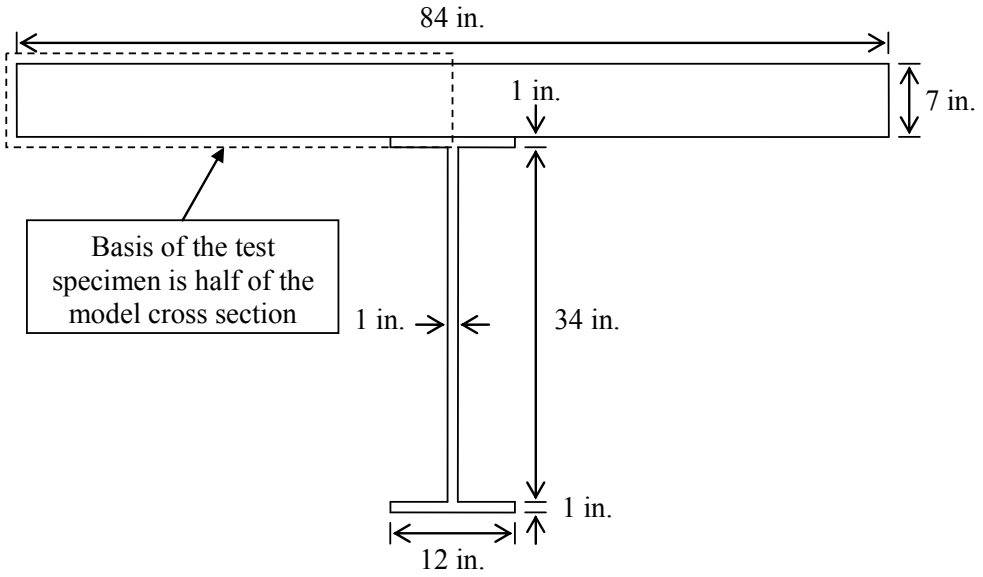

Figure 3.14: Cross-section of prototype composite bridge used to develop direct-shear test specimens

3.3.1 Concrete Test Blocks

Concrete test blocks were cast using fiberglass waffle-slab forms, measuring 23-1/2 in. square by 12 in. deep. The concrete test blocks were cast using the inside of the form. Four 4-3/8 in. tall plastic reinforcing chairs were placed inside the form on which a 22-1/4 x 22-1/4 x 5/8-in. piece of plywood was set. The form created a concrete block measuring 22-1/4 to 23-1/2-in. square, and 7 in. thick (see Figure 3.15).

The reinforcing cage was composed of two layers of reinforcement tied to four #3 stirrups located at the corners. Each layer consisted of two #4 bars and two #5 bars in each the longitudinal and transverse directions. The configuration and dimensions are shown in Figure 3.16.

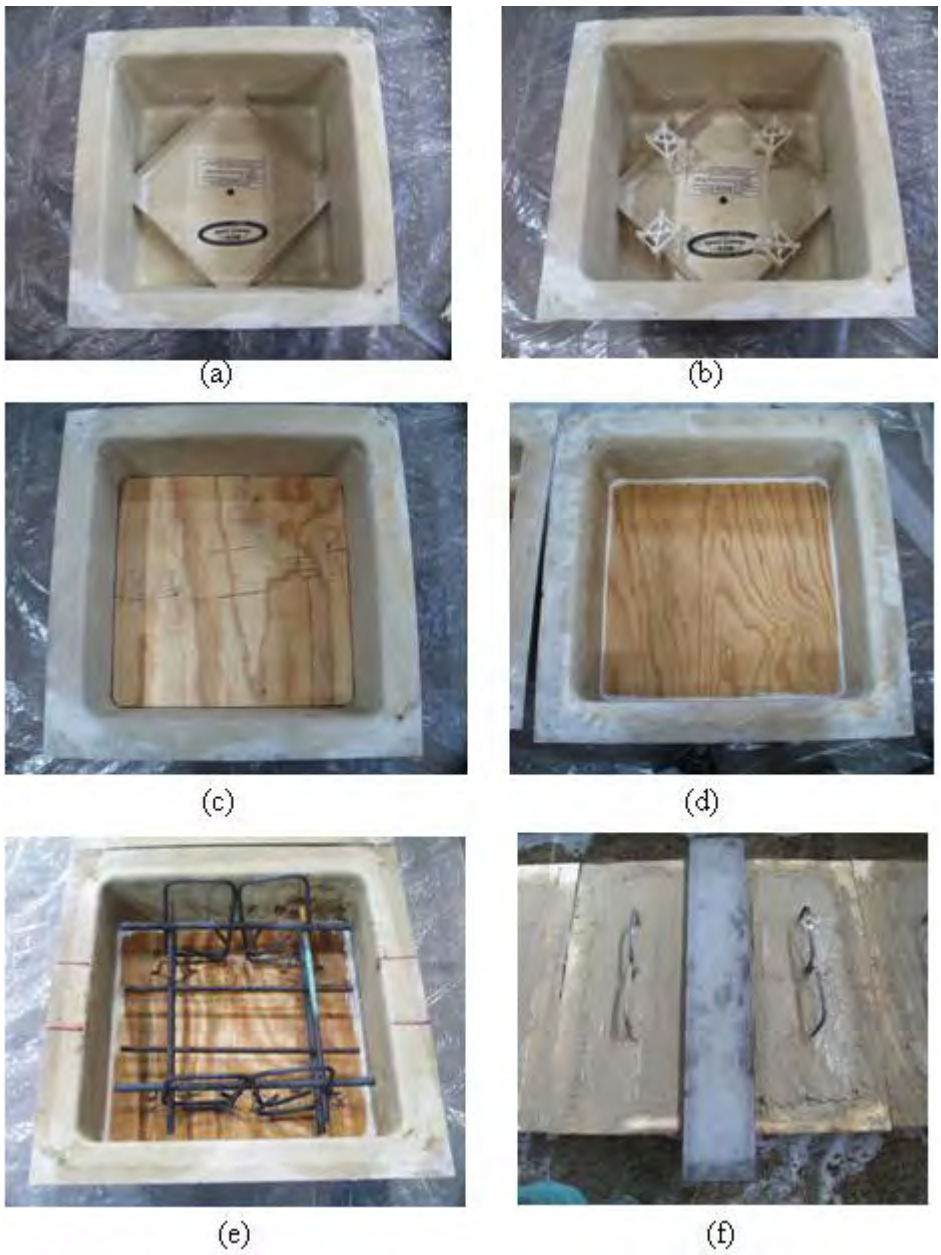

Figure 3.15: (a) Empty waffle slab form; (b) form with plastic reinforcing chairs; (c) form with plywood; (d) form with plywood and caulk; (e) form with reinforcing cage; (f) cast concrete with steel test plate

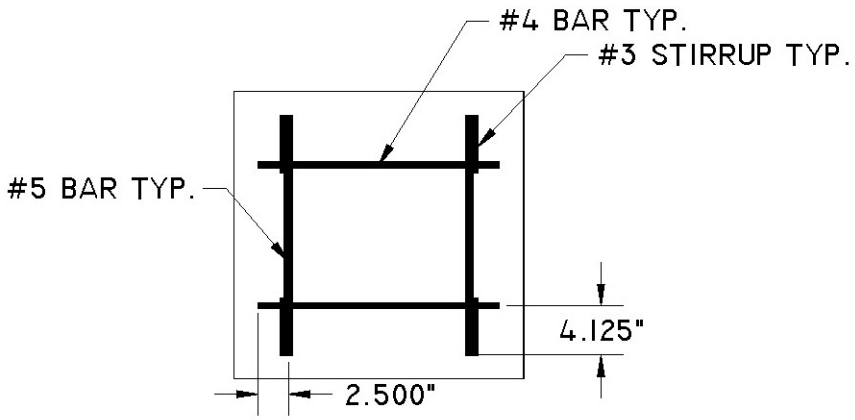

(a) Top View

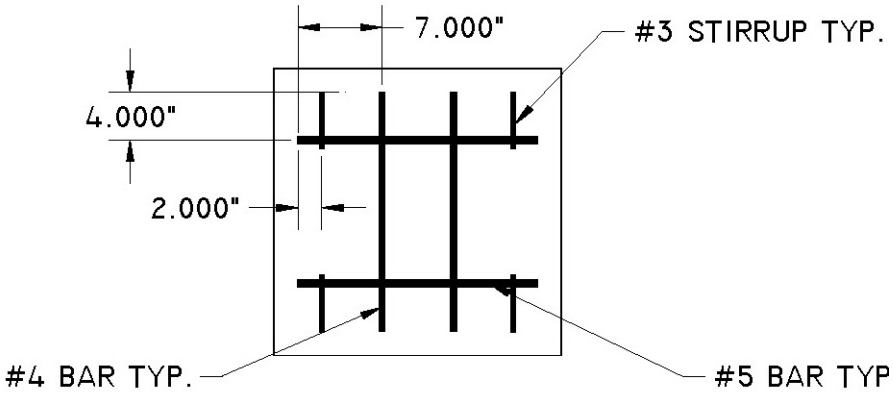

(b) Bottom View

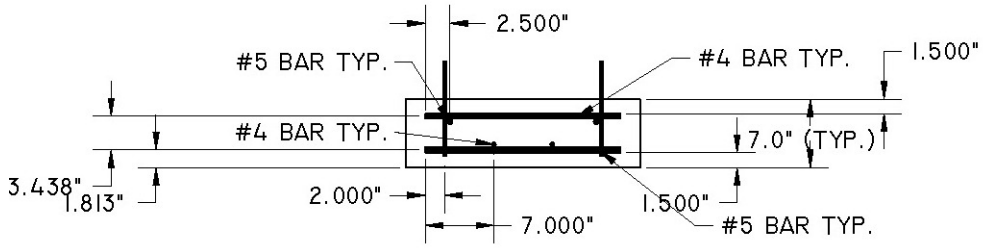

(c) Section View

Figure 3.16: Reinforcing cage for single-shear connector test specimen

The concrete was ordered as Mix Design #261 (f_c' =3,000 psi) from Capitol Aggregates in Austin, Texas. The cast blocks were covered with plastic and sprinkled with water twice daily for 5 days after casting. Test cylinders were covered with plastic and kept next to the test blocks. To determine compressive strength, cylinder tests were performed at 7, 14, 21, and 28 days, and

on four later occasions during static testing. Results are shown in Figure 3.17. Note that the compressive strength of the concrete was in the range of 3000 to 3500 psi.

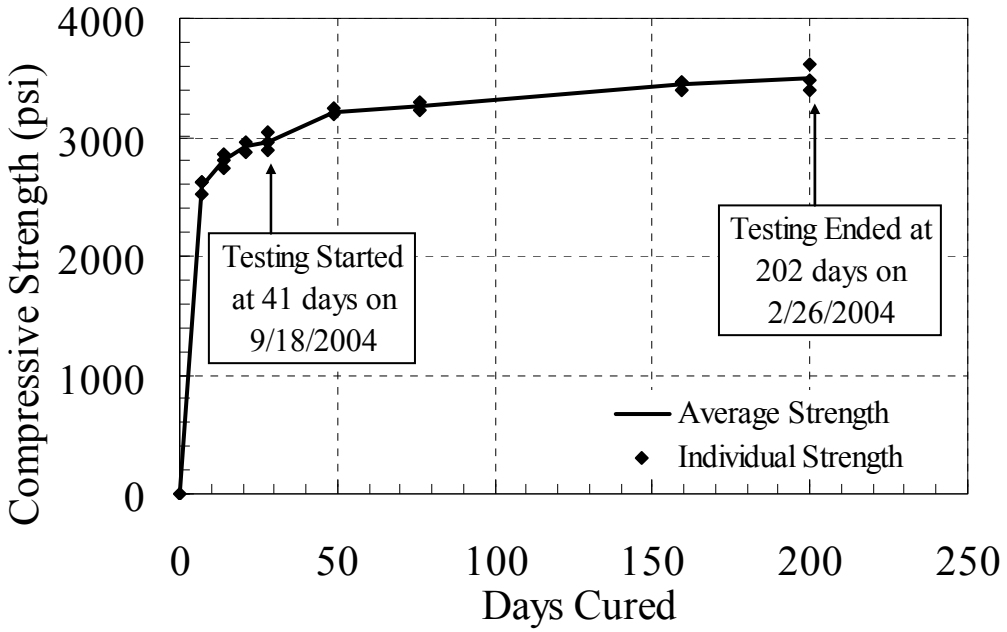

Figure 3.17: Concrete compressive strength of test specimens versus time

3.3.2 Steel Test Plates

Fifty 36- x 6- x 1-in. A36 steel plates were ordered for the test specimens. A 1-5/16 in. diameter hole centered 2-1/2 in., from one end was drilled in each plate for the attachment with the clevis. A tension coupon test was performed on a sample plate to determine the material properties of the steel plates. The average static yield strength was 39.9 ksi; the average dynamic yield strength, 43.0 ksi; and the average ultimate tensile strength, 66.9 ksi.

3.3.3 Grout

Several shear connection methods require grouting to fill the drilled holes during the installation. For the selection of the grout material, the following qualities were necessary: suitable for traffic applications, fast setting, high early compressive strength, low shrinkage, and simple application.

Five Star™ Highway Patch met all of those requirements and was selected for use in this study. This is a fast-setting grout typically used in traffic areas, including bridges. It is a one-component material with a specified compressive strength of 2000 psi at 2 hours, 5100 psi at 24 hours, 7000 psi at 7 days. Due to its high early strength, roads can be opened to traffic 2 hours after application (Five Star Products 2006).

3.3.4 Shear Connectors

All connectors tested had 3/4-in. nominal diameter except the WEDGB connector (0.7 in. dia.). Table 3.1 shows nominal strengths of the shear connectors used for each shear connection method and anchor materials of which the corresponding shear connectors are made. For the

3MEPX connection method, 3M DP-460 NS Epoxy was used. Its specified shear capacity is 4650 psi at 73° F and 1360 psi at 180° F.

Table 3.1: Properties of connector materials

Shear connector	Minimum specified yield strength (ksi)	Minimum specified ultimate tensile strength (ksi)	Material specifications
CIPST	50	60	AISI C-1015
POSST			
STWPL			
DBLNB	130	150	SAE J429 - Grade 8
HTFGB	92	120	ASTM A325
KWIKB	41	75	ASTM A510
MAXIB	105	125	ASTM A193-B7
POSTR	36	60	ANSI C1018
HASAA	58	72.5	ISO 898 Class 5.8
HITTZ	70	87	ASTM A510
WEDGB	130.5	145	Case hardened AISI 1020/1040

3.4 Setup for Single Connector Shear Test

3.4.1 Test Setup

Each connection method introduced in the previous section was subjected to a screening process based on structural performance, constructability, practicality, and cost. Those that showed promise in each category were recommended for further investigation under fatigue tests.

To assess the load-slip behavior of each connector under static loads, two possible testing methods were investigated: push-out tests and direct-shear tests. The push-out test is widely used among researchers to test shear connectors. A test specimen consists of two slabs connected to the flanges of a single steel girder with welded shear studs (Figure 2.2). The load is applied at the center of the steel girder until the studs fail in shear. With this type of test, the load-slip behavior of a group of shear connectors is obtained. Depending on support conditions used, additional friction at the steel-concrete interface or tensile forces on the connectors are typically introduced which may misrepresent conditions in an actual composite beam.

With a direct shear test setup, on the other hand, a group of connectors as well as individual connectors can be tested. The main advantage of the direct shear test is that it can be designed to minimize eccentricity between the applied load and the concrete. Therefore, the direct-shear test setup shown in Figure 3.18 was chosen for the testing of individual shear

connectors. With this method the load is applied closer to the steel-concrete interface. Details of this direct-shear test setup and advantages over the push-out test are discussed in Schaap (2004).

3.4.2 Instrumentation

The instrumentation and data acquisition system consists of the hydraulic actuator load cell for measuring applied load, a washer load cell for measuring anchor tension, and two displacement transducers, for measuring slip. The load cell attached to the hydraulic actuator had a 100-kip capacity. The measurement output was given to the nearest pound and was accurate to within 0.5%, based on a statistical evaluation of the output. The load cell is located in the test setup between the hydraulic actuator and the clevis.

Several setups included a 7/8-in. diameter washer load cell, intended to measure anchor clamping force (see Figure 3.19). The washer load cell measurement was given to the thousandth of a pound, but it was only accurate to within 20% of the output in the experiments, based on the same statistical evaluation.

The displacement transducer, shown in Figure 3.20, were direct current differential transformers (DCDT) that receive a DC input, convert that input to AC within the device, and then convert the output signal back to DC. The DCDT has a precision of 0.0001 in., and it was accurate to 0.2% of the displacement reading, based on the same statistical analysis.

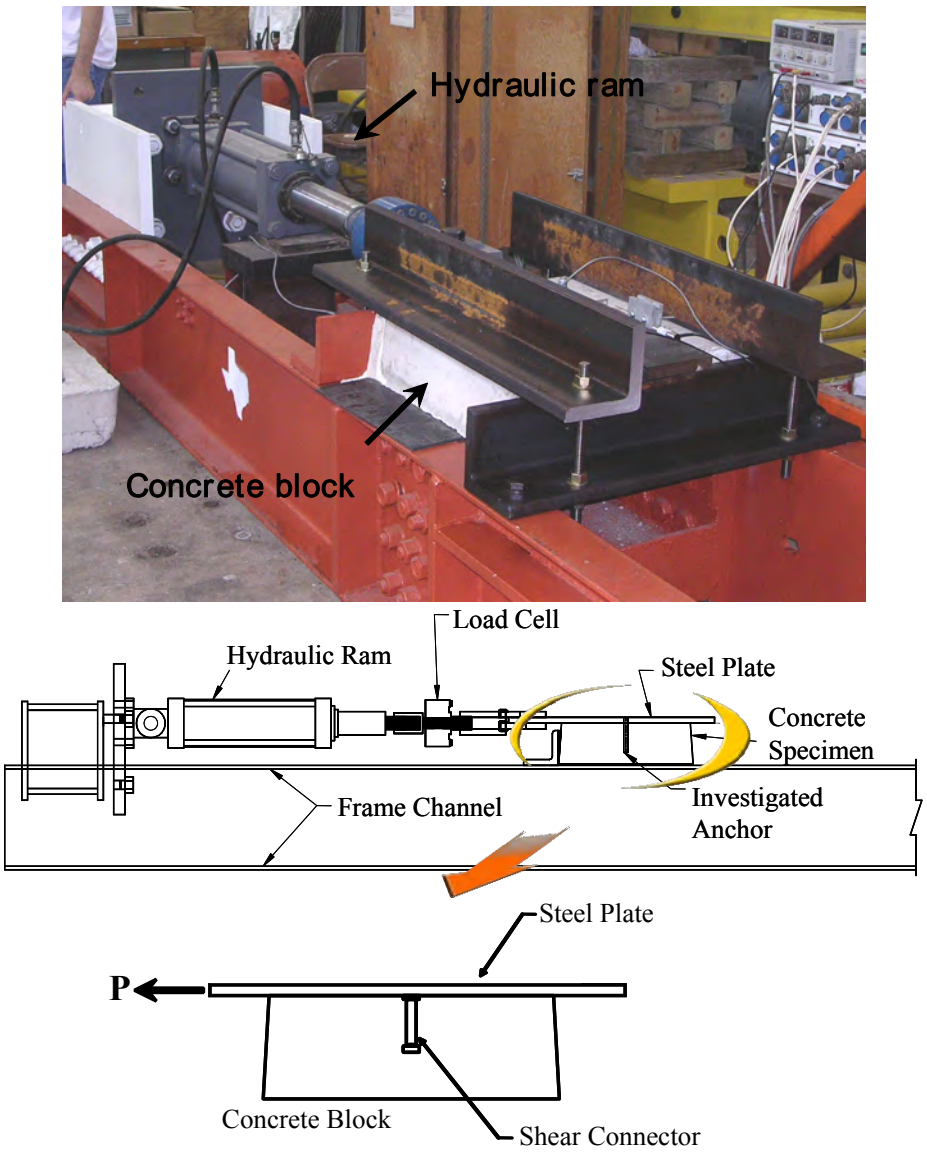

Figure 3.18: Test setup and test specimen for single-shear connector tests

Figure 3.19: Washer load cell

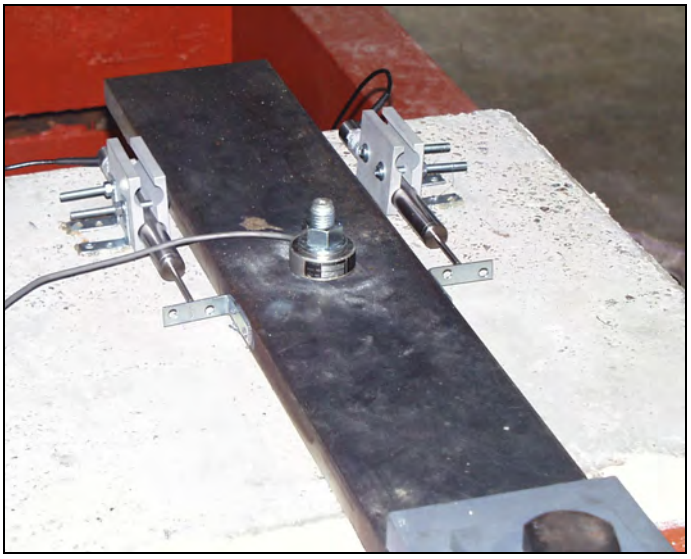

Figure 3.20: DCDTs and load washer

Instrumentation was connected to a standard bridge completion box, scanner, and personal computer. LabVIEW 7 Data Acquisition software was used to continuously obtain input every half-second while testing.

3.4.3 Test Procedure

The direct-shear, single-connector shear tests of this study were carried out using the following sequence of steps:

1) The steel test plates were connected to the concrete test blocks by the shear connectors, and the concrete test blocks were restrained by the reaction frame.

2) The hydraulic actuator, whose capacity was 100 kips, was operated using a 10,000-psi capacity pneumatic oil pump and a manual regulator to apply load to the steel test plates at rates ranging from 0.1 to 0.3 kips per second.

3) Load was applied until the connector failed or the concrete test block had developed a significant crack through its entire section.

3.5 Test Results and Discussion

This section briefly discusses structural behavior of the shear connectors tested under static loading. Three replicate tests were conducted for most of the connection method, although in some cases, either more or less replicates were tested. A total of 50 single-shear connector, direct-shear tests were performed with 3/4 -in. diameter shear connectors and the 3MEPX connection method. More detailed descriptions of the load-slip relationship and failure modes can be found in Hungerford (2004) and Schaap (2004).

3.5.1 Typical Load-Slip Behavior and Failure Mode

Although the load-slip behaviors of each type of shear connectors varied in many respects, all load-slip curves shared a few common characteristics, shown in Figure 3.21. The typical characteristics of a load-slip curve for a shear connector are the following: slip without load, load without slip, connection stiffness, ultimate strength, plastic deformation, and failure.

An anchor may have load without slip if it has initial pre-tension. An anchor may have slip with nearly zero load if a gap exists between the anchor and the concrete or steel. The connection stiffness is the stiffness of the anchor-concrete system after the anchor has slid into bearing. The ultimate strength of the shear connector is the maximum load experienced by the shear connector. After a typical short descending branch, failure of the shear connector marks the end of the load-slip response. The plastic deformation of the shear connector is defined as slip before failure without losing strength after the transition from elastic to inelastic deformation.

Most of the test specimens failed by fracture of the connector, with the failure surfaces suggesting fracture due to shear or a combination of shear and tension. Some of the test specimens experienced significant lifting of steel plates (1/2 in. max.). These tests were stopped before connector fracture due to the concern of damaging the test setup and instrumentation. For these specimens, the test was stopped after the maximum load significant deformation was observed.

Four different failure modes were observed during the tests:

1) Fracture of the shear stud just above the weld pool at the base of the shear stud (see Figure 3.22)

2) Fracture at through threaded portion of connector (see Figure 3.23)

3) Fracture of the connector at the steel-concrete interface (see Figure 3.24)

4) Bond failure at the steel-concrete interface in brittle manner (for 3MEPX) (see Figure 3.25)

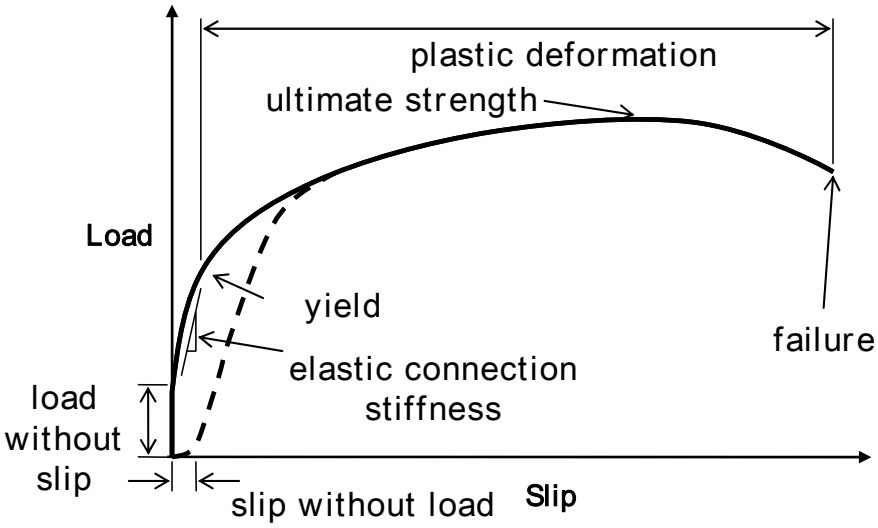

Figure 3.21: Typical characteristics of a load-slip curve

Figure 3.22: Typical failure of welded stud above the weld pool

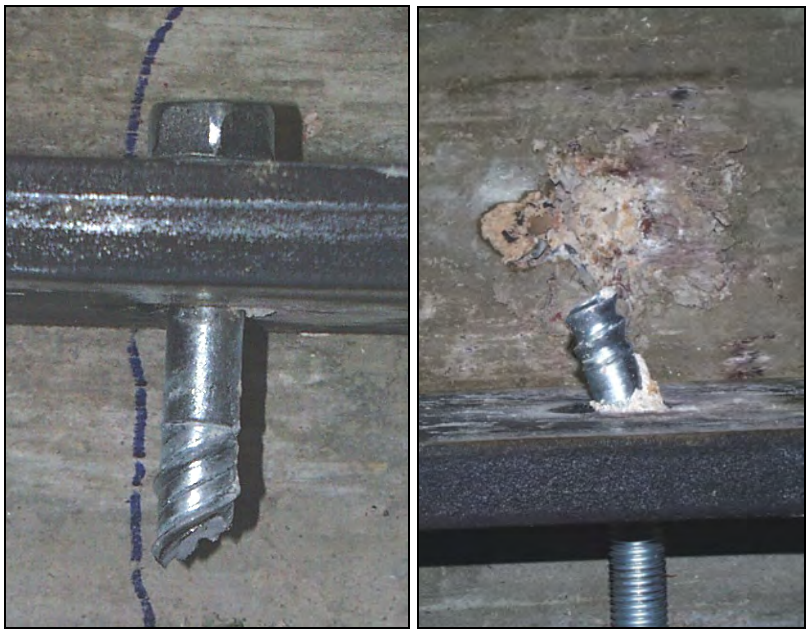

Figure 3.23: Typical failures at threads below the shear plane (WEDGB, HITTZ)

Figure 3.24: HAS-E adhesive anchor failure at the shear plane

Figure 3.25: Epoxy plate failure of the concrete below the adhered surface (3MEPX)

3.5.2 Average Load-Slip Behavior

Load-slip curves for replicate tests of each type of shear connectors were averaged and reported in Figure 3.26. The cast-in-place shear stud is also shown as a reference. The 3MEPX method is not shown in this figure, because it experienced no slip until failure at an average load of 55.4 kips.

Most of the post-installed shear connectors tested in this study showed higher strength than CIPST connector. This indicates that a smaller number of post-installed shear connectors is required compared to the welded shear studs to reach an expected composite ratio. It is considered that the higher strength of the post-installed shear connectors is due primarily to the high strength steels used in the connectors. The DBLNB and HTFGB connectors use high strength bolts which showed substantially higher strength than the conventional CIPST connector.

However, strength is not the only factor important in the performance of a post-installed shear connector. For example, connectors that require large slip before developing significant shear resistance, such as the MAXIB and KWIKB connectors, may require unacceptably large displacements of a retrofitted bridge girder to develop the composite strength of the girder.

The HTFGB, POSTR, MAXIB, KWIKB, HASAA, and HITTZ connectors were pre-tensioned during the installation. As a result, slip at the steel-concrete interface is almost zero before friction is overcome. However, the friction is overcome at relatively low loads except for the HTFGB. It is considered that initial zero slip for the HASAA connector is partly due to the overflow of excess HY 150 adhesive which cause bonding of the concrete and steel.

3.5.3 Discussion

3.5.3.1. Structural Performance

Static loading test results for the post-installed shear connectors, including the conventional welded stud shear connectors (CIPST), are summarized in Table 3.2. Maximum slip is the slip at shear connector failure. Strength and slip capacity of post-installed shear connectors are compared with the CIPST connector in the table.

Three criteria were considered to evaluate the structural performance of the post-installed shear connectors: strength, stiffness, and slip capacity. Most shear connectors tested in this study showed higher strength than CIPST connector. However, they showed significant variation in their stiffness and maximum slip capacity.

High strength shear connectors are desirable because fewer connectors will be needed to reach a required shear connection ratio. In a retrofit situation, this is desirable from the perspective of construction time and cost. However, it appears that the shear resistance developed by a connector at low levels of slip may be the most meaningful measure of the structural effectiveness of the corresponding connection method. The shear resistance developed at large slip may not contribute to the strength and stiffness of a composite beam.

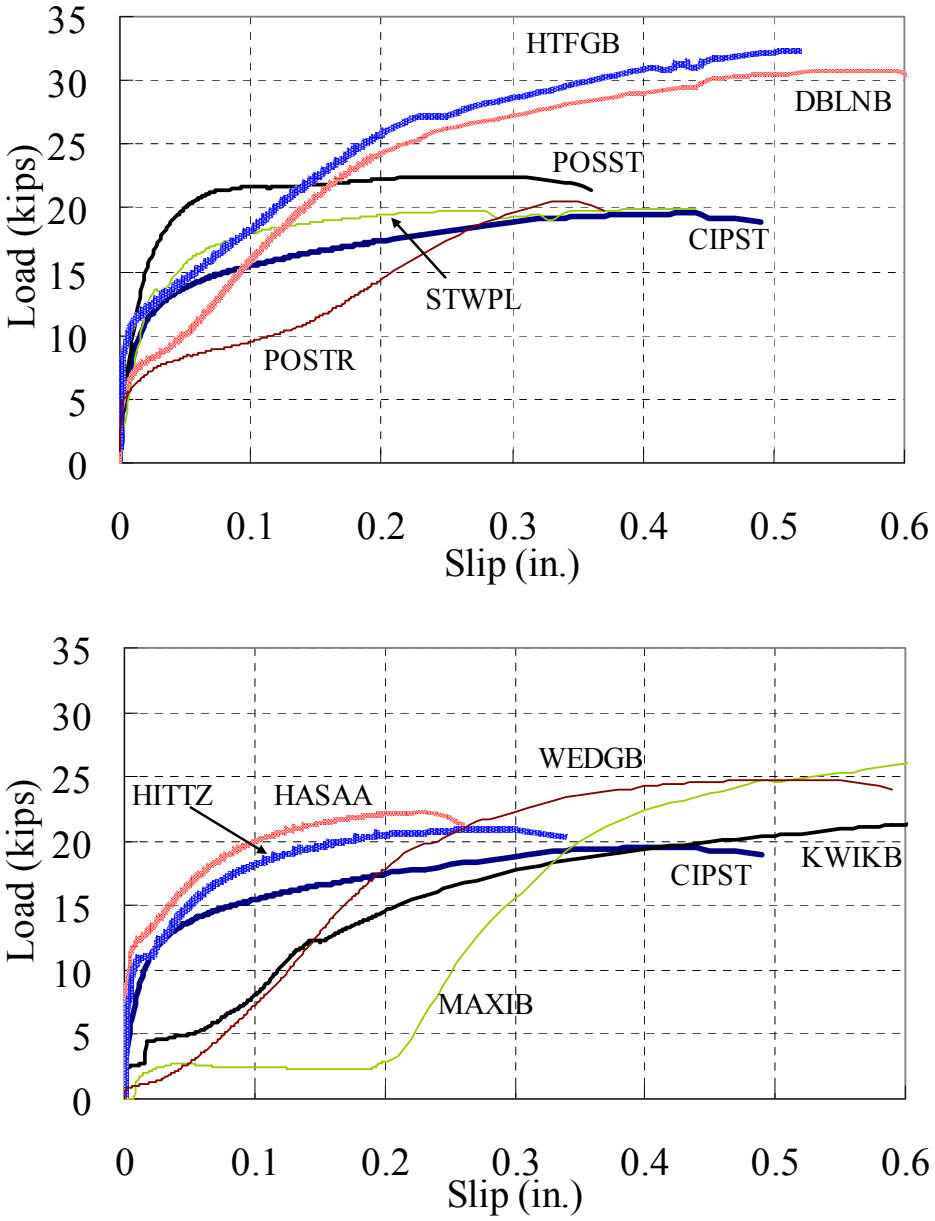

Figure 3.26: Load-slip curves for post-installed shear connectors

The shear resistance at a slip of 0.2 in. was chosen as a key parameter for comparative evaluation of the strength of various shear connectors, and a criteria for selecting a limited number of post-installed shear connectors for further testing under fatigue loading. According to Equation 2.6, which approximates the load-slip curve for a stud shear connector, a 3/4-inch diameter CIPST connector in 3,000 psi concrete attains approximately 95% of its ultimate strength at a slip of 0.1 in., and 99% of its ultimate strength at a slip of 0.2 in. Strength evaluations showed that seven shear connection methods performed at least as well as the cast-in-place welded stud shear connector at the slip limit of 0.2 in.: POSST, STWPL, DBLNB, HTFGB, HASAA, WEDGS, and 3MEPX.

The slip capacity of the shear connectors tested in this study is also significant. It is generally useful as an index of a connection method's ability to continue to resist load while deforming inelastically. Several post-installed shear connectors tested here are made of higher-strength, less-ductile steel than that of CIPST connector, and therefore have smaller slip capacities.

Table 3.2: Summary of various connector test results

Connection method	Max. Load (kips)	Max. Slip (in.)	Strength ratio at 0.2 in. slip	Strength ratio	Slip ratio
CIPST	19.57	0.58	1.00	1.00	1.00
POSST	22.46	0.37	1.36	1.15	0.64
STWPL	19.95	0.49	1.07	1.02	0.84
DBLNB	30.81	0.61	0.72	1.57	1.05
HTFGB	32.38	0.52	1.09	1.65	0.90
KWIKB	23.72	1.06	0.40	1.21	1.83
MAXIB	33.68	1.29	0.20	1.72	2.22
POSTR	20.53	0.39	0.62	1.05	0.67
HASAA	22.21	0.26	1.19	1.14	0.45
HITTZ	21.00	0.36	1.01	1.07	0.62
WEDGB	24.80	0.61	0.11	1.27	1.05
3MEXP	55.4	0	-	2.96	0

Shaded: Selected connection methods for further tests under fatigue loading

3.5.3.2 Selection for Further Testing

Of all the post-installed shear connectors described in this chapter, the most promising were chosen for further testing under fatigue loading. Structural performance, constructability, and installation cost were the issues considered in selecting post-installed shear connectors for further testing. From a structural performance perspective, it was decided to select the seven shear connectors which showed higher strength at critical design slip of 0.2 in. for further evaluation under fatigue loading. Constructability and installation cost are discussed in detail after the results of the fatigue tests are presented in the next chapter.

Chapter 4. Single-Shear Connector Tests: Phase II—Fatigue and Further Static Tests

4.1 Introduction

The Phase I tests described in Chapter 3 focused on evaluating a variety of different post-installed shear connector concepts and identifying those with the most promising static strength characteristics. As discussed in Chapter 3, this resulted in the selection of seven shear connectors for further assessment under fatigue loads.

The primary purpose of the Phase II tests described in this chapter was to investigate the fatigue performance of single-shear connectors at two distinct load levels: below the yield stress (high-cycle fatigue) and above the yield stress (low-cycle fatigue). High cycle fatigue tests were conducted first, and the connectors that showed good high-cycle fatigue performance were then tested in low-cycle fatigue. Additional static tests were also performed to gather more information on the load-slip behavior of each connector. All single-shear connector tests were performed using the direct shear test setup.

4.2 Test Setup and Procedure

4.2.1 Direct Shear Test Setup

The same direct shear test setup used for the Phase I testes was also used for Phase II. However, the test setup was modified based on experiences gained in the Phase I tests. The direct shear test setup used in the Phase II tests is shown in Figure 4.1. Compared to the Phase I tests, the setup was modified in the following manner.

An alignment coupler was placed between the load cell and the clevis, as shown in Figure 4.1. The coupler is a universal joint that allows additional movement in the loading apparatus, permitting better alignment of the applied load and reducing wear on the components during the fatigue tests.

A 3/4-in. diameter threaded clamping rod was added to the back of the steel plate, to prevent the back of the specimen plate from lifting during testing. Two 3-1/2 in. square steel plates, one with a 3/4-in. diameter hole and the other with a 3/4-in. x 2-in. slotted hole, were used as washers on each side of the test plate. To minimize friction due to clamping, strips of Teflon were glued to the washer plates, permitting the clamping plates to slide independently during loading. In addition, to minimize bending of the steel plate during testing, 32-1/2 x 3 x 1/4-in. stiffeners were welded to the outer edges of the steel plate.

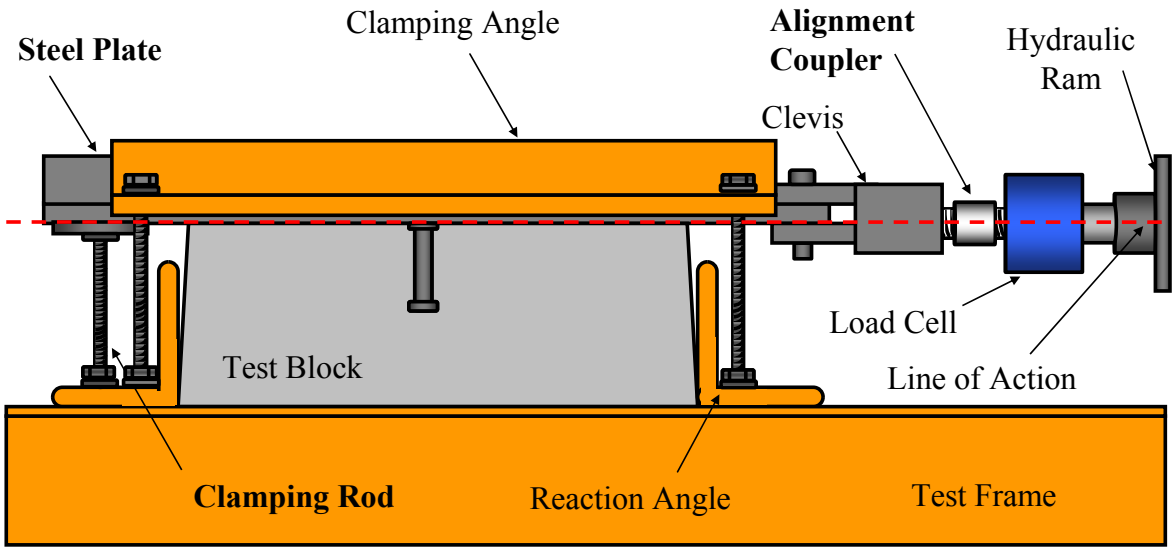

Figure 4.1: Side view of direct shear test setup

4.2.2 Instrumentation and Load Control

For the fatigue tests, a 30-gpm MTS hydraulic pump was used and loading of the test specimens was controlled by an MTS 407 single-channel servo-controller with automatic shutoff based on specified load, displacement, or error limits (MTS 2000).

For the static tests, the controller facilitated load monitoring, and its shutoff mechanism provided additional safety in the case of connector failure. The controller was found to be most useful, however, for cyclic tests, easily permitting automatic cycling between specified loads or displacements at a specified frequency. For the high-cycle fatigue tests, run under load control, the mean load, half the loading amplitude, loading frequency, and type of waveform were specified. For the low-cycle fatigue tests, run under displacement control, the corresponding displacement values were specified. During testing, the instantaneous load or displacement value, accumulated number of cycles, and the error between command and feedback signals were displayed on the controller monitor. For load-controlled tests, the controller was programmed to shut off hydraulic pressure once either connector failure or a predetermined number of cycles was reached. For displacement-controlled tests, hydraulic pressure was shut off manually following connector failure.

4.2.3 Test Procedure

4.2.3.1 Static Tests

Static tests were performed in Phase II to obtain additional load-slip behavior of each type of connector, to supplement the data collected in Phase I. These tests provided information on connection stiffness, ultimate strength, and ductility. Data gathered were compared to those of Phase I of single-shear connector test results, and were also used to plan the fatigue tests.

4.2.3.2 High-Cycle Fatigue Tests

Tests in high-cycle fatigue were performed to assess the fatigue performance of shear connectors under repeated service loads. For these tests, stress range was used as the primary test variable and the corresponding fatigue life of each connector was measured as the number of cycles to failure, permitting construction of S-N curves as discussed in Chapter 2.

Stress ranges typical of those used by earlier researchers for the fatigue assessment of welded studs were also used for CIPST specimens in these tests. This enabled a direct comparison of results. For all other connection methods, a single test was performed for each type of connector at a stress range already used for the CIPST specimens. Depending on the response of each connector, the subsequent stress ranges were adjusted as needed. The selected stress ranges were chosen to lie below the yield stress of the connector material.

The cyclic tests were controlled by applying a specified load range. Load ranges were determined by multiplying the effective shear stress area of each connector by the desired stress range. To prevent inadvertent reversal of load a minimum load of 0.9 kips was specified for each load range. For most tests, a constant mean value was used, eliminating mean load as a variable. For tests with high stress ranges, however, the mean load was adjusted to keep the maximum load below the yield strength of the connector.

The tests were started with an initial static loading before the application of cyclic loads, permitting comparison of the load-displacement data between high-cycle fatigue and static tests. The static load was applied by first manually increasing the load up to the upper limit of the load range (maximum load). Next, the load was reduced down to the lower limit (minimum load). Finally, the load was increased up to the mean load which corresponds to the "set point" in the 407 Controller.

Once the "set point" was reached, half of the loading amplitude (span) and the loading frequency were specified in the controller. Cyclic loading was then applied until connector failure. A fatigue test was typically stopped if a connector showed no signs of failure after 5 million loading cycles. Several specimens that did not fail were loaded statically up to failure.

4.2.3.3 Low-Cycle Fatigue Tests

Shear connectors that showed adequate performance under high-cycle fatigue were also tested in low-cycle fatigue. The purpose of these tests was to assess the behavior of a shear connector subjected to multiple overloads.

The procedure for the low-cycle fatigue tests followed the same steps as for high-cycle fatigue tests, with the only difference being that displacement control was used instead of load control. This required modifications only in the data acquisition process as explained in Section 4.2.3.2. Because instantaneous load values were not tracked by the controller, the tests could not be automatically stopped after connector failure. These tests were stopped manually and the number of load cycles was displayed on the controller monitor. Specimens that remained intact up to 4,000 cycles were tested statically to failure to determine their residual ultimate strength.

4.3 Test matrix

4.3.1 Static Tests

Additional static tests were performed to supplement the data collected in Phase I. One static test per connection method was conducted in Phase II, except that replicate tests were performed for POSST method. A total of seven static tests were performed.

4.3.2 High-Cycle Fatigue Tests

To understand the fatigue performance of the post-installed shear connectors, test at various stress ranges are needed. Due to the unknown fatigue lives of the majority of connectors investigated and time constraints, only three tests per connection method were initially scheduled. The CIPST method was the only exception with five tests and four different stress ranges, intended to create more reliable benchmark data for comparison with retrofit alternatives. Table 4.1 is the test matrix of stress ranges for each connection method. For the CIPST connector at 10 ksi, and the POSST at 20 ksi, two specimens were tested, as indicated in Table 4.1. A total of 20 high-cycle fatigue tests were performed on shear connectors. Each test generated a point on the S-N curves.

Table 4.1: Test matrix for high-cycle fatigue tests

Shear Connection Methods with Tested Stress Ranges					
CIPST	POSST	DBLNB	HTFGB	WEDGB	HASAA
25 ksi	25 ksi	56 ksi	45 ksi	38 ksi	40 ksi
20 ksi	20 ksi (2)	38 ksi	35 ksi	33 ksi	35 ksi
15 ksi	15 ksi	31 ksi		28 ksi	30 ksi
10 ksi (2)					

4.3.3 Low-Cycle Fatigue Tests

For the low cycle fatigue tests, the connectors were tested under displacement control. This required the selection of a displacement range that forced the connector beyond its yield strength. In light of static test results, a displacement range between 0.1 in. and 0.2 in. was selected for each specimen. The specimens were tested until failure or 4000 displacement cycles were reached. At least two tests were performed per connector type (1 test for the CIPST method), for a total of 10 tests.

4.4 Material Properties

4.4.1 Concrete

The concrete used for the test specimens was ordered from Capitol Aggregates in Austin, Texas (Mixture Design #261) and had a target 28 day compressive strength of 3,000 psi. Concrete strength was evaluated by cylinder tests at 7, 14, 21, and 28 days using the 6- x 12-in. cylinders. Average concrete strength was determined as 2960 psi at 28 days. The increase in average concrete strength within the first 28 days is shown in Figure 4.2. Additional cylinder

tests were performed regularly throughout the testing program. Further data on concrete strength is given in Kayir (2006).

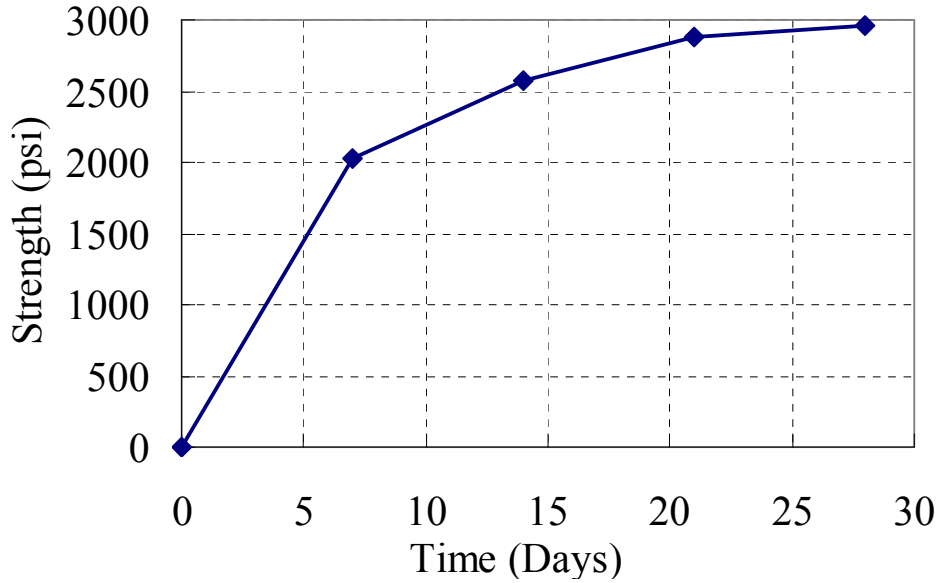

Figure 4.2: Average concrete compressive strength up to 28 days

4.4.2 Steel Plate

The 1-inch thick steel plates used for the test specimens were specified to be ASTM A36 steel. Based on the mill report provided, the steel had a yield strength of 48.1 ksi and an ultimate tensile strength of 71.9 ksi. The plates' dimensions were 6- x 1- x 40-in. To prevent bending of the steel plates during testing, 32-1/2 x 3- x 1/4-in. steel plates were welded on as stiffeners.

4.4.3 Grout

Five Star® Highway Patch was also used for POSST and DBLNB methods. The strength of the grout used in each specimen is provided in Kayir (2006).

4.4.4 Shear Connector Materials

Tests were conducted to determine the material strength properties of the shear connectors. Shear tests were conducted on the headed shear studs used for CIPST specimens and POSST specimens, the ASTM A193 B7 threaded rod used for DBLNB specimens, the Wedge-Bolt concrete screw used for WEDGB specimens, the standard ASTM A325 bolt used for HTFGB specimens, and the Hilti HAS-E threaded rod used for HASAA specimens. ASTM A193 B7 rod was used for DBLNB instead of SAE J429—Grade 8 tap bolt which was used in phase I single-shear connector tests. ASTM A193 B7 rod has rolled threads, which is believed to have better fatigue resistance than the SAE J429 – Grade 8 tap bolt with cut threads.

Individual anchors were tested in single shear using a customized bolt testing apparatus. Details about the test setup and procedures are presented in Kayir (2006). Table 4.2 presents the measured mean ultimate shear strength. Results are presented in terms of stress, by taking the measured shear force at failure and dividing by the area of the connector. For threaded rods, the

area was taken as 80% of the gross area of the connector as in *AISC LRFD Specification for Structural Steel Buildings* (2005). Also listed in Table 4.2 is the estimated ultimate tensile strength of the connector materials. The ultimate tensile strength was estimated by assuming that the shear strength of the material is equal to 60% of the tensile strength. It was also assumed that the net area in tension for threaded rods was 75% of the gross area. Finally, Table 4.2 also lists the minimum specified tensile strength for the connector materials. Observe that the actual strength of the connectors was significantly greater than the minimum specified values.

4.5 Test Results

This section summarizes the results from static, high-cycle fatigue, and low-cycle fatigue tests conducted on the CIPST and the post-installed shear connectors. The reported results include the load-slip behavior of connections under static loading, fatigue strength under high-cycle and low-cycle fatigue, and the failure modes of each specimen. Test results are discussed in greater detail in Kayir (2006).

Table 4.2: Experimental and theoretical ultimate shear strength of connectors

Connector Type	Measured Ultimate Shear Strength (ksi)	Estimated Ultimate Tensile Strength (ksi)	Minimum Specified Ultimate Tensile Strength (ksi)
CIPST & POSST	48.7	81.2	60
DBLNB	86.6	144.3	120
HTFGB	82.7	137.8	120
HASAA	70.1	116.8	72.5
WEDGB	100.6	167.7	145

4.5.1 Specimen Designation

Specimen designations start with applied connection method. It is followed by a two-digit number. For static and low-cycle fatigue tests, this number represents the sequence of the tests. The order of static tests starts from the static tests in the Phase I tests. For high-cycle fatigue tests, the number is the stress range based on the estimated shear area. The last two letters represent the applied loading type. Figure 4.3 describes the specimen designation system.

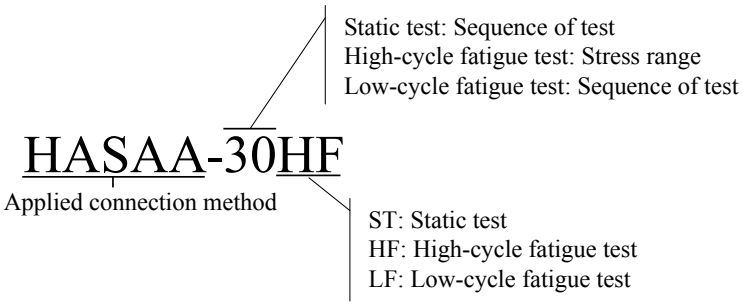

Figure 4.3: Specimen designation system

4.5.2 Static Test Results

In Phase II, one of each of the investigated shear-connection methods was tested under static loading. Load-slip curves for each specimen are shown in Figure 4.4 along with the average load-slip curve for CIPST specimens tested in Phase I. (CIPST-Average). The load-slip curve for Specimen 3MEPX-04ST with the Epoxy Plate method is not included in Figure 4.4. This specimen resisted 63.8 kips with essentially no slip, and then failed with no ductility.

The ultimate shear strength of the connectors ranged between 21.1 kips for the Specimen POSST-04ST and 63.8 kips for Specimen 3MEPX-04ST. Ultimate slip capacities of the connectors varied from 0.001 in. for Specimen 3MEPX-ST to 0.70 in. for Specimen WEDGB-S. Most failures occurred as a result of shearing of the connector at the steel-concrete interface, except Specimens WEDGB-04ST and HTFGB-04ST, for which failure occurred through the connector below the steel-concrete interface, and Specimen 3MEPX-04ST, which failed below the adhered surface of the concrete.

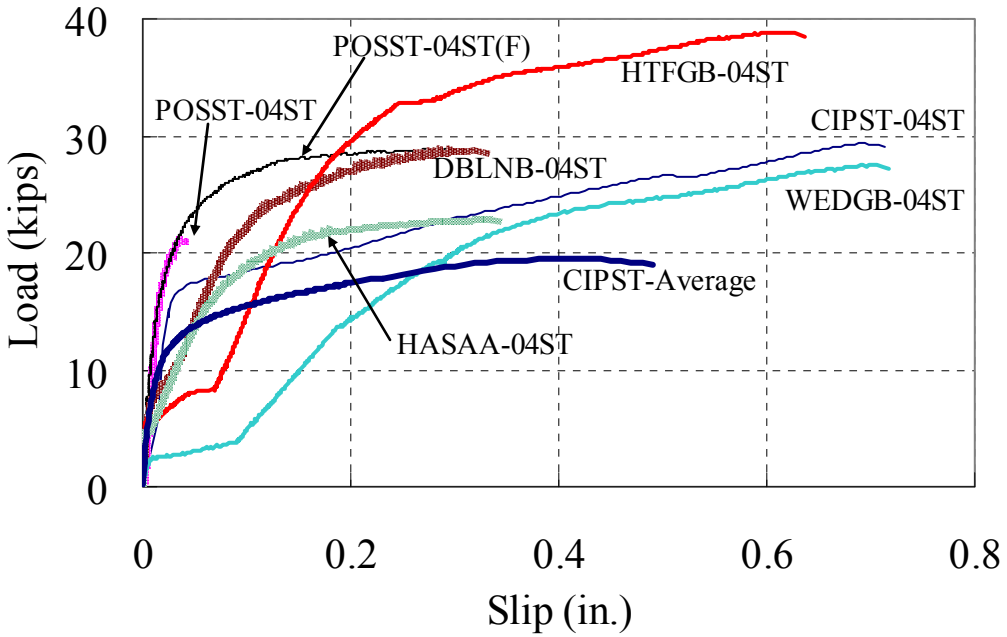

Figure 4.4: Load-slip curves for post-installed shear connectors

4.5.3 High-Cycle Fatigue Test Results

This section presents results from 20 high-cycle fatigue tests conducted at predetermined stress ranges for each shear connection method. Due to the brittle behavior exhibited by Specimen 3MEPX specimens, 3MEPX specimens were not tested in high-cycle fatigue and were excluded from further consideration.

Each high-cycle fatigue test started with an initial application of monotonic load followed by the application of load cycles until failure, as previously described in Section 4.2.3.2. Each specimen was tested either until failure occurred or until at least 5 million loading cycles was reached.

Test results are summarized in Figure 4.5. Specimens for which testing was stopped before connector failure are shown with arrows adjacent to the data points. Stress ranges were calculated based on the effective shear area of each connector at the steel-concrete interface. Figure 4.5 also shows the S-N curve adopted by AASHTO LRFD for welded stud shear connectors. The AASHTO S-N curve was based on the mean behavior of welded stud shear connectors under high-cycle fatigue loading from push-out tests. Slutter and Fisher (1966) report that push-out test results conservatively estimate the behavior of shear connectors, so push-out tests are assumed to represent a lower bound of shear connector failure in real beams.

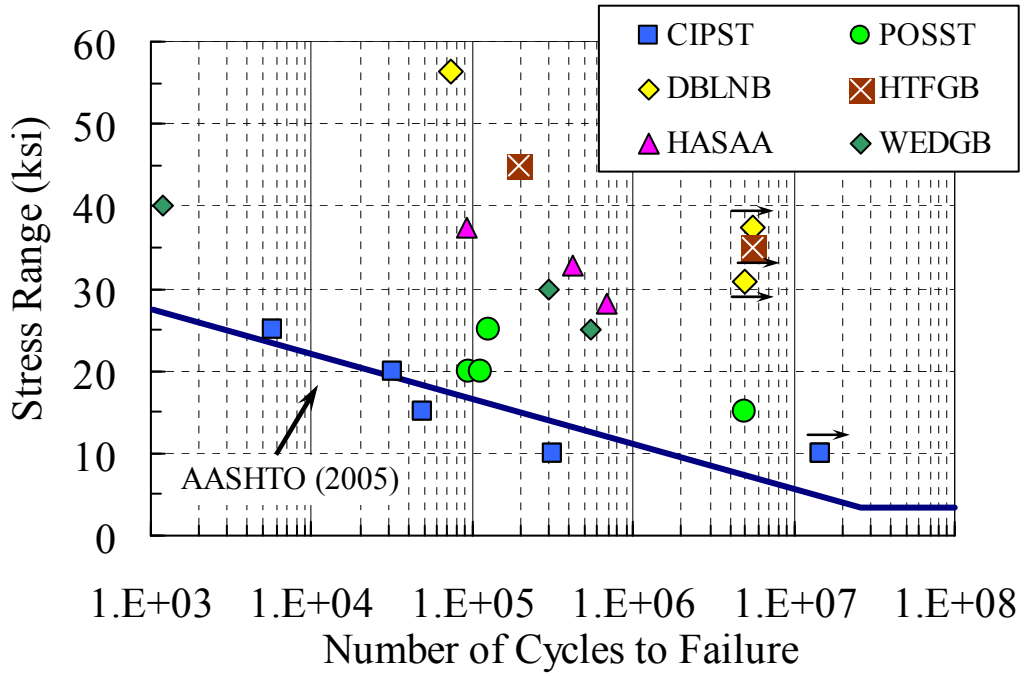

Figure 4.5: S-N data for test specimens

As shown in Figure 4.5, post-installed shear connectors generally shows better fatigue strength than the conventional CIPST connectors. HTFGB and DBLNB connectors show significantly higher fatigue strength than CIPST connectors. These two connectors appear to exhibit an endurance limit at about a 35 ksi stress range, whereas AASHTO LRFD defines the endurance limit of welded stud shear connectors as 3.5 ksi. POSST connectors which require welding for installation show less fatigue endurance than the other types of post-installed shear connectors which do not require welding. DBLNB connectors using a high strength rod (ASTM

A193 B7 rod) with rolled threads showed higher fatigue strength than HASAA connectors using a rod (HAS-E anchor) with cut threads. Specimens DBLNB-38HF and DBLNB-31HF were tested under static loading after the high-cycle fatigue tests. Specimen DBLNB-38HF reached an ultimate load of 29.0 kips, while Specimen DBLNB-31HF reached 29.4 kips.

Load-slip readings for connectors were recorded during the initial application of monotonic load and intermittently throughout high cyclic testing, to assess degradation in stiffness under high-cycle fatigue loading. The resulting load-slip curves showed increasing slip and decreasing stiffness with cycling for all connectors, with the changes varying with stress range and connection type. In Figure 4.6 are shown the static and cyclic load-slip curves for Specimen CIPST-25HF, representative of the general trend observed in the load-slip behavior of all investigated connectors.

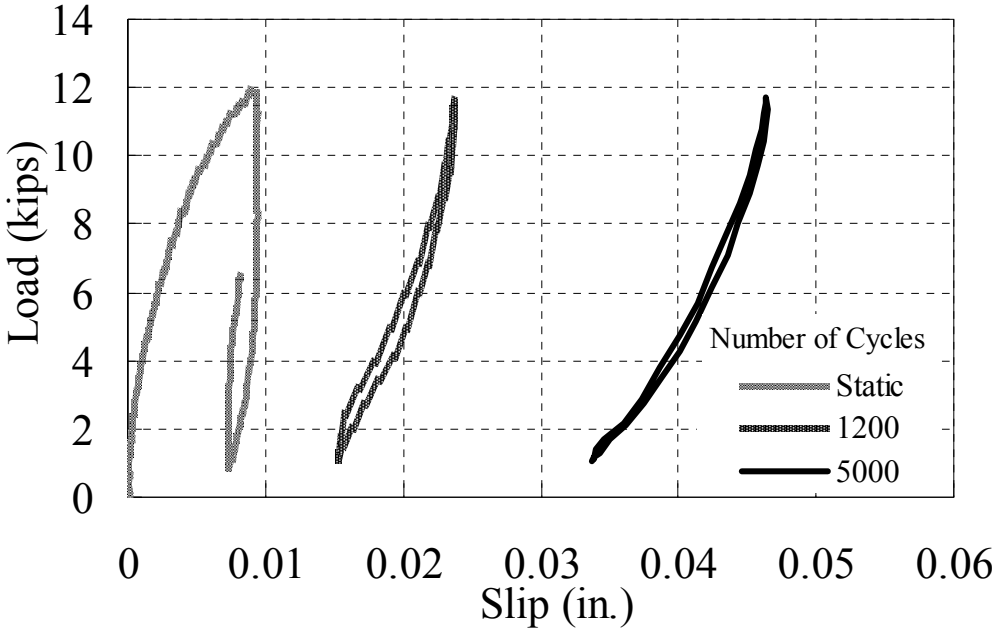

Figure 4.6: Static and cyclic load-slip curves for Specimen CIPST25

Failure modes of the single-shear connector test specimens under high-cycle fatigue loading were similar to those under static loading except Specimens DBLNB-56HF, HASAA-38HF, and HASAA-33HF. The failure plane of Specimen DBLNB-56HF corresponded to the level at which the second nut on the threaded rod ended (see Figure 4.7). Significant crushing of both the grout and concrete was observed in front of the connector. This may be attributed to the local crushing of concrete. This may have shifted the reaction on the connector below the steel-concrete interface resulting in the observed failure mode.

Figure 4.7: Failed Specimen DBLNB-56HF

Fatigue failure of Specimens HASAA-38HF and HASAA-33HF occurred at two locations through the connectors, above and below the steel-concrete interface. The failed Specimen HASAA-38HF is shown in Figure 4.8 and the failed connector is shown in Figure 4.9. This type of failure may be due to the presence of HY 150 adhesive in the hole in the steel plate. It is likely that the adhesive provided a restraint for part of the connector in the steel plate, preventing the slip of the connector within the hole. This possibly resulted in two reactions on the connector: below the steel-concrete interface (inside the concrete block) and above the steel-concrete interface (inside the steel plate). This may have caused stress concentrations at the reaction points, causing the connector to fail in double shear. Local crushing of concrete was also observed in front of the connector.

a)

b)

Figure 4.8: Failed Specimen HASAA-38HF: a) concrete block, b) steel plate

Figure 4.9: HAS-E anchor failed at two locations (Specimen HASAA40)

4.5.4 Low-Cycle Fatigue Test Results

Shear connection methods that performed well under high-cycle fatigue were tested under low-cycle fatigue. Specimens were tested cyclically under displacement control until either failure or 4,000 cycles was reached. As described previously in Section 4.3.3, a maximum displacement of 0.2 in. and a minimum displacement of 0.1 in. were applied to each specimen.

Table 4.3 summarizes the results obtained from the low-cycle fatigue tests. All post-installed shear connector specimens performed better than Specimen CIPST-01LF, which failed immediately upon the application of fatigue cycles. Failure occurred only in Specimen HTFGB-01LF, which had previously been subjected to 5.6 million cycles of fatigue loading under a 35 ksi stress range (HTFBG-35HF). Specimens that remained intact up to 4,000 cycles (5,000 cycles for HTFGB-02LF) were finally tested statically to failure. Results of these static tests are also given in Table 4.3. Figure 4.10 shows typical load–slip behavior under static load after 4,000 cycles of fatigue load. Residual slip due to the inelastic behavior during the low cycle loading was about 0.15 in. for the specimens under low-cycle loading.

Table 4.3: Summary of results for low-cycle fatigue tests

Specimen	Number of Cycles to Failure	Failed Component & Location	Residual Strength (kips)	Slip at failure (in.)
CIPST1	-	Weld roots	-	-
DBLNB1	>4000	No Failure	29.91	0.27
DBLNB2	>4000	No Failure	32.46	0.30
HTFGB1	1250	First roots of thread	-	-
HTFGB2	>5000	No Failure	18.01	0.77
HTFGB3	>4000	No Failure	37.45	1.00
HASAA1	>4000	No Failure	23.57	0.31
HASAA2	>4000	No Failure	21.83	0.30
WEDGB1	>4000	No Failure	28.38	0.73
WEDGB2	>4000	No Failure	27.83	1.00

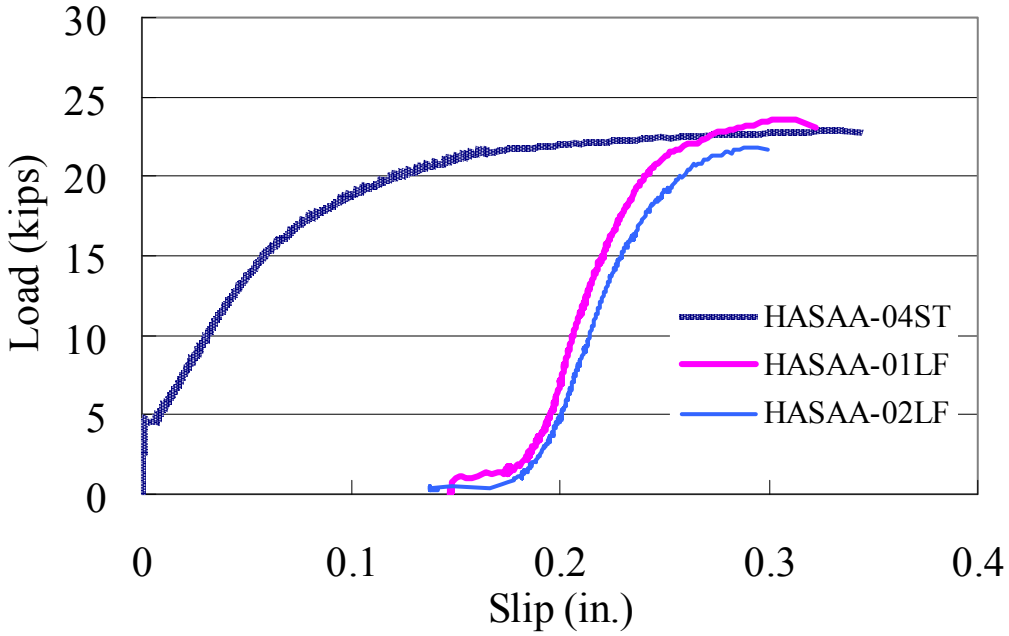

Figure 4.10: Load-slip behavior after low-cycle fatigue loading (HASAA)

The load sustained by the connector at each displacement cycle was recorded during each test, permitting the development of a load-time graph for each specimen. The load-time graph for Specimen DBLNB-01LF is shown in Figure 4.11 and is representative of the trend observed for each specimen. The graph indicates a considerable reduction in the load applied to the connector with each cycle to constant displacement amplitude. This load reduction is due to decreasing lateral stiffness of the connector as the concrete around the connector crushes. The decrease in applied load continues until a somewhat constant load is reached. Load reversal starts with the monotonic application of the displacement range and continues throughout the 4000 displacement cycles. This suggests that the connector behaves inelastically and endures loading in the opposite direction to achieve the required minimum displacement. Load reversal was not observed for the WEDGB specimens.

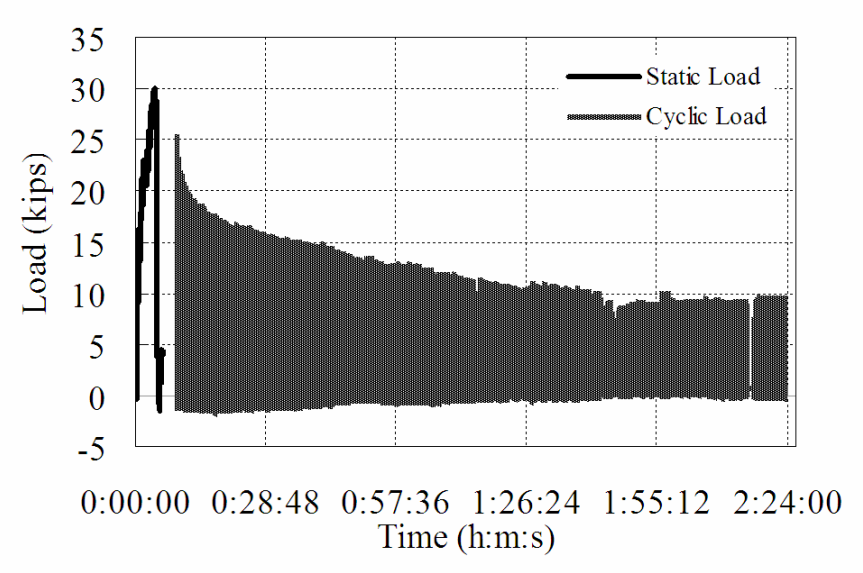

Figure 4.11: Change in load resisted by connector over time (Specimen DBLNB-01LF)

4.6 Discussion of Test Results

4.6.1 Static Tests

4.6.1.1 Load-Slip Behavior

Different shapes of load-slip curves can be observed for each specimen. Factors that contribute to the different load-slip behaviors include differences in the amount of pretension in each connector, the ductility of the connectors, and the stiffness, overall slip capacity, and ultimate shear strength of the connection.

The WEDGB and HTFGB specimens experienced at least twice as much overall slip as the other post-installed shear connectors. This may imply that connectors confined by either grout (POSST and DBLNB) or adhesive (HASAA), experience less overall slip than connectors that are less confined (WEDGB and HTFGB). This is a reasonable observation, since a more confined connector will not deform as much as a connector with less confinement. Also, a higher strength grout, adhesive, or concrete may limit the amount of deformation a connector experiences prior to failure. Thus, while providing high-strength concrete, grout, or adhesive around the anchor may increase the connector's strength and stiffness, it may also decrease its ductility.

Figure 4.12 shows the ultimate strength, the load at 0.2 in. of slip, and the ultimate slip capacity of each post-installed shear connector as a percent of the corresponding values obtained for CIPST connectors. These values are average values of four test specimens for each connection method except HASAA and DBLNB methods. Three test results were used for HASAA connection method and one test result was used for DBLNB connection method. Specimen HASAA-03ST showed uncommon behavior due to the overflow of excess HY 150 adhesive which cause bonding of the concrete and the steel plate. Specimen DBLNB-04ST used

ASTM A193 B7 threaded rod for its anchor material, whereas the other DBLNB specimens used SAE J429 – Grade 8 tap bolt. Thus, only Specimen DBLNB-04ST was compared with CIPST specimens for the connection method. For the POSST method, POSST-04ST(F) was used instead of POSST-04ST because of the premature failure of shear connector due to a weld defect.

As shown in Figure 4.12, post-installed shear connectors show higher ultimate strength than CIPST connectors except HASAA connectors. The HASAA method shows higher load at 0.2 in. of slip. However, most of post-installed shear connectors show less slip capacity than CIPST connector. This can be attributed to the use of high strength grout and high strength connector materials.

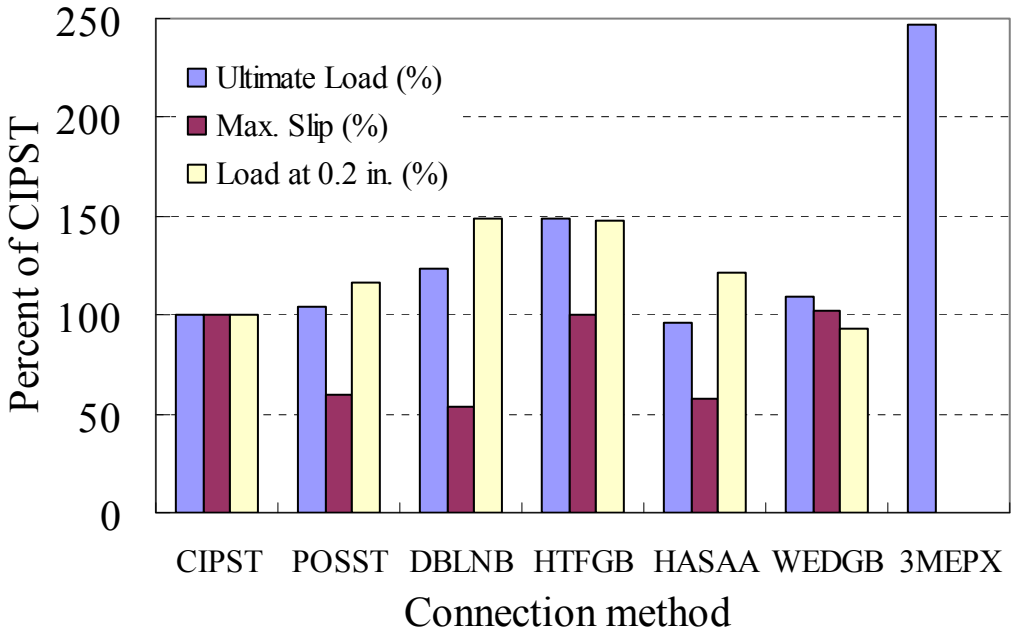

Figure 4.12: Comparison of load and ultimate slip capacity as a percentage of corresponding values for CIPST connectors

4.6.1.2 Predicting Ultimate Strength

Design equations for predicting the ultimate shear strength of cast-in-place and post-installed connectors are available in design codes and specifications as well as in the literature. In the following pages experimentally measured ultimate loads are compared to the capacities predicted by the above equations. The experimental values used in these comparisons include those obtained in this chapter and Chapter 3. Each experimental value is compared to a predicted value calculated from the above equations.

Tables 4.4 and 4.5 show comparisons for four different cases belonging to three different categories: equations governed by the strength of the concrete, equations governed by the strength of the connector steel, and equations governed by a combination of the strength of the both materials. The variable f'_{avg} was computed using a weighted average of measured values for f'_c (concrete compressive strength) and f'_g (grout compressive strength) based on the crushed zone in front of the connector, as described in Kayir (2006). Load ratios representing the quotient

of the experimental load divided by the predicted load also are given for each specimen. Load ratios less than 1.0 indicate that the predicted strength was higher than the experimentally measured ultimate strength (in other words, the predicted strength was unconservative). Load ratios for both tables are compared in Figure 4.13 and 4.14. Variables and corresponding values used in each equation are described in greater detail in Kayir (2006).

Loads ratios for Equation 2.2 are compared in Figure 4.13. The equation governed by the compressive strength of concrete conservatively underestimates the ultimate shear strength of almost all post-installed shear connectors except that of POSST specimens and Specimen DBLNB-04ST. Except for Specimen CIPST-01ST and Specimen CIPST-04ST, the ultimate load of all welded shear studs is overestimated.

Figure 4.14 shows a comparison of experimental and predicted ultimate strength values for Equation 2.3 proposed by Oehlers and Johnson (1987). This equation includes material properties of both concrete and connector steel for the prediction of ultimate strength of shear connectors. As indicated in Figure 4.14, ultimate load values predicted by Equation 2.3 are generally unconservative.

Figure 4.14 also presents comparisons of experimental and predicted values for the ultimate load of each specimen for Equation 2.4 and 2.5. Predicted values are calculated using equations that are governed by the ultimate strength of the connector steel. These equations are the ultimate tensile strength of steel ($A_s f_u$), which is used in Equation 2.4, and the ultimate shear strength of steel ($0.6 A_s f_u$), which is used in Equation 2.5. The ultimate tensile strength equation gives an unconservative estimate of the ultimate load for all specimens. The ultimate shear strength equation more conservatively estimates the ultimate load. However, it still results in unconservative results for many cases.

Based on those comparisons it appears that none of the existing equations conservatively predicts the experimentally observed ultimate load for all shear connectors tested in this current research. Variability in experimental data is also clearly apparent. As an alternative to the existing shear connector strength design equations discussed earlier, the following equation is proposed for estimating the shear strength of post-installed connectors for design purposes:

$$Q_u = 0.5\, A_s f_u \qquad \textit{(Eq. 4.1)}$$

This equation corresponds to one-half the ultimate tensile strength of the connector steel. Predicted ultimate load values and corresponding load ratios for this formula are presented in Table 4.6. Load ratios are compared in Figure 4.15, and it can be observed that the proposed equation provides a conservative estimate of ultimate shear strength for post-installed shear connectors, except the WEDGB connectors. For the DBLNB, HTFGB, and HASAA specimens, the predicted strength is 10 to 25 percent lower than the experimentally measured ultimate strength. This suggests that the proposed Equation 4.1 is not excessively conservative.

Table 4.4: Comparison of experimental and predicted values for ultimate load (Equations 2.2 and 2.3)

Specimen ID.	Test Result (kips)[a]	Eq. (2.2) (kips)[b]	Load Ratio (a/b)	Eq. (2.3) (kips)[c]	Load Ratio (a/c)
CIPST-01ST	24.3	22.5	1.08	-	-
CIPST-02ST	21.7	22.5	0.96	-	-
CIPST-03ST	17.8	22.5	0.79	-	-
CIPST-04ST	29.4	22.4	1.31	24.0	1.23
POSST-01ST	22.8	27.6	0.82	-	-
POSST-02ST	22.4	29.2	0.77	-	-
POSST-03ST	23.3	29.2	0.80	-	-
POSST-04ST(F)	28.8	35.9	0.80	38.2	0.75
DBLNB-01ST	31.1	18.8	1.66	-	-
DBLNB-02ST	30.6	18.8	1.63	-	-
DBLNB-03ST	28.4	18.8	1.51	-	-
DBLNB-04ST	28.9	35.7	0.81	46.3	0.62
HTFGB-01ST	30.7	23.2	1.32	-	-
HTFGB-02ST	34.3	23.2	1.48	-	-
HTFGB-03ST	33.5	23.2	1.45	-	-
HTFGB-04ST	38.8	24.1	1.61	35.7	1.09
HASAA-01ST	22.7	18.5	1.23	-	-
HASAA-02ST	21.8	18.5	1.18	-	-
HASAA-03ST	23.1	18.5	1.25	-	-
HASAA-04ST	22.9	19.6	1.17	26.0	0.88
WEDGB-01ST	23.0	20.9	1.10		
WEDGB-02ST	23.8	20.9	1.14		
WEDGB-03ST	27.6	20.9	1.32		
WEDGB-04ST	27.5	21.5	1.28	35.9	0.77

Table 4.5: Comparison of experimental and predicted values for ultimate load (Equations 2.4 and 2.5)

Specimen ID.	Test Result (kips)[a]	Eq. (2.4) (kips)[b]	Load Ratio (a/b)	Eq. (2.5) (kips)[c]	Load Ratio (a/c)
CIPST-04ST	29.4	35.9	0.82	21.5	1.37
POSST-04ST(F)	28.8	35.9	0.80	21.5	1.34
DBLNB-04ST	28.9	51.0	0.57	30.6	0.94
HTFGB-04ST	38.8	60.9	0.64	36.5	1.06
HASAA-04ST	22.9	41.3	0.55	24.8	0.92
WEDGB-04ST	27.5	64.6	0.43	38.7	0.71

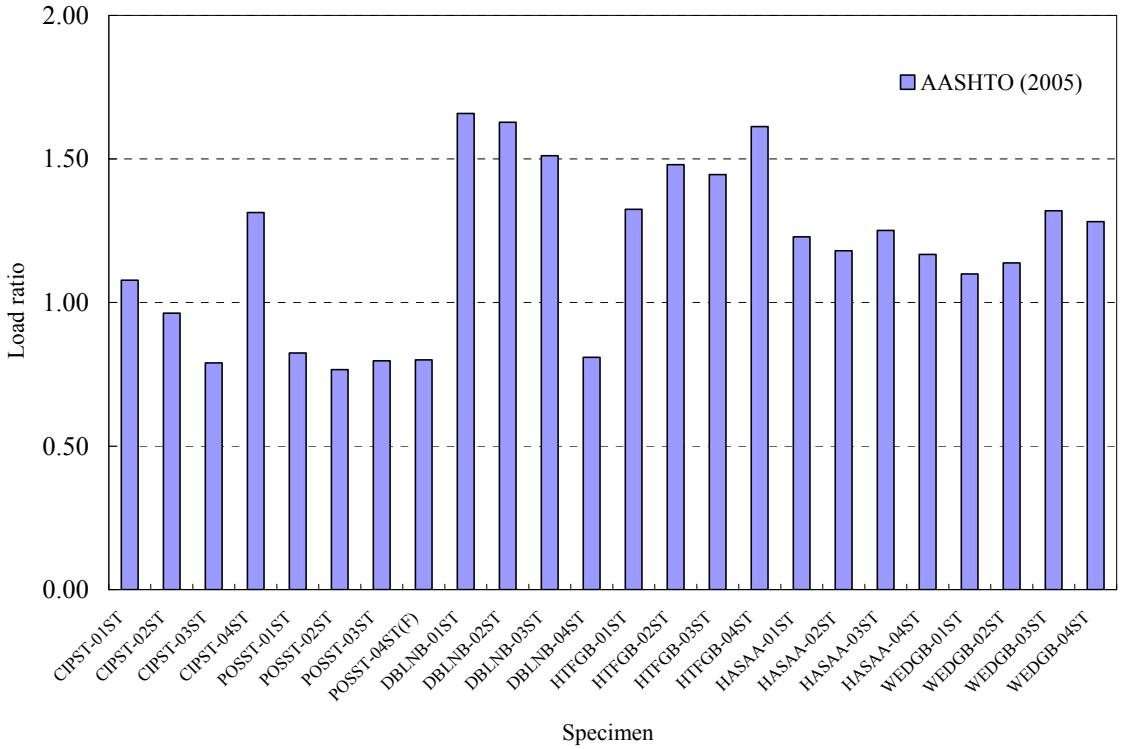

Figure 4.13: Comparison of load ratios

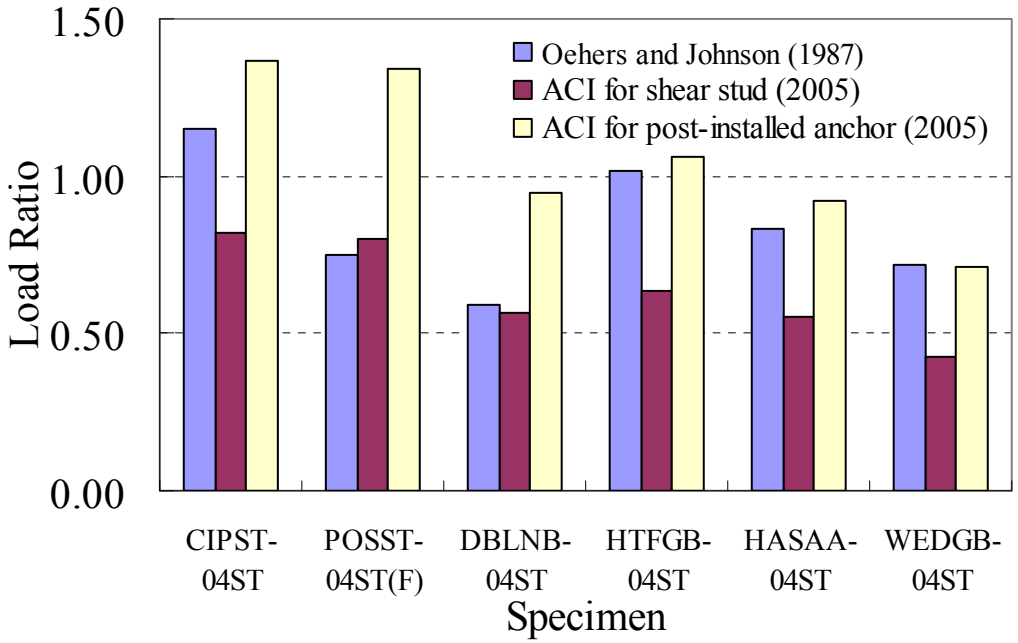

Figure 4.14: Comparison of load ratios

Table 4.6: Comparison of experimental and predicted values for ultimate load (Equation 4.1)

Specimen ID.	Test Result (kips)[a]	Eq. (4.1) (kips)[b]	Load Ratio (a/b)
CIPST-04ST	29.4	17.9	1.64
POSST-04ST(F)	28.8	17.9	1.61
DBLNB-04ST	28.9	25.5	1.13
HTFGB-04ST	38.8	30.4	1.27
HASAA-04ST	22.9	20.6	1.11
WEDGB-04ST	27.5	32.3	0.85

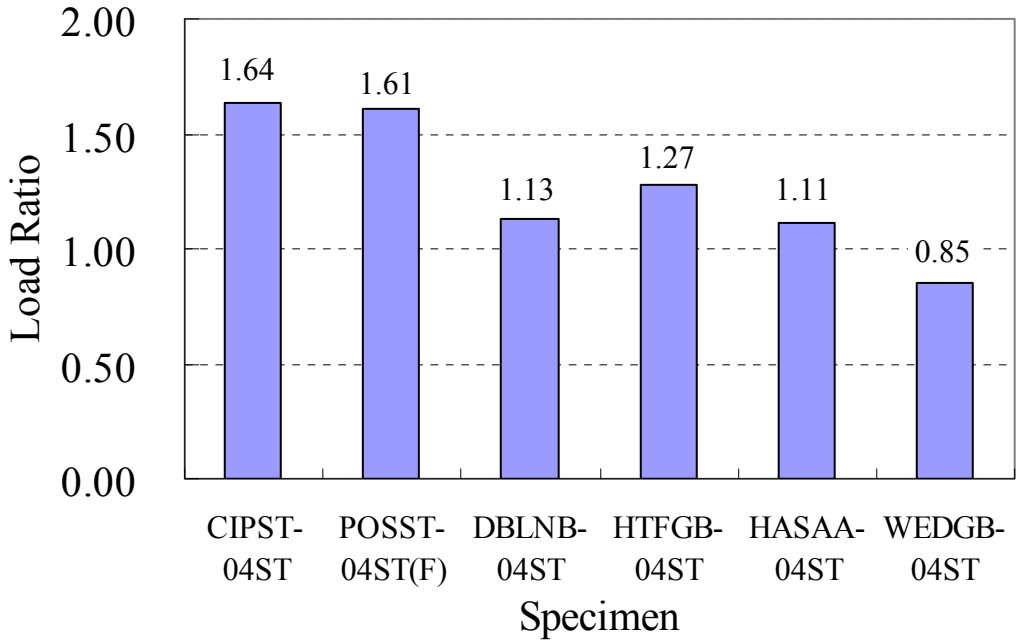

Figure 4.15: Comparison of load ratios (Equation 4.1)

4.6.2 High-Cycle Fatigue Tests

4.6.2.1 Comparison with Past Research

Among the seven shear connection methods, 3MEPX method was eliminated from further consideration under fatigue loading. Although this connection method exhibited the highest ultimate shear strength, it also had problematic aspects, including its brittle nature (essentially zero ductility), the potential difficulties and cost of construction, and concerns regarding its long-term durability.

In Figure 4.16, all data for the CIPST specimens are plotted with data from past fatigue tests conducted on push-out type specimens. Data from past tests published in the literature were previously presented in Chapter 2. The fatigue design curve in *AASHTO LRFD* is also shown in the figure as a benchmark for comparison with the fatigue data for post-installed shear connectors.

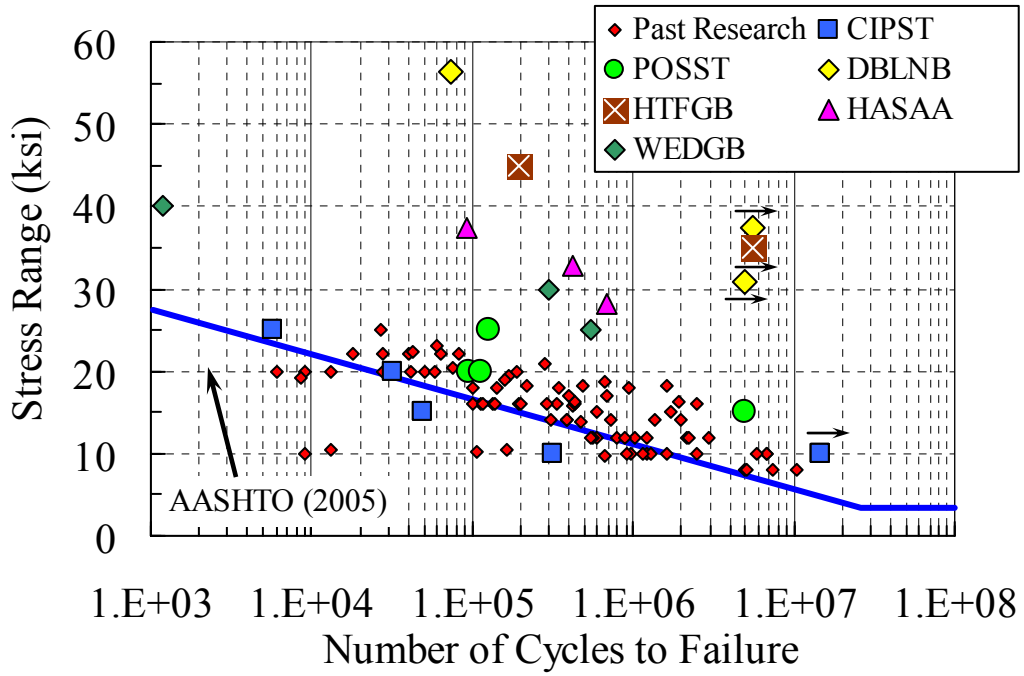

Figure 4.16: Comparison of S-N data from past research with current data

Data from the current fatigue tests for the cast-in place welded stud are generally similar to the data from past research. It is clear from Figure 4.16 that S-N data from past tests show considerable scatter. In general, data from the current tests fall within the overall scatter band of the data from past tests. Thus, even though the current tests were not conducted on push-out type specimens, the direct-shear single connector test setup used for the current tests gives fatigue results comparable to push-out type specimens.

Scatter in fatigue life is evident at every level of stress range in the past data. This scatter may be the result of many factors, including variability in material properties, variability in stud weld quality, and intrinsic variability in fatigue life. The presence of scatter suggests that many tests are needed to adequately characterize the fatigue behavior of shear connectors.

All specimens with post-installed shear connectors had improved fatigue life compared to the CIPST specimens. The superior fatigue performance of DBLNB and HTFGB specimens is readily apparent in this figure. Failure was achieved for DBLNB specimens only at a stress range 56 ksi. Specimen DBLNB-38HF and DBLNB-31HF did not fail and are shown as runnout specimens with arrows next to the corresponding data points. Specimen HTFGB-35HF did not fail after 5 million cycles of fatigue loading. .

4.6.2.2 Effect of Fatigue Loading on Subsequent Ultimate Strength

Several specimens with post-installed shear connectors did not fail under fatigue loading. To determine the effect of fatigue loading on ultimate strength, these runout specimens, after fatigue loading, were loaded statically to failure. In Table 4.7, ultimate strengths obtained from residual static tests (that is, static tests conducted after fatigue loading) are compared, along with the corresponding load ratios (residual ultimate load divided by ultimate load from initial static

test). The load ratios are all essentially unity, suggesting that the application of 5 million or more high-cycle fatigue cycles did not reduce the ultimate strength of the connectors.

Table 4.7: Comparison of static strength to residual strength for connectors previously subjected to fatigue loading

Specimen	Residual Ultimate Load (kips)	Ultimate Load from Initial Static Test (kips)	Load Ratio
POSST-15HF(F)	29.0	28.8	1.00
DBLNB-38	29.0	28.9	1.00
DBLNB-31	29.4	28.9	1.01

4.6.2.3 Predicting Fatigue Strength

AASHTO Specifications define fatigue endurance of stud shear connectors as a function of stress range. Slutter and Fisher (1996) report that concrete strength does not significantly affect fatigue endurance of stud shear connectors.

Due to the time and cost of high-cycle fatigue tests, only a limited number of post-installed shear connectors was tested under high-cycle fatigue loading. As discussed, because of the large scatter in fatigue test results, a significant number of shear connectors should be tested to understand the fatigue characteristics of shear connectors.

In this test program, post-installed shear connectors with high strength anchor materials showed superior fatigue endurance. Threads are in the plane of shear for DBLNB specimens. The threads of ASTM A193 B7 rods were rolled, not cut. Cut threads may potentially have a lower fatigue life. Based on the test results in Figure 4.16, Equation 4.2 is recommended for the fatigue endurance limit for HTFGB (ASTM A325 bolts with threaded not in the plane of shear) and DBLNB (ASTM A193 B7 threaded rods) connectors. This value appears to be endurance limits for those specimens under high-cycle fatigue loading.

$$Z_r = 35ksi \times A_s \qquad \textit{(Eq. 4.2)}$$

where Z_r is the allowable range of shear force on the connector, in kips; and A_s is the effective shear area of the connector, which can be estimated as 80% of the gross area of threaded connectors.

Due to the intrinsic scatter of fatigue test results, more tests would be desirable to better define fatigue endurance of other types of post-installed shear connectors under higher stress ranges.

4.6.3 Low-Cycle Fatigue Tests

As discussed in Chapter 2, loads applied to shear connectors beyond their elastic limit are best evaluated from a standpoint of imposed displacement. This approach takes the view that the demands placed on the shear connectors in a composite beam can be viewed as a displacement (slip) demand at the steel-concrete interface rather than as a shear force demand. Consequently,

the low-cycle fatigue tests were conducted by applying selected displacement cycles to the connectors, rather than applying load cycles, as was done in the high-cycle fatigue tests.

Fatigue failure was not obtained for specimens tested under low-cycle fatigue, except for Specimen HTFGB-01LF, which had been previously subjected to 5 million loading cycles in the high-cycle fatigue tests (HTFGB-35HF). Also, Specimen CIPST-01LF could not be properly tested under low-cycle fatigue due to a defective weld.

After 4,000 displacement cycles were applied, the residual static strength of each specimen was evaluated and the load-slip curves were captured. Values for ultimate strength and slip, and load at 0.2 in. of slip, are reported in Table 4.8. These values are compared to those obtained from initial static tests and the load and slip ratios are given (the residual static test value divided by the initial static test value). Load and slip ratios are compared in a bar chart form in Figure 4.17.

Table 4.8: Comparison of values obtained in residual static tests and initial static tests

Specimen	Residual Ultimate Load		Residual Ultimate Slip		Load at 0.2 in.	
	Exp. Load (kips)	Load Ratio	Exp. Slip (in.)	Slip Ratio	Exp. Load (kips)	Load Ratio
DBLNB-01LF	32.5	1.13	0.30	0.91	9.2	0.34
DBLNB-02LF	34.6	1.20	0.32	0.95	11.1	0.41
HTFGB-02LF	18.0	0.52	0.77	1.23	4.9	0.18
HTFGB-03LF	37.5	1.08	1.00	1.60	4.7	0.17
HASAA-01LF	23.6	1.05	0.32	0.89	6.9	0.31
HASAA-02LF	21.8	0.97	0.30	0.83	4.8	0.22
WEDGB-01LF	28.4	1.11	0.73	1.14	1.7	0.10
WEDGB-02LF	27.8	1.09	1.00	1.57	2.2	0.13

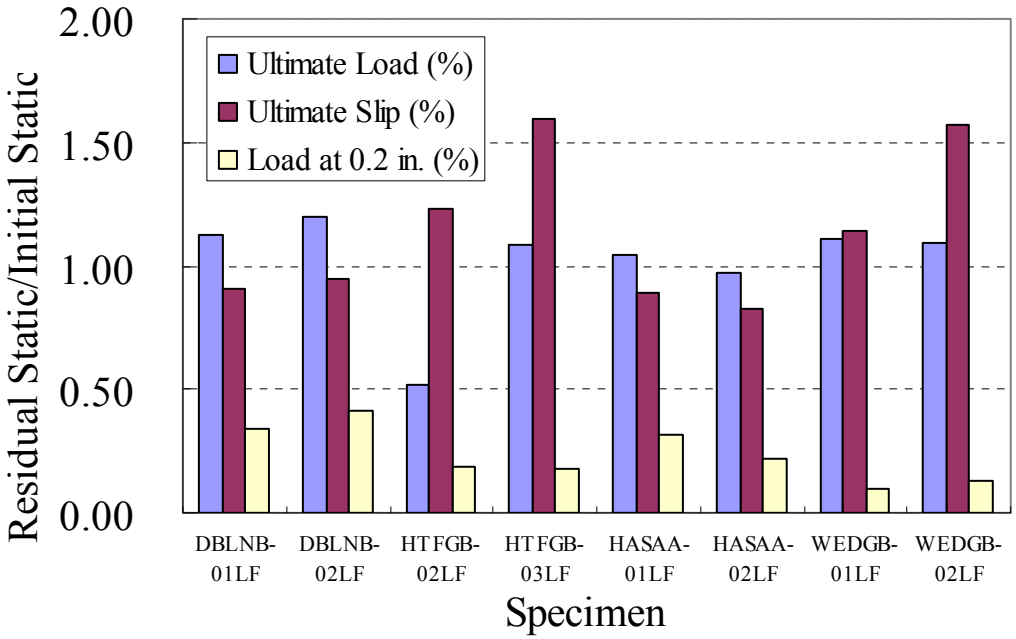

Figure 4.17: Ratios of residual to initial static load capacities

It can be seen in Figure 4.17 that the static capacities of the post-installed shear connectors were not significantly affected by low-cycle fatigue loading except Specimen HTFGB-02LF. In Specimen HTFGB-02LF, the connector failed inside the steel plate. It is considered that the first root of the threads is vulnerable to fatigue loading. This failure mode under fatigue loading was observed in Specimen HTFGB-45HF and all WEDGB specimens.

The ultimate slip experienced by each specimen is almost matched the values observed in initial static tests except Specimen HTFGB-03LF and Specimen WDEGB-02LF. These specimens showed a significant increase in ultimate slip. At a slip of 0.2 in., a significant decrease in load is apparent for all specimens. The slip of 0.2 in. coincides with the maximum displacement applied to each specimen during fatigue cycles.

It appears that a high number of displacement cycles had no significant effect on the ultimate strength of the shear connectors. Increasing damage of the concrete in front of the connector with each displacement cycle may have reduced the confinement around the connector, and, as the connector deformed inelastically, resulted in less load applied to the connector with each displacement cycle. As a result, the possibility of degradation in the connector material and a low-cycle fatigue failure could have been reduced.

4.6.4 Constructability and Cost Considerations

Thus far, the structural effectiveness of retrofit shear connectors has been evaluated and results from static and fatigue tests have been discussed. The objective of the single-shear connector tests, however, was not just to evaluate the structural performance of post-installed shear connectors, but also to evaluate the connectors from the perspective of constructability and cost. These issues are discussed in this section. This discussion is based primarily on experience gained with the connectors in constructing the test specimens, combined with consideration of how these experiences may be related to connector installation in an actual bridge. Six

connection methods are discussed for constructability and cost evaluation. Comparative connector costs and relative ease of installation are given in Table 4.9 for the connection methods discussed in this chapter.

The POSST method is the only retrofit method using a welded shear stud, and also the only method that can be installed completely from the top of a bridge. Static and fatigue tests, however, showed that the behavior of this connection depends heavily on the quality of the stud weld. This prompts the need for inspections of the weld quality in a field application. For welded studs in new construction, stud welds are typically inspected by a non-destructive "bend test" in which a number of shear studs are bent a specified amount. This technique is not easy to use for the POSST method, since no room is available to bend the stud inside a 3.5-in. diameter hole. Consequently, some other stud weld inspection technique would be needed, and it is unclear if another practical method is available.

Like the Post-Installed Welded Stud (and Stud Welded to Plate) method, the Double-Nut Bolt requires coring holes through the concrete slab. Unlike the Post-Installed Welded Stud, however, installation of this connector requires access from underneath the bridge as well as from the top. The smaller diameter hole (2-in.) used with the Double-Nut Bolt may require less time and effort to drill than the 3.5-in. core used with the Post-Installed Welded Stud.

The High-Tension, Friction Grip Bolt was found to be the hardest of all tested connectors to install in a laboratory setting. Drilling two different size holes was cumbersome in the laboratory, and could be even more difficult on a real bridge. This method also requires access both from the top and the bottom of the slab.

The Adhesive Anchor was found to be one of the easiest connectors to install in a laboratory setting. This connector can be installed in a bridge with minimal damage to the concrete slab from under the bridge. The only drawback of the installation process is the time needed for the adhesive to cure. For a 68 $^{\circ}F$ temperature a 50 min. curing time is required for the adhesive used in the tests. During this time the adhesive should not be disturbed, which may require traffic to be stopped on a bridge.

The Concrete Screw was the easiest connector to install. This one-piece screw requires drilling only from the bottom of the bridge. The concrete screw can be easily installed while the bridge is in service; it requires no grout or adhesive and can resist load immediately after installation.

The Epoxy Plate method has several installation disadvantages. First, a long curing time of 7 days is required for the epoxy used in the tests. During this time, it may be necessary to restrict traffic on the bridge. Second, the epoxy is brittle, which means no slip can be observed between the steel girder and concrete deck prior to failure. This would require high safety factors to be used in design. Finally, the effects of weathering and extreme temperature on epoxy durability are also unknown for this type of application.

Costs listed in Table 4.9 include materials (connectors, grout and adhesive as applicable), but do not include labor costs, as little information was available on actual labor requirements for each method. The comparative cost analysis was performed assuming 300 connectors (the number required for a 50-ft long span with six girders, with rows of two connectors, spaced longitudinally at 2 ft.). Costs are normalized to the cost of the cast-in-place, welded headed studs. Costs for 3MEPX method were estimated assuming that the adhered area was approximately equal to that of two cast-in-place welded studs spaced at 2 ft, with an additional safety factor of about 1.5 due to the brittle failure of the connection. No other connection

methods were so adjusted for relative strength or failure mode. Cost evaluation results are listed in Table 4.9.

Table 4.9: Normalized material costs of connection methods

Connection Method Designation	Relative Ease of Installation	Normalized Material Cost
CIPST	Easy	1.0
POSST	Easy	3.1
DBLNB	Medium	11.9
HTFGB	Hard	3.9
HASAA	Easy	10.5
WEDGB	Easy	3.3
3MEPX	Medium	45.2

4.6.5 Selection of Post-Installed Shear Connectors for Full-Scale Beam Tests

The next stage of the overall research program was to conduct full-scale tests on composite beams retrofitted with post-installed shear connectors. Because only a small number of large-scale tests could be conducted, only a limited number of post-installed shear connectors could be evaluated in these tests. Two types of post-installed shear connection methods, the HASAA and DBLNB connection methods, were selected for full-scale beam tests based on evaluations of the structural performance, cost, and constructability of post-installed shear connectors.

The Double-Nut Bolt (DBLNB) was selected for full-scale beam tests, because it has higher strength at early slip than the cast-in-place welded stud, comparable ultimate strength, and superior high-cycle and low-cycle fatigue life. The Double-Nut Bolt has the longest high-cycle fatigue life of all connectors investigated in this study. Constructability issues discussed for the Post-Installed Welded Stud also apply to the Double-Nut bolt. For the Double-Nut Bolt, however, a smaller diameter hole through the slab and less grout is required, which makes this method more constructible.

Static tests on the Adhesive Anchor (HASAA) showed higher static strength and less ultimate slip capacity than the cast-in-place welded stud. Specimens tested under high and low-cycle tests showed better fatigue performance, as well. This anchor is easy to install from under the bridge and its installation is minimally destructive to the concrete slab. Except for the time needed for the adhesive to cure, fast installation with minimum traffic disruption is possible. Due to its satisfactory structural performance, easy construction, and reasonable cost, the Adhesive Anchor was selected for full-scale beam tests. In high-cycle fatigue, however, HASAA connectors had lower fatigue strength than DBLNB connectors. More tests are required to understand fatigue characteristics of the HAE-S anchor enough to apply the connection methods to real bridges. As mentioned in Section 4.6.2.3, fatigue endurance of shear connectors are not significantly influenced by confined concrete. Therefore, it was decided to use ASTM A193 B7 threaded rod for HASAA connectors for full-scale beam tests. ASTM A193 B7 threaded rod was

used for DBLNB connectors and its fatigue endurance is better understood and design recommendation in Equation 4.6 can be used for the rod.

Chapter 5. Full-Scale Beam Tests

5.1 Introduction

In the previous chapters, several types of post-installed shear connectors were tested under static, high-cycle fatigue, and low-cycle fatigue loading using the direct shear test setup. Based on the test results, two types of shear connectors were recommended for further evaluation in full-scale beam tests: the double nut bolt (DBLNB) and the adhesive anchor (HASAA). Two full-scale partially composite beams retrofitted with DBLNB and HASAA connectors were tested under static loading. One non-composite beam was also tested as a benchmark to compare the structural performance of retrofitted partially composite beams with existing non-composite beams.

The selected post-installed shear connectors were installed using procedures which could be used in an actual field application. Thus, constructability issues for the connection methods could also be evaluated during the construction of the specimens in the laboratory.

5.2 Test Program

5.2.1 Test Specimens

Three full-scale specimens consisting of a steel beam and concrete slab were constructed and tested. Specimens were designed based on the configurations of potential prototype bridges examined as described in Chapter 3. The specimen name starts with the connection method, as in the single shear tests. It is followed by the composite ratio in percentage. For the full-scale beam test specimens, the specimen name ends with "BS" which stands for Beam Static test. The beam specimens were each a 38-ft long, simply supported span, with a point load applied at mid-span.

5.2.1.1 Non-Composite Beam (NON-00BS)

The non-composite steel girder and concrete slab beam which simulates existing bridge girders is a simply supported beam with a 38ft long span. A W30x99 section was used for the steel beam and the concrete slab was 84-in. wide and 7-in. deep as shown in Figure 5.1. For the steel girder, ASTM A992 steel was used instead of ASTM A36 steel which was typically used for the existing bridge girders, since ASTM A36 steel was no longer available in wide-flange shapes. ASTM A992 steel has a specified yield stress between 50 to 65 ksi and a minimum tensile strength 65 ksi. To simulate the prototype bridge, #4 and #5 Gr. 60 rebars were placed with 6 in. spacing in the transverse direction. In the longitudinal direction, #4 bars were placed with 12 in. spacing (see Figures 5.1 and 5.2). These reinforcement details were recommended by a project advisor at TxDOT. Web stiffeners were welded at the center and both ends of the specimen to prevent local failures at the load and support points.

Concrete formwork was hung on the steel beam flanges to simulate unshored construction, as shown in Figure 5.3. Before building rebar cages on the formwork, the top of the formwork was cleaned and coated with form oil. The concrete slab was cast with ready-mix concrete using a 1-cubic yard bucket. The concrete was vibrated and screeded. The 6- x 12-in. concrete cylinders were made for concrete cylinder tests, and the concrete cylinders were placed

by the test specimen to be cured in the same environment with the test specimens. After casting, the exposed surface of the concrete was covered with plastic sheets for 5 days under moist conditions. The concrete formwork was removed from the specimen 7 days after the casting, and reused for the other specimens.

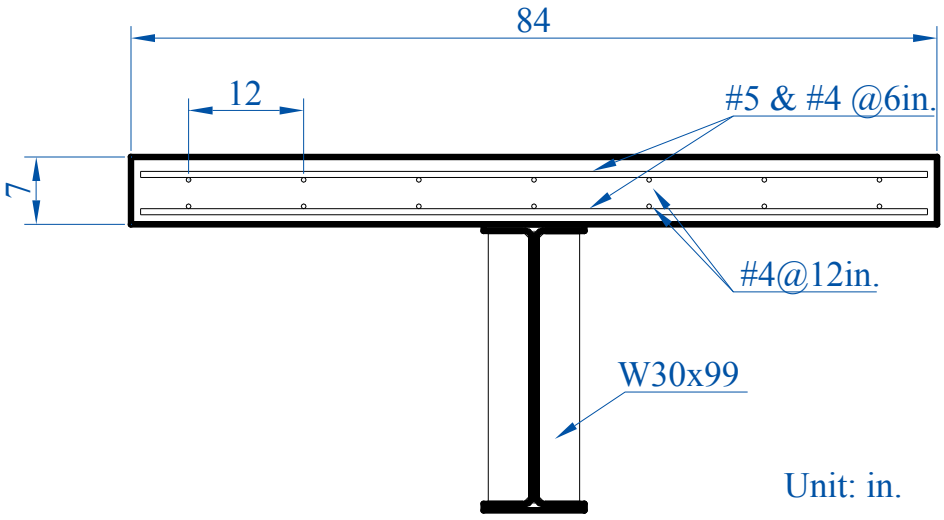

Figure 5.1: Details of specimen cross-section

Figure 5.2: Reinforcement layout

Figure 5.3: Concrete formwork

5.2.1.2 Design of Partially Composite Specimens (DBLNB-30BS, HASAA-30BS)

The two specimens constructed using post-installed shear connectors were both designed as partially composite. Figure 5.4 shows the computed load-carrying capacity of the test specimens with respect to their composite ratio. These strength values were calculated using minimum specified concrete strength (f'_c = 3000 psi) and the minimum specified strength of the steel (f_y = 50 ksi). The contribution of the longitudinal reinforcing bars was neglected in the strength calculation. The minimum specified tensile strength of ASTM 193 B7 threaded rod, used for both the DBLNB and HASSAA post-installed shear connectors, is 125ksi. For the full-scale beam tests, 7/8 in. diameter threaded rod was used for the connectors to reduce the number of shear connectors installed. Based on Equation 4.1, the shear capacity of each connector is 30.1 kips, and this value was used in the beam strength calculations plotted in Figure 5.4.

Ultimate strength of the partially composite beam was calculated using simple plastic analysis, as described in Chapter 2. Based on these calculations, the non-composite beam has a capacity of 137 kips. The fully-composite beam has a strength of 236 kips, approximately 70% greater than the non-composite beam. As shown in Figure 5.4, partially composite beams also show a significant increase in ultimate strength compared to the non-composite case, even with low values of composite ratio. Based on this analysis, it was decided to design the two partially composite beam specimens with a 30% composite ratio. Even with only a 30% composite ratio, a 47% increase in ultimate load-carrying capacity is predicted compared to the non-composite beam. To achieve a 30% composite ratio, 16 shear connectors for each shear span, or a total 32 shear connectors are required. The shear strength of each shear connector was determined using Equation 4.1. The effective shear area was taken 80% of unthreaded gross area. That is, the

connector shear strength was computed as $0.5A_s f_u$, where f_u is 125 ksi, and A_s is 0.48 in^2. This results is 30.1 kips per shear connector.

Also, the specimens were tested only under static load; fatigue strength of the shear connectors was checked with Equation 2.4 and Equation 4.2. Fatigue load was calculated with the design truck described in *AASHTO LRFD* with a spacing of 30 ft between 32-kip axles. Under this truck load, the maximum shear force sustained by the shear connectors is 164.4 kips. Therefore, each shear connectors in one shear span sustains 10.27 kips. Since the diameter of the shear connectors is 7/8 in., stress range in each shear connector is 21.36 ksi (= 10.27 kips / 0.48 in^2), which satisfies Equation 4.2.

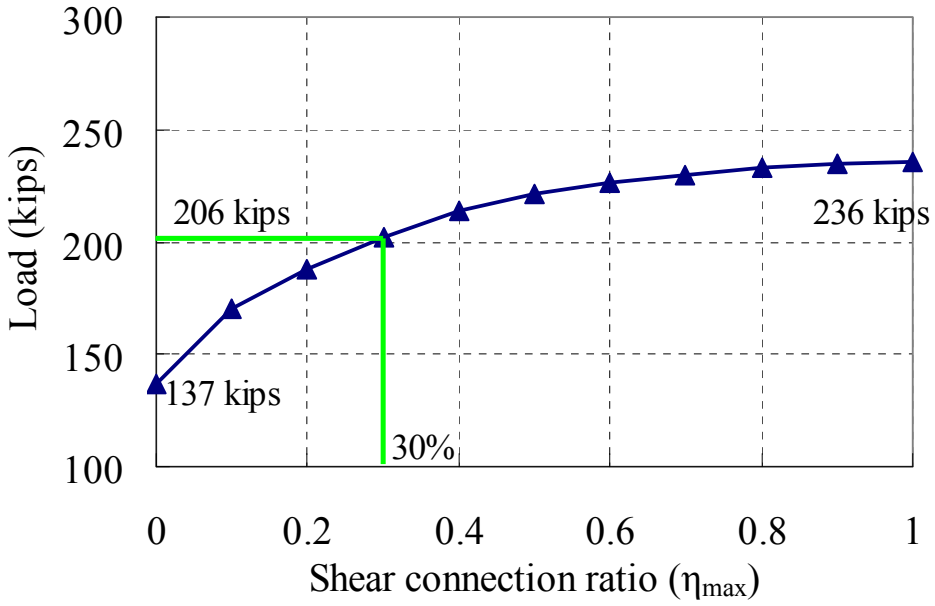

Figure 5.4: Predicted load capacity of test specimens versus shear connection ration (based on minimum specified material properties)

5.2.1.3 Installation of Post-Installed Shear Connectors (DBLNB-30BS, HASAA-30BS)

Installation of the post-installed shear connectors in the full-scale beam specimens was different from installation of the connectors in the individual small blocks used in the single connector tests described in Chapters 3 and 4. Both of the methods used for the full-scale composite beam specimens required access underneath the beam. For the HASAA connection method, holes needed to be drilled from the bottom of the beam top flange and into the concrete slab.

5.2.1.3.1 Installation of Shear Connectors for Specimen DBLNB-30BS

Installation of the DBLNB connectors required access from both the top and the bottom of the slab. Drilling through both the concrete slab and the steel beam flange was completed from the top and tightening of the connector was done underneath the slab using an impact wrench to reach required pretension in the connector. Following is the procedure used to install the DBLNB shear connectors.

1) A 2.5-in. diameter hole was drilled into the concrete slab from the top using a Hilti DD200 coring machine. A DD-BL U4 diamond core bit was used for the coring operation (see Figure 5.5). This core bit is designed for coring a wide range of concrete and medium steel reinforcing. A constant water supply is needed to keep the drill bit cool. It took 5 to 10 minutes to complete each hole through the concrete slab.

2) A 15/16-in. diameter hole was drilled through the steel beam top flange from the top side of the slab using a portable magnetic drill. A 10 in. long drill bit was used to the drill holes from the top of the slab. A hollow round bar was placed inside of the cored hole in the concrete to serve as a guide for the steel drill bit. This guide also helped to keep the inside surface of the concrete clean from machine oil (see Figure 5.6). To fix the coring machine and the magnetic drill to the concrete slab surface, a 1 in. thick steel plate was anchored to the concrete slab using four concrete anchors.

3) A 7.25-in long ASTM A193 B7 rod was placed from the top to provide a 5-in. embedment length. Figure 5.7 shows the concrete surface after drilling. The connector was tightened to a pretension of 39 kips using an impact wrench. "Squirter" Direct Tension Indicating (SDTI) washers were used to confirm the required pretension as shown in Figure 5.8. This washer has several bumps on the surface. Under this bump, orange-color silicone is embedded. As a bolt is tightened, the silicone material comes out and gives a visual indication of bolt tension. This washer first tested using the Skidmore-Wilhelm Bolt-Tension Calibrator and checked to determine the amount of silicone coming out to achieve the specified pretension.

4) Grout was poured to fill the gap. Five Star® Highway Patch was used for the grout materials. Five Star® Highway Patch is fast setting, high strength grout which is used for repair of highways and bridges.

Figure 5.5: Coring and drilling into the specimen

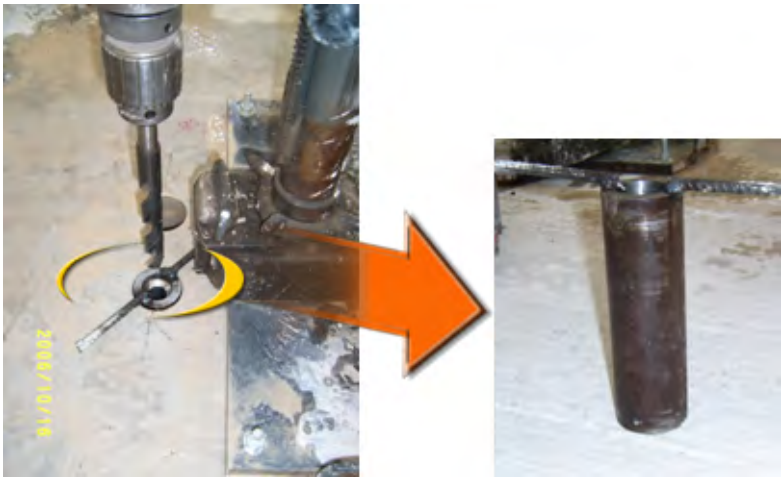

Figure 5.6: Drilling through beam flange

Figure 5.7: Drilled holes for DBLNB installation

Figure 5.8: Use of "Squirter" Direct Tension Indicating (SDTI) washer

5.2.1.3.2 Installation of Shear Connectors for Specimen HASAA-30BS

The same 7/8-in. diameter ASTM A193 B7 threaded rods used for the DBLNB-30BS specimen were also used for the HASAA shear connectors in specimen HASAA-30BS. Following is the procedure used to install the HASAA shear connectors.

1) A 15/16-in. diameter hole was drilled through the steel flange from the bottom of the slab. A portable slugger drill with magnetic base was used to drill the hole (see Figure 5.9a).

2) A 5-in. deep hole was drilled into the concrete from the bottom using a 7/8-in. drill bit and a Hilti TE-55 rotary hammer drill as shown in Figure 5.9b. The 15/16-in. diameter holes are required to install HASAA shear connectors according to the installation manual provided by Hilti (Hilti 2006). A 15/16-in. diameter carbide-tipped drill bit did not fit into the 15/16-in. diameter hole through the steel beam flange. Therefore, a 7/8-in. diameter drill bit was used to drill the hole in the concrete and worked to make the hole larger.

3) The drilled hole was cleaned using a wire brush and compressed air before injecting adhesive.

4) Hilti HIT HY 150 adhesive was injected in the hole using the HIT-MD 2000 manual dispenser. Eight to nine holes can be completed with an 11.1-fluid ounce cartridge pack. The adhesive was viscous enough not to run down during the upward application.

5) An anchor rod was inserted with a twisting motion. The rod can be adjusted during the specified gel time, but should not be disturbed between the gel time and cure time. The gel time and the cure time are 6 min. and 50 min. at 68° F. Adhesive that overflowed was wiped off, leaving adhesive filling the gap between the oversized hole in the steel flange and the anchor. The hole in the concrete slab was not perfectly vertical, so the rod was self-braced and was not required to be held during the cure time to prevent from falling.

6) After the gel time, the rod was fastened with specified torque (125 lb-ft) using a torque wrench.

a) Drilling through the steel flange

b) Drilling into the concrete

c) Injecting adhesive

d) Tightening with torque wrench

Figure 5.9: Installation of HASAA shear connectors

5.2.2 Material Properties

5.2.2.1 Concrete and Grout

Concrete for the full-scale tests was delivered in a ready-mix truck from Capitol Aggregates in Austin, Texas (Mixture Design #308). The design compressive strength was 3,000 psi with 3/4 in. river aggregate. Concrete slump tests were performed for each test specimen before casting concrete. Current TxDOT Specifications requires 4 in. ± 1 in. slump for concrete for a bridge slab. The 3,000 psi concrete compressive strength was required for the test program to simulate older existing bridges, so that concrete with higher slump was accepted.

Concrete cylinders were cured in the same environment with the test specimens. The design strength of the concrete slabs was 3,000 psi, but the compressive strength of the concrete for Specimen NON-00BS was over 6,000 psi on the day of testing. However, it was considered that this did not significantly affect the test results for this non-composite specimen, because the contribution of concrete slab to the total flexural strength for the non-composite beams is less than 5%. The concrete slump test and the compressive test results for each test specimens are listed in Table 5.1.

Five Star® Highway Patch was used to fill the gap in the slab after installation of DBLNB shear connectors. This is a fast setting high strength grout. The manufacture specifies that roads can be opened to traffic 2 hours after application due to its high early strength. Its specified compressive strength at 2 hours is 2,000 psi. Its measured compressive strength was 5,800 psi at 2 days, 7,000 psi at 7 days, and 7570 psi on the test day for Specimen DBLNB-30BS.

Table 5.1: Concrete slump and compressive strength

Specimen	Slump (in.)	Compressive strength (f_c', psi.)	
		28 days	Test day
NON-00BS	3	5,190	6,250
DBLNB-00BS	7	3,560	3,680
HASAA-00BS	4	3,500	3,610

5.2.2.2 Steel Beams and Reinforcing Bars

The steel beams used for the full-scale tests were produced by Nucor-Yamato Steel Company. The three beams were from the same heat of steel and steel coupons were taken from one test specimen. Four steel coupons were taken, two from the beam web and two from the beam flange.

The Grade 60 reinforced bars used in the specimens has a minimum yield stress of 60ksi and a minimum ultimate tensile strength 90ksi. Tension tests were conducted on the #4 longitudinal reinforcing bars.

Three static yield stresses were measured in the yield plateau and averaged to determine the yield stress for both the steel girder coupons and the reinforcing bars. Test results are shown in Table 5.2 and 5.3.

Table 5.2: Steel coupon test results

Section	Static yield stress (f_y, ksi)	Ultimate strength (f_u, ksi)	Elongation (%)
Flange	56.9	77.4	38
Web	60.9	78.6	36

Table 5.3: Reinforcing bar test results

Specimen	Static yield stress (f_y , ksi)	Ultimate strength (f_u , ksi)	Elongation (%)
NON-00B	61.6	103.5	35
DBLNB-30B	61.6	103.5	35
HASAA-30B	57.6	99.2	37

5.2.2.3 Shear Connectors

ASTM A193 B7 threaded rod has a minimum specified yield stress 105 ksi and minimum ultimate tensile strength 125 ksi. All of shear connectors for the composite beam tests were cut from rods from the same production lot. The threaded rods were tested in shear and tension using a customized bolt testing apparatuses. Figure 5.10 shows sections of threaded roads after the tests.

Only the ultimate strengths for shear and tension were determined from the tests. The measured ultimate shear and tensile strength for the threaded rod were 91.1 ksi and 147 ksi. Note that the measured shear strength of the rod is 62% of the measured tensile strength.

a) Failure sections in shear *b) Failure section in tension*

Figure 5.10: ASTM A193 B7 rods after shear and tension tests

5.2.3 Test Setup

5.2.3.1 Details of Test Setup

The specimens were each a 38-ft long, simply supported span, with a point load applied at mid-span. The test setup is shown in Figure 5.11. A roller support was provided at one end of the beam and hinge support at the other end. Bracing was provided at each end of the beam to prevent the concrete slab from overturning due to the possibility of small eccentricities in the loading. These braces were attached in manner so that they do not restrain longitudinal movement of the concrete slab.

Two 100-ton capacity hydraulic rams were used to apply a concentrated load at the mid-span of the specimen. A load cell was placed at the loading point and measured the load applied by these hydraulic rams. To prevent lateral torsional buckling of the beam during concrete casting and to provide for safety during testing of the specimen, lateral bracing was placed at the center of the beam. Teflon sheets were used at the interface of the bracing and the steel beam to minimize frictional forces. For Specimen Non-00BS (non-composite specimen), four shear studs were installed on the beam flange at the center of the beam, to help maintain safety of the setup during testing. Since they are at located at the center of the beam, little or no composite action is expected to be developed as a result of these studs. To easily detect yielding of the steel beam, whitewash was painted around the center of the steel beam.

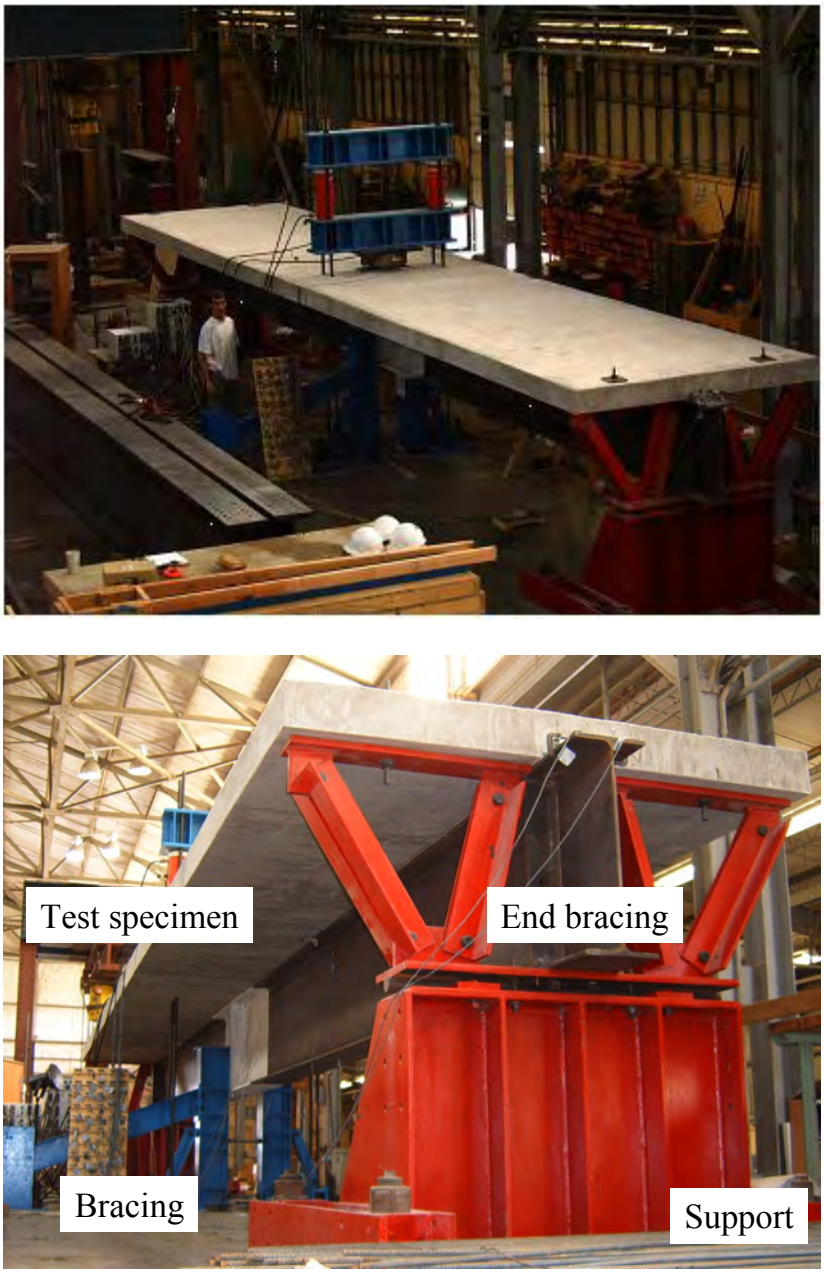

Figure 5.11: Test setup

5.2.3.2 Instrumentation

Vertical deflection, slip between the concrete slab and the steel beam flange, and longitudinal strain in both the steel beam and reinforcing bars in the concrete slab were measured during the test. Two string potentiometers at the center of the beam and one at each quarter point of the beam were installed to measure vertical deflection during the tests. Slip at the interface between the concrete slab and the steel beam were also measured at the center and quarter points of the beam. Figure 5.12 shows two linear potentiometers at the one end of the beam for measuring slip. Strain gages were used to measure longitudinal strain of the composite beam at

the center and 6 in. from the center. The location of the strain gages at a beam cross-section is shown in Figure 5.13.

Loading was applied by two 100-ton capacity hydraulic rams which were operated using a 10,000-psi capacity pneumatically driven oil pump. Test data were read every at 5 kip loading intervals in the elastic range. When the test specimen yielded, data were read at increments of 0.25-in. center deflection.

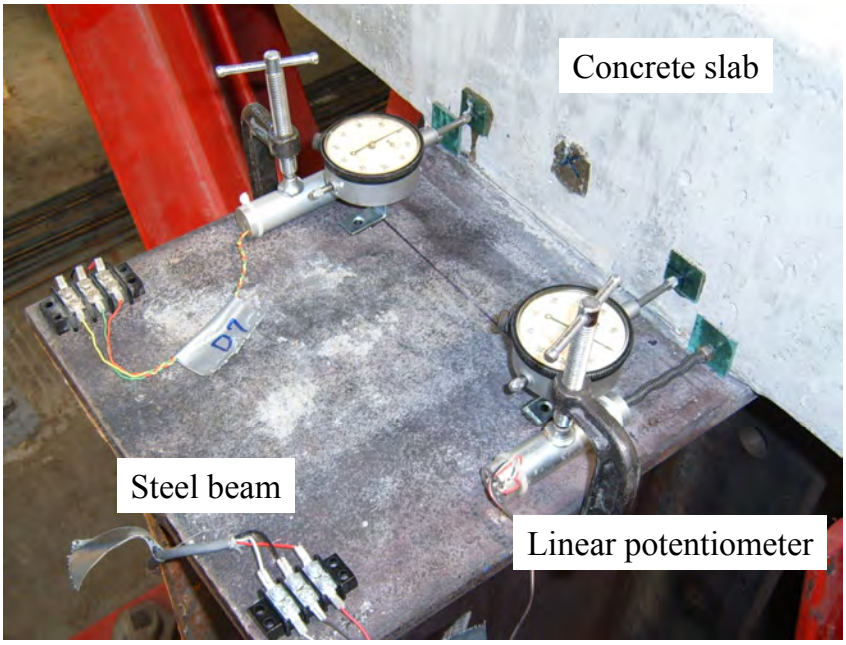

Figure 5.12: Linear potentiometers for measuring slip at the end of the specimen

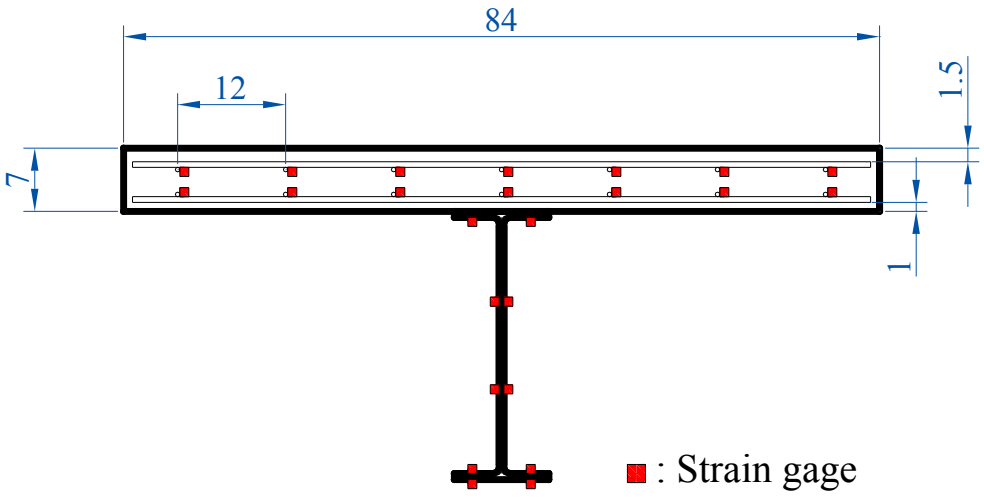

Figure 5.13: Strain gage locations

5.3 Test Results

During each test, in addition to electronically recording data, the specimens were visually examined for phenomena such as cracks in the concrete slab, yielding and local buckling in the steel beam and failure of the post-installed shear connectors. The observations of various phenomena during the tests are described in this section. Load versus center deflection curves for each test specimen are shown in Figure 5.14.

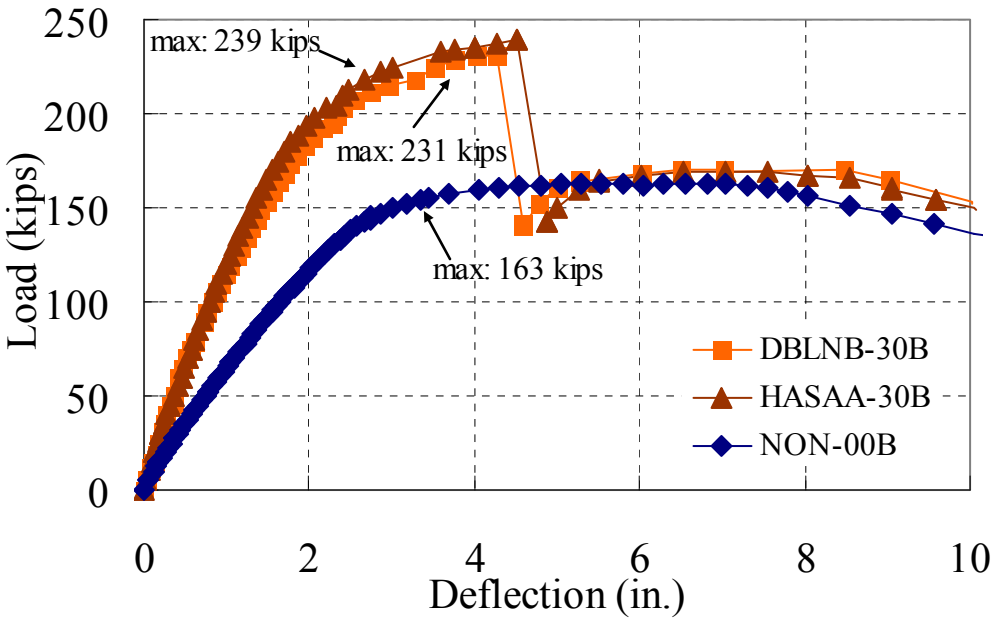

Figure 5.14: Load-deflection curves for the test specimens

5.3.1 Specimen NON-00BS

Specimen NON-00BS was the baseline non-composite specimen. As indicated by the load-deflection plot in Figure 5.14, this specimen showed highly ductile response, as might be expected for a compact, laterally supported steel beam.

The specimen showed a slight reduction in stiffness at around 40-kips loading. Nonlinear behavior at this early stage might be attributed to breaking bond between the steel beam and concrete slab, and possibly due to small movements at the supports. At 70 kips, the first cracks were observed on the bottom of the slab. At 90 kips, more cracks were detected on the bottom of the slab, with the spacing between cracks ranging from 10 in. to 15 in. Whitewash flaking on the bottom flange was detected at 100 kips loading. However, at this point, there was no apparent sign of yielding on the load-deflection plot. At a load of 130 kips, flaking of whitewash on both the top and bottom flanges indicated significant yielding of the beam. Specimen NON-00BS started to lose stiffness at 150kips, so the load was applied by displacement control instead of force control.

At 4-in. deflection, more cracks were detected on the bottom of the slab between the existing cracks. Flaking of whitewash on the web was also observed. At 5-in. deflection, some cracks on the side of the concrete slab propagated horizontally, suggesting imminent crushing of

the concrete at the top of the slab. At 6.5-in. deflection, both flange and web local buckling were observed in the steel beam. Flange buckling occurred only on one side and started about half of the beam depth away from the center of the beam. Crack widths on the bottom of the concrete slab were about 1/16 in. At about 6.8-in. deflection, Specimen NON-00BS reached its ultimate strength which was 163.1 kips. Beyond 6.8 in. deflection, the strength of Specimen NON-00BS started to reduce due to local flange and web buckling in the W30x99 beam. At 7.5-in. deflection, flange buckling occurred on the other side of the beam flange. Figure 5.15 shows cracks in the slab, and local buckling of steel beam at 11-in. deflection. The test stopped at 11.5-in. deflection for safety reasons. No crushing on the top of the concrete was observed after the test. An overall view of the specimen at 11.5-in. deflection is shown in Figure 5.16

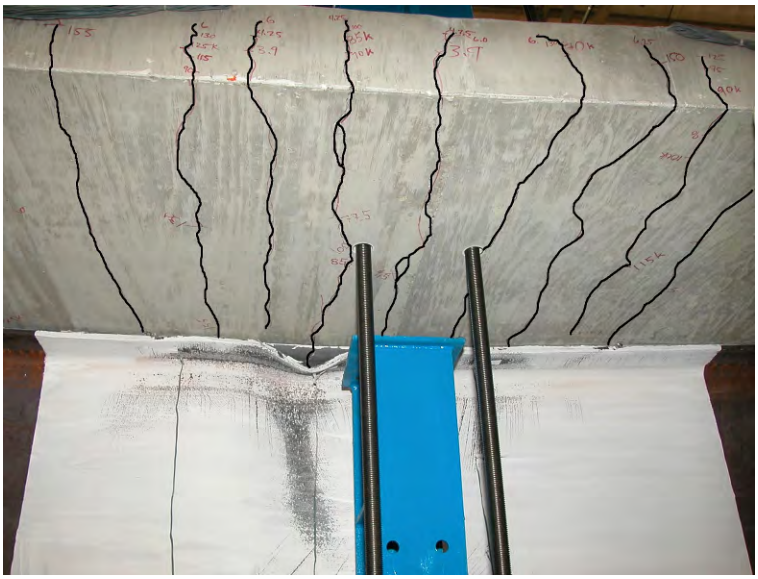

Figure 5.15: Specimen NON-00BS—Cracks in the slab and beam local buckling (11-in. deflection)

Figure 5.16: Specimen NON-00BS – Overall view of specimen at end of test (11.5-in. deflection)

5.3.2 Specimen DBLNB-30BS

Specimen DBLNB-30BS was constructed with DBLNB (double nut bolt) shear connectors. It was designed as 30% composite based on the specified strength of concrete, steel beam, and DBLNB shear connector. In total, 32 shear connectors (16 in each shear span) were installed in the beam, and were distributed uniformly along the length of the beam.

Figure 5.14 shows the load-deflection response for Specimen DBLNB-30BS. Compared to Specimen NON-00BS, Specimen DBLNB-30BS showed much higher strength and stiffness. The specimen showed a sudden strength drop after the peak load due to the failure of multiple shear connectors. After the strength drop, however, Specimen DBLNB-30BS showed very similar behavior to Specimen NON-00BS.

The initial stiffness of Specimen DBLNB-30BS was much higher than Specimen NON-00BS. From around 65 kips, Specimen DBLNB-30BS started losing stiffness. This can likely be attributed to the nonlinear behavior of the shear connectors near the supports. It is also considered that the friction force between the connector and steel beam was overcome, so that the threaded rod slipped in the oversized hole in the steel beam flange. At 130 kips, flaking of whitewash was detected on the bottom beam flange and on the beam web. The first crack on the concrete slab was detected at a load of 200 kips. The cracks were observed only on the edge of the slab and did not propagate on the bottom of the slab. Spacing of the cracks on the concrete slab edge was 5 to 8 in. At a load of 220 kips, some cracks on the concrete slab propagated to the bottom. At 220 kips, the stiffness of the specimen reduced significantly, so that the load was applied by displacement control instead of load control.

At 3.25-in. deflection, some cracks in the concrete slab propagated to the center of the slab. Most cracks propagated to the center and the width of the cracks was less than 1/32 in (see Figure 5.17). At 4.25-in. deflection, one shear connector located near the south support failed with a loud noise. No sudden drop of load, however, was detected due to this failure. This can likely be attributed to the redistribution of shear force among the shear connectors. From the single connector tests (Chapter 4), the DBLNB connector exhibits less ductility than the conventional CIPST shear connectors. This can be attributed to the high strength of the connector material and high strength of the grout used to fill the hole after installation of the connectors. At 4.5-in. deflection, more than 10 shear connectors fractured essentially simultaneously. Accordingly, the strength of the specimen dropped suddenly, as seen in the load-deflection plot in Figure 5.14. In addition, cracks on the side of the concrete slab propagated toward the top of the slab. However, there was no sign of crushing of concrete on the top of the slab.

After the multiple fractures of shear connectors, the structural behavior of Specimen DBLNB-30BS was similar to that of non-composite Specimen NON-00BS as shown in Figure 5.14. At 5-in. deflection, top flange local buckling occurred at the first shear connector location from the center of the beam. For Specimen NON-00BS, first beam flange local buckling was detected at 6.5-in. deflection. At 6.0-in. deflection, beam flange buckling was detected on both sides of the flange and web local buckling was also observed. Another shear connector failure was observed for each 8- and 8.5-in. deflection. Figure 5.18 shows slab cracks and steel beam local buckling at 8-in. deflection. The test stopped at 10-in. deflection for safety reasons.

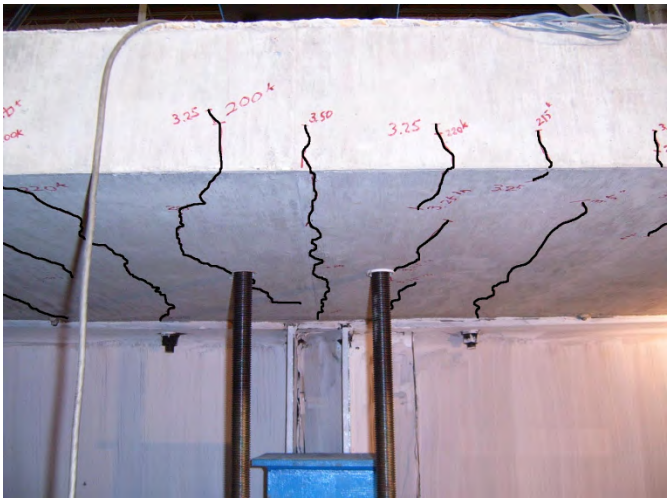

Figure 5.17: Specimen DBLNB-30BS—Cracks on the bottom of the concrete slab (3.25-in deflection)

Figure 5.18: Specimen DBLNB-30BS—Flange and web local buckling (8-in. deflection)

5.3.3 Specimen HASAA-30BS

Specimen HASAA-30BS was constructed with HASAA (adhesive anchor) shear connectors. It was designed as 30% composite beam based on the specified strength of concrete, steel beam, and HASAA shear connector. Sixteen shear connectors in a shear span, 32 shear connectors in total, were installed in the beam. The number and location of shear connectors installed in Specimen HASAA-30BS was same as for Specimen DBLNB-30BS.

Figure 5.14 shows the load-deflection response for Specimen HASAA-30BS. This specimen showed behavior that was very similar to that of Specimen DBLNB-30BS. Specimen HASAA-30BS showed much higher strength and stiffness than Specimen NON-00BS. A sudden drop in strength after the peak load was observed due to the failure of multiple shear connectors. After the strength drop, Specimen HASAA-30BS showed very similar behavior to the non-composite Specimen NON-00BS.

A small amount of whitewash flaking was detected on the bottom beam web at a load of 120 kips. At 190 kips, flaking of whitewash was also observed on the bottom flange. The first crack on the concrete slab was observed at a load of 200 kips. At 210 kips, the crack propagated to the center of the slab. At 220 kips, several cracks were observed on the bottom of concrete slab. Spacing of the cracks was 5 to 8 in. At 225 kips, the stiffness of the specimen reduced significantly, so the load was applied by displacement control instead of load control. Figure 5.19 shows concrete cracks at 4.25-in. deflection. Between 4.75- and 5.00-in. deflection, multiple connectors fractured consecutively. Thirteen shear connectors out of sixteen failed in the south shear span. The deflection of the beam after the failure was 4.87 in.

After failure of multiple shear connectors, the behavior of Specimen HASAA-30BS was very similar to the behavior of non-composite Specimen NON-00BS. Beam flange local buckling was first observed at 5.25-in. deflection and web local buckling was detected at 6-in. deflection. Crack widths on the concrete slab were about 0.04 in. at 5.25-in. deflection. The test was stopped at 10-in. deflection for safety reason.

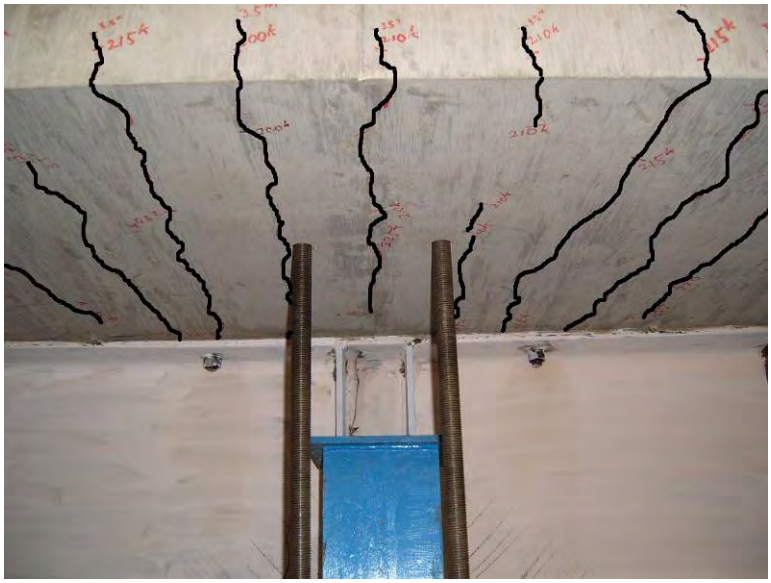

Figure 5.19: Specimen HASAA-30BS—Cracks on the bottom of the concrete slab (4.25-in deflection)

5.4 Discussion of Full-Scale Beam Tests

In this section, results of the full-scale composite beam tests are discussed in greater detail, including considerations of overall stiffness and strength of the specimens, and comparison with the individual shear connector test results for the corresponding shear connection methods. Constructability issues are also discussed for each connection method.

5.4.1 Stiffness and Strength

Figure 5.20 shows the load-deflection relations for the test specimens along with theoretical values. Solid lines represent the theoretical initial stiffness and ultimate load carrying capacity of the non-composite beam and the dashed lines represent the values for the retrofitted composite beams.

The theoretical stiffness and strength of the non-composite specimen (NON-00BS) is based on the steel beam only. No contribution of the concrete slab for stiffness or strength is included. The theoretical strength of the specimen was computed using the actual measured yield strength values for the W30x99 test beam (see Table 5.2).

The theoretical stiffness of the partially composite specimens (DBLNB-30BS and HASAA-30BS) was determined using an effective moment of inertia, computed using Equation 2.25. The theoretical strength of these specimens was based on simple plastic cross-sectional analysis, as described in Section 2.5.1.2. In computing the theoretical strength, the actual measured yield strength of the steel beam and compressive strength of the concrete were used. Shear connector strength was computed as $0.5\ A_s f_u$, per Equation 4.1. In this calculation, A_s was taken as 80% of the gross area of the 7/8" diameter threaded rod. That is, $A_s = 0.80 \times \pi\,(7/8'' \div 2)^2 = 0.48$ in^2. For the ultimate tensile strength of the shear connector material f_u, the measured value of 147 ksi was used (see Section 5.2.2.3).

The behavior of non-composite Specimen NON-00BS, which represents an existing bridge girder without any shear connectors, basically reflected the behavior of a bare steel beam. Specimen NON-00BS shows only slightly higher stiffness and strength than the bare beam. By comparing the theoretical strength and stiffness (which are based on the steel beam only) with the measured load-deflection response, the contribution of the concrete slab towards stiffness and strength of the girder appears to be negligible. Note also that load-deflection response of Specimen NON-00BS exhibited excellent ductility, a desirable attribute for a bridge girder.

The composite beams retrofitted with the post-installed shear connectors showed much higher stiffness and strength than the non-composite Specimen NON-00BS as expected. Recall that the composite ratio of the specimens was relatively low (30%) and the spacing between the connectors was 28.5 in. which is much larger than the spacing required for a fully composite beam. Despite the relatively small number of shear connectors provided in these specimens, a 40% increase in strength was achieved compared to the non-composite specimen, demonstrating the efficiency of partially composite design.

The measured ultimate strength of the test specimens showed good agreement compared to the theoretical values. Specimen HASAA-30BS shows slightly higher strength and ductility than Specimen DBLNB-30BS. The reason for the small difference in strength and ductility between HASAA-30BS and DBLNB-30BS is difficult to determine from this limited test data, but may simply reflect intrinsic variability in structural performance.

The strength of the shear connectors controls the strength of the partially composite beams. The strength of the DBLNB and HASAA shear connectors is controlled by fracture of the connector. Based on the individual shear connector tests, fracture of the DBLNB and HASAA occurs at a smaller slip value than conventional welded shear studs. That is, the DBLNB and HASAA connectors are somewhat less ductile than the conventional welded shear stud. The overall load-deflection response of the retrofitted partially composite beam specimens also showed relatively non-ductile behavior, compared to the non-composite specimen.

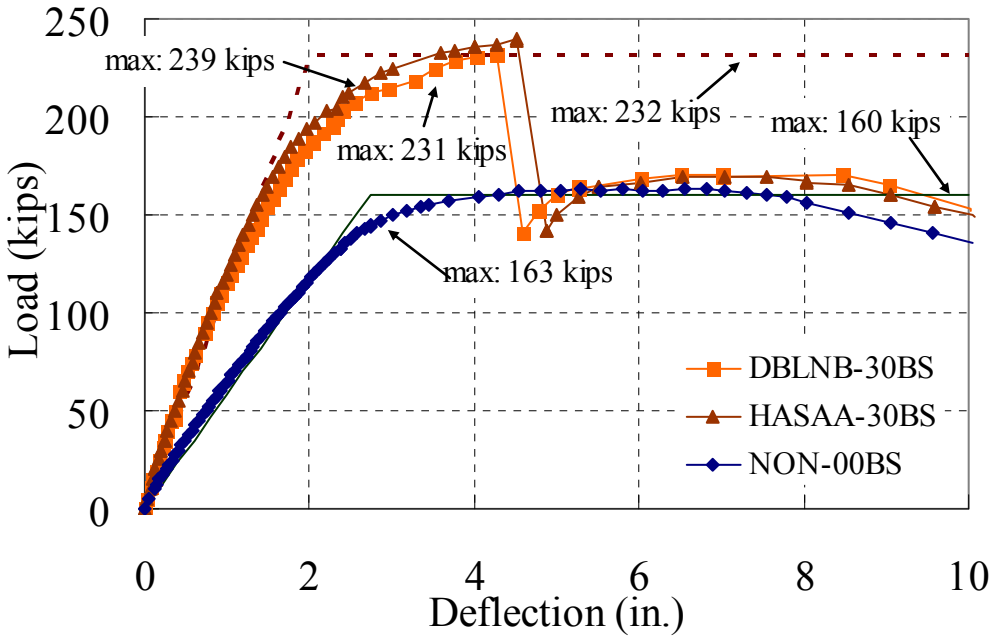

Figure 5.20: Test results compared with theoretical values of stiffness and strength

5.4.2 Failure Modes

As mentioned in Section 5.3.1, Specimen NON-00BS showed very ductile behavior without any sudden strength drop during the test. Cracks on the bottom of the concrete slab occurred at low load levels. This suggests the lack of significant composite action between the concrete slab and the steel beam. In Specimen DBLNB-30BS and Specimen HASAA-30BS, cracks were observed on the bottom of the concrete slab at much higher loads than the non-composite beam. After shear connectors failed, both the retrofitted specimens showed similar concrete crack patterns as Specimen NON-00BS. In all of the specimens, there were no concrete crushing even at large deflections, although cracks on the side of concrete slab propagated horizontally, which suggests imminent concrete crushing on the top of the slab.

For non-composite Specimen NON-00BS, the ultimate strength of the girder was controlled by achieving the fully plastic moment of the W30x99 beam. This section is compact for local buckling. That is, the section is capable of developing its plastic moment prior to the occurrence of local flange or web buckling. Further, the compression flange was well braced against lateral torsional buckling. Consequently, because the beam section is compact and the beam was well braced, it was capable of developing its plastic moment, and maintaining its plastic moment through large inelastic deformations. The ultimate loss of strength of this specimen, which occurred at very large deflections, was due to local flange and web buckling. Note that the presence of the slab did not prevent local buckling of the top flange, although it may have delayed it.

In contrast to Specimen NON-00BS, the two retrofitted partially composite beams showed a sudden strength drop when the shear connectors fractured. Figure 5.21 shows failed sections of the shear connectors for Specimen DBLNB-30BS and Specimen HASAA-30BS. The appearance of the fracture surfaces suggest that the DBLNB shear connectors failed in a

combination of tension and shear, whereas HASAA shear connectors failed primarily due to shear. After failure of the shear connector, both of the retrofitted partially composite beams showed behavior that was very similar to the non-composite beam specimen. Thus, while the retrofitted beam specimens showed a sudden strength drop when the shear connectors failed, the specimens had substantial residual strength and ductility, as they revert back to non-composite beams.

All of the test specimens exhibited local flange and web buckling at large deflections. However, the loss of strength drop due to the buckling was quite gradual. Typical local buckling at large deflections is shown in Figure 5.22.

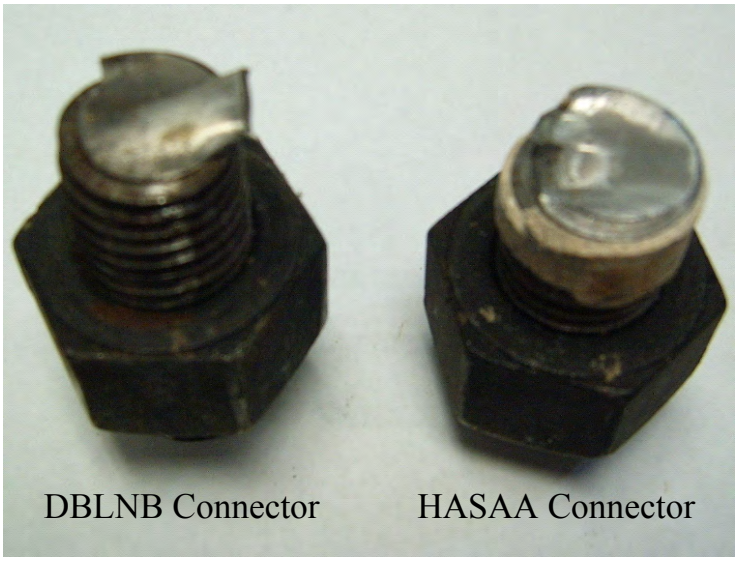

Figure 5.21: Failed sections of shear connectors

Figure 5.22: Typical beam local flange and web buckling at large displacements

5.4.3 Interface Slip and Neutral Axis Locations

All of the test specimens showed an increase in slip at the interface between the concrete slab and the steel beam with increase in load. Figure 5.23 shows the interface slip at the ends of Specimen NON-00BS. Slip increased linearly with load at the early stages of loading. After local buckling of the web and flange occurred, slip on the south end with the hinge support increased continuously, whereas the slip on the north end decreased.

Specimen DBLNB-30BS showed much less slip at the early stages of loading (see Figure 5.24). At 60 kips loading, the slope of the load-slip curve decreases, but still shows linear behavior. It is possible that friction between the connector and steel beam due to tensioning of the shear connectors was overcome and shear connector slip occurred in the oversized holes. Specimen HASAA-30BS did not show a sudden change of slope in the load-slip curves (see Figure 5.25). In Specimen HASAA-30BS, the oversized holes were filled with HY 150 adhesive during installation. After shear connector failure, both retrofitted partially composite beams showed a continuous increase in slip on the south end of the beams as in Specimen NON-00BS.

Specimens DBLNB-30BS and HASAA-30BS showed beam end slip values, at the point of connector failure and sudden strength loss, of 0.23 in. and 0.27 in., respectively. These values are 26% and 31% of the shear connector diameter (7/8 in.), which are less than the values from the single-shear connector tests. It appears that more single-shear connector tests are necessary to characterize single-shear connector behavior including its strength and slip capacity.

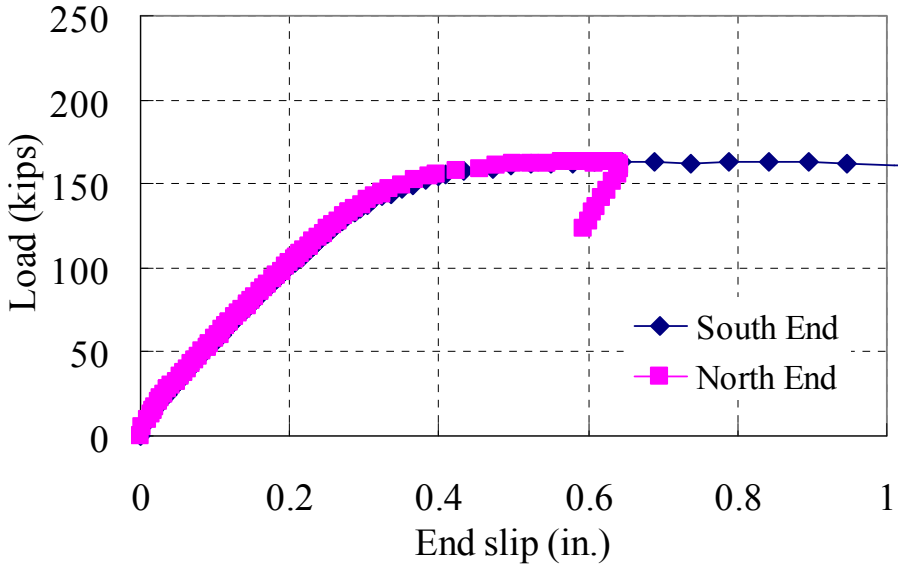

Figure 5.23: Slip at the ends of Specimen NON-00BS

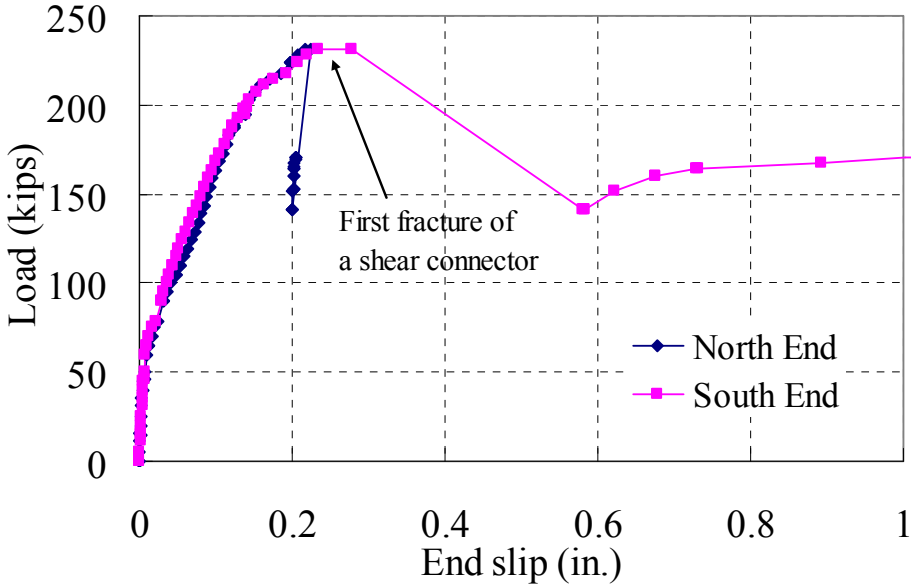

Figure 5.24: Slip at the ends of Specimen DBLNB-30BS

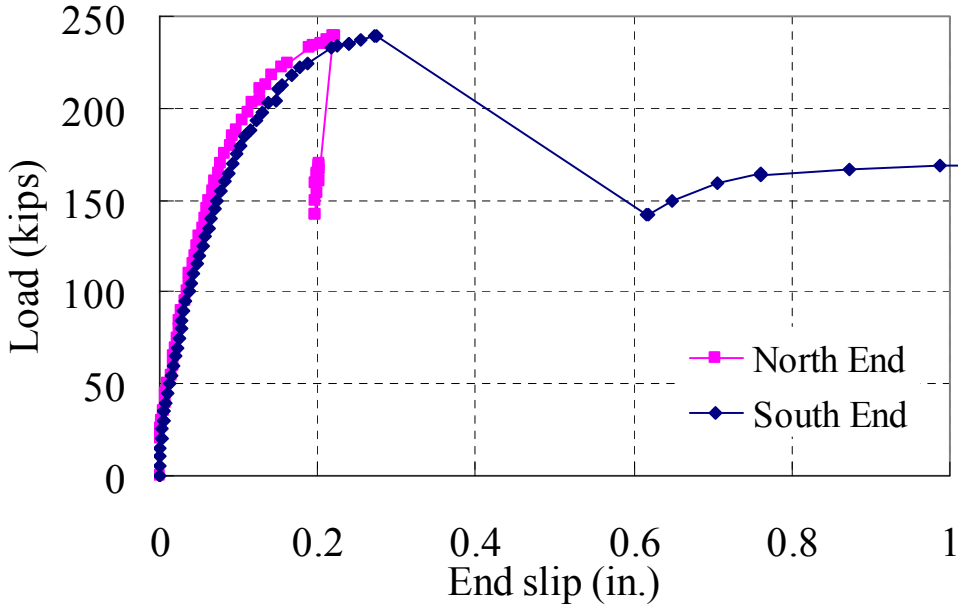

Figure 5.25: Slip at the ends of Specimen HASAA-30BS

Composite action in the retrofitted partially composite beams can be further evaluated by locating the neutral axis during the tests. For non-composite behavior, the neutral axis is expected to be at mid-height of the steel beam. For composite behavior, the neutral axis moves toward the top flange. Figure 5.26 shows the measured neutral axis location at mid-span of the girder at various load levels throughout the tests. Neutral axis locations were obtained by interpolating strain data read from the strain gages on the beam section.

For Specimen NON-00BS, the neutral axis was located near mid height of the steel section at most load levels, as expected. At very low load levels at the start of the test, the neutral axis was located higher up in the cross-section, suggesting some degree of composite action. This early composite action may have been due to bond and/or friction between the steel and concrete. However, as indicated in Figure 5.26, this composite action only occurred at very low load levels. Once the load exceed about 10% of the girder's full capacity, this composite action ended, and the girder subsequently behaved in an almost purely non-composite manner. When evaluating existing non-composite bridges, it is sometimes surmised that some degree of composite action can be considered when load rating the girders, resulting from bond and friction between the steel and concrete. However, the test results for Specimen NON-00BS suggest that such "unintended" composite action should not be relied upon in evaluating the strength of existing non-composite girders. A similar conclusion was reached after an extensive series of field load tests on non-composite steel girders in TxDOT Project 0-1741 (Bowen and Engelhardt 2003).

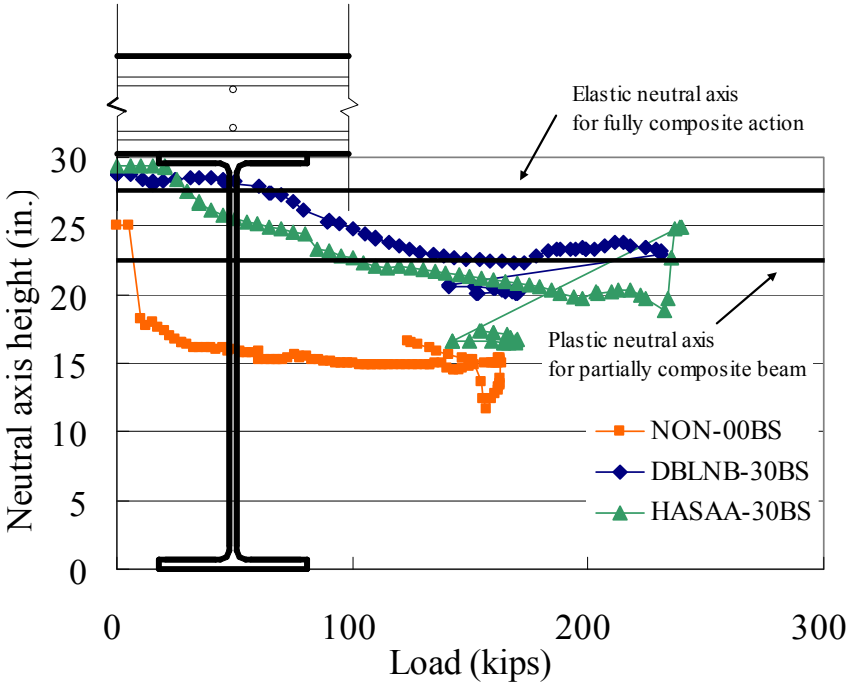

Figure 5.26: Neutral axis locations of test specimens

For the retrofitted partially composite beams, the neutral axis stayed above mid-height of the steel section at all load levels, as indicated in Figure 5.26. Specimen DBLNB-30BS and Specimen HASAA-30BS showed almost full composite action in the early stages of loading, likely due to the friction at the steel-concrete interface. However, the neutral axis moved down as the load increased, indicting partial composite interaction between the steel beam and concrete slab.

5.4.4 Constructability

In addition to assessing the structural performance of the retrofitted girders, constructability related issues for the two shear connection methods were also evaluated during

the full-scale beam tests. Procedures used to install the shear connectors in the test specimens are similar to the procedures that would likely be used on an actual bridge, allowing for an assessment of construction related difficulties.

5.4.4.1 Double-Nut Bolt (DBLNB) Method

For the DBLNB connection method, access from both the top and the bottom of the concrete slab is needed to install the shear connectors. For each connector, a 2.5-in. diameter hole was made in the slab, using a core drilling machine from the top of the slab. In the laboratory, it took 5 to 10 minutes to complete a hole. The core drill bit hit and cut through transverse reinforcing bars frequently during the drilling operation. The top transverse reinforcing bars function to resist negative moment in the transverse direction of the slab, and cutting a number of these bars may adversely affect the structural integrity of the slab. The longitudinal reinforcing bars function primarily as temperature reinforcement, so cutting these bars is less consequential. In field applications, a reinforcing bar locator can potentially be used to help avoid cutting through reinforcing bars.

After completing the 2.5-in. diameter holes in the slab, a 15/16-in. diameter hole was drilled through the top flange of the steel beam, centered in the 2.5-in. hole in the slab. The holes in the top flanges were also made from the top of the slab using a magnetic drill with a long drill bit. In the laboratory, a 1-in. thick steel plate was anchored on the concrete slab to hold the magnetic drill. Also, as described in Section 5.2.1.3.1, a hollow round bar was placed inside of the cored hole in the concrete to serve as a guide for the steel drill bit. Tightening of a connector using an impact wrench from the bottom of the slab generally took less than 30 seconds. Load Indicator washers were used to control the pretension on the connector. Grout that was used to fill the gap in the concrete slab had a specified strength of 2000psi at 2 hours and 5100psi at 24 hours. Traffic may need to be stopped until the grout gains a reasonable degree of strength.

5.4.4.2 Adhesive Anchor (HASAA) Method

Compared to the DBLNB connection method, installation of the HASAA connectors can be completed entirely from underneath the slab. As a first step, 15/16-in. diameter holes were drilled through the top flange of the steel beam. These holes were drilled from underneath the slab, using a magnetically mounted slugger drill. It took 1 to 2 minutes to complete a hole. Only 6 to 8 holes were drilled with one annular slugger cutter bit because the drill bit was easily worn when it hit the concrete. This may increase construction cost of the connection method. However, the drill bit can be used repeatedly after sharpening.

As the next step, a 5-in. deep hole was drilled into the concrete from beneath the slab, using a hammer drill. In the laboratory, a Hilti TE-55 hammer drill was used for this purpose. Hilti HY 150 adhesive was used to install HASAA connectors. A potential drawback of this installation process is the cure time for the adhesive. For a 68^{o}F temperature a 50 min. curing time is required for the adhesive used in the tests. During this time the adhesive should not be disturbed, which may require traffic to be stopped on the bridge.

Chapter 6. Summary, Conclusions, and Preliminary Design Recommendations

6.1 Summary

This study investigated methods to strengthen existing non-composite steel bridge girders by the development of composite action between the steel girder and concrete slab. More specifically, the objective of this study was to identify structurally efficient and practical ways to post-install shear connectors in existing bridges. Various types of post-installed shear connection methods were tested under static, high-cycle fatigue, and low-cycle fatigue loads using a direct-shear test setup. Based on the results of single-shear connector tests, full-scale beam tests were performed under static load to evaluate system performance of the beams retrofitted for partial composite action with post-installed shear connectors.

First, using a direct-shear test setup, various post-installed shear connectors were tested under monotonically increasing loads to examine the load-slip behavior of the connectors, and characterize their stiffness, strength, and ductility. Conventional cast-in-place welded studs, which are widely used for new construction, were also tested as a benchmark to assess the structural behavior of the post-installed shear connectors.

For the post-installed shear connection methods that showed acceptable performance under static loads, their structural performance was further evaluated through cyclic tests. High-cycle and low-cycle fatigue tests were conducted to assess the comparative behavior of these shear connectors subjected to repeated service loads and overloads, respectively. The performance of shear connectors under fatigue loading was also compared to that of the conventional cast-in-place welded stud.

The post-installed shear connectors that showed the most promising structural performance under static and fatigue loading were then selected for further evaluation in full-scale beam tests. A total of three full-scale beam tests were conducted. Two full-scale non-composite beams were built and retrofitted with different post-installed shear connectors. One non-composite beam was also tested as a benchmark to compare the structural performance of the retrofitted partially composite beams. In constructing the full-scale beam test specimens, the installation processes of the two shear connection methods were also evaluated.

6.2 Conclusions

The results of this study clearly demonstrate that the strength and stiffness of existing non-composite steel bridge girders can be increased significantly by post-installing shear connectors. Development of composite action between the existing steel girder and concrete slab through the installation of post-installed shear connectors appears to be a structurally efficient and cost-effective approach to retrofit existing bridges. The addition of post-installed shear connectors can increase the load capacity of existing steel girders on the order of 40 to 50%. Some more specific conclusions of this project are as follows:

- Of the various types of post-installed shear connectors investigated in this study, the most promising, from a structural performance and constructability point of view are:

  - double-nut bolt
  - adhesive anchor
  - high tension friction grip bolt.

- These connectors consist of high strength bolts or threaded rods placed in holes that are drilled in the concrete slab and top flange of the steel girder. The holes are filled with high strength grout (double-nut bolt and high tension friction grip bolt) or structural adhesive (adhesive anchor). Installation of the double-nut bolt and high tension friction grip bolt require construction operations on both the top and bottom sides of the concrete slab. The adhesive anchor, on the other hand, can be completely installed from underneath the slab, thereby minimizing traffic disruptions on the bridge.

- Static tests on these three post-installed connectors show strength levels that are similar or greater than conventional welded studs. Fatigue tests on these post-installed connectors show significantly better fatigue lives than conventional welded studs. The excellent fatigue performance of these three post-installed shear connectors is attributed, in large part, to the fact that no welds are involved in their installation.

- A preliminary recommendation was developed for computing the static strength of the post-installed shear connectors. The recommended equation is as follows:

$$Q_u = 0.5\, A_s f_u \qquad \textit{(Eq. 6.1)}$$

  where:
  Q_u = ultimate strength of the shear connector (kips)
  A_s = effective cross-sectional area of shear connector (in^2)
  f_u = ultimate tensile strength of shear connector material (ksi)

  For threaded connectors, as used in the double-nut bolt, adhesive anchor and high tension friction grip bolt, it is recommended that A_s be taken as 80% of the gross unthreaded cross-sectional area of the connector.

  Equation 6.1 differs considerably from the existing AASHTO shear connector strength equations for conventional welded shear studs, but is believed to provide a reasonable and conservative estimate of the strength of the post-installed shear connectors, based on the tests conducted in this study.

- A limited number of high-cycle fatigue tests on the post-installed shear connectors showed fatigue lives that are significantly better than conventional welded shear studs, as noted earlier. However, not enough fatigue tests were conducted to confidently recommend an S-N relationship for design purposes. Due to the intrinsic variability of fatigue test results, additional fatigue tests would be desirable to better identify a design S-N curve for the post-installed shear connectors.

Nonetheless, based on the limited available data, a preliminary simplified recommendation for checking fatigue of post-installed shear connectors made of ASTM A325 bolts or of ASTM A193 B7 threaded rods is to assume a fatigue endurance limit of 35 ksi. That is, if the stress range on the effective shear area of the connector is less than 35 ksi, then a fatigue failure appears unlikely. The effective shear area of the threaded connectors can be taken as 80% of the gross cross-sectional area of the connector.

- It is recommended that *partial* composite design be used as a basis for determining the number of post-installed shear connectors that will be used to strengthen an existing bridge girder. Current *AASHTO Specifications* only recognize full composite design for steel bridge girders, and do not include provisions for partial composite design. The absence of partially composite design provisions in AASHTO likely reflects the fact that fatigue design requirements, than static strength requirements, normally control the required number of welded shear studs on a composite girder. Thus, the use of partially composite design is not normally used for new composite bridge girders. However, because of the outstanding fatigue characteristics of the post-installed shear connectors, fatigue is not likely to control the required number of shear connectors, thereby enabling partial composite design. The cost of post-installed shear connectors for an existing bridge is likely to be far greater than the cost of welded studs for new construction. Full composite design will therefore likely be very costly for strengthening existing bridges. Thus, the economic viability of strengthening existing non-composite bridges by post-installing shear connectors depends largely on the use of partial composite design.

- To evaluate overall system performance of a steel bridge girder strengthened with post-installed shear connectors, three large scale beam tests were conducted. These tests were conducted on a 38-ft long simply supported span, with a point load applied at mid-span. Each specimen consisted of a W30x99 steel girder with a 7-in. thick by 7-ft wide reinforced concrete slab on top. For one of the three specimens, no shear connectors were provided, to provide baseline data on the strength and stiffness of a non-composite girder. The test of the non-composite specimen showed that the stiffness and ultimate strength of the girder was controlled by the stiffness and strength of the W30x99 girder, with a negligible contribution from the slab. At very low load levels, the non-composite specimen exhibited some degree of composite action, likely due to bond at the steel-concrete interface. However, this composite action only occurred at very low load levels. Once the load exceed about 10% of the girder's full capacity, this composite action ended, and the girder subsequently behaved in an almost purely non-composite manner. When evaluating existing non-composite bridges, it is sometimes surmised that some degree of composite action can be considered when load rating the girders, resulting from bond and friction between the steel and concrete. However, the test results for the non-composite specimen suggest that such "unintended" composite action should not be relied upon in evaluating the strength of existing non-composite girders.

- Two large scale beam specimens were retrofitted with post-installed shear connectors; one with double-nut bolts and the other with adhesive anchors. Due to cost constraints, a large scale beam test was not conducted with the high tension

friction grip bolt. Each of the retrofitted beam specimens were designed as partially composite, with a 30% shear connection ratio. That is, the number of shear connectors installed in these specimens was only 30% of the number required for full composite design. This resulted in a pair of shear connectors (one on either side of the beam web) located at intervals of 28.5-in. along the length of the beam. The ultimate strength of the specimen retrofitted with double-nut bolt shear connectors was 42% greater than the baseline non-composite specimen. Similarly, the ultimate strength of the specimen retrofitted with adhesive anchors was 47% greater than the baseline non-composite specimens. Consequently, a large increase in strength, on the order of 45%, was achieved with a relatively small number of shear connectors, demonstrating the efficiency of partial composite design. Further, the elastic stiffness of the retrofitted beams was about 90 to 100% greater than the baseline non-composite specimen.

- The strength of the retrofitted beams was controlled by the strength of the shear connectors. When the shear connectors failed, the strength of the retrofitted beams dropped sharply, to a level corresponding to the non-composite specimen. That is, once the shear connectors failed, the behavior of the retrofitted beams reverted back to the original non-composite condition. The retrofitted beams exhibited less ductility than the baseline non-composite specimen.
- The strength of the retrofitted beams was well predicted by simple plastic cross-sectional analysis for partial composite behavior, with shear connector strength computed per Eq. 6.1. Thus, it appears that the strength of retrofitted beams can be computed using simple and well established design procedures for partial composite beams. These procedures are available in many texts on steel design, and are also reviewed in Chapter 2 of this report (see Section 2.5.1.2). Similarly, the stiffness of the retrofitted beams was well predicted using the simple expression for the effective moment of inertia for partial composite girders that is provided in the commentary to the *AISC Specification for Structural Steel Buildings* (see Eq. 2.25 in this report).

6.3 Preliminary Design Recommendations

Based on the results of this study, a preliminary design approach for strengthening existing steel bridge girders by post-installing shear connectors can be suggested. Preliminary design recommendations are as follows:

- Full-scale beam tests were conducted only with the double nut bolt and the adhesive anchor. Pending the availability of additional large scale beam tests, it is recommended that one of these two post-installed shear connectors be used for bridge girder retrofit.
- Use of either 3/4-in. or 7/8-in. diameter shear connectors is recommended, as these are the diameters tested in this research study. Other diameters may be suitable, although test data would be desirable to evaluate their performance.
- For the double nut bolt, the use of either ASTM A325 bolts or ASTM A193 B7 threaded rods is suggested. For the adhesive anchor, the use of ASTM A193 B7 threaded rods, or equivalent, is suggested.

- Use of partial composite design is recommended as an overall basis for strengthening steel bridge girders with post-installed shear connectors. Use of a composite ratio less than 30% is not recommended, due to the lack of test results in this range. The flexural strength of the retrofitted partial composite cross-section can be computed using simple plastic cross-section analysis.
- The use of Equation 6.1 is recommended for computing the strength of post-installed shear connectors.
- Pending the availability of additional fatigue test results, it is suggested that the fatigue strength of post-installed shear connectors be checked using Equation 4.2, where the stress range on the connector is determined with elastic analysis. Due to the superior fatigue strength of the post-installed shear connectors, it is anticipated that fatigue will not normally control the required number of shear connectors.
- It is recommended that general requirements concerning clear cover, edge distance, and minimum distance between shear connectors in *AASHTO Standard Specifications* be followed. AASHTO limits the maximum distance between shear connectors to 24-in. This limit will often be violated in a partial composite design. The full-scale beam tests conducted in this study also violated this limit, with no apparent detrimental effects. Consequently, there appears to be no need to limit the maximum spacing of shear connectors to 24-in.

6.4 Recommendations for Further Research

Following are several recommendations for further research related to strengthening existing non-composite beams by post-installing shear connectors:

- Additional single connector shear tests under fatigue loading are needed to better characterize the S-N relationship for the post-installed shear connectors, as well as to characterize the variability in fatigue performance.
- Additional full-scale beam tests would be desirable to evaluate the system performance of retrofitted partial composite beams with other types of post-installed shear connectors (such as the high tension friction grip bolts), different composite ratios, and various connector spacings.
- Finite element studies are needed to evaluate the performance of this strengthening technique for a wider range of conditions than tested, including larger span lengths and different sizes of steel girders.
- Studies are needed to evaluate the use of this strengthening technique in negative moment regions.

References

AASHTO (2005). “LRFD Bridge Design Specifications Interim Customary U.S. Units, 3rd Edition.” American Association of State Highway and Transportation Officials, Washington, D.C.

AASHTO (2002). “Standard Bridge Design Specifications (2002) 17th Edition.” American Association of State Highway and Transportation Officials, Washington, D.C.

ACI (2005). “Building Code Requirements for Structural Concrete (ACI 318-05) and Commentary (ACI 318R-05).” American Concrete Institute, Farmington Hills, Michigan, 2005.

AISC (2005). “Steel Construction Manual Thirteenth Edition.” American Institute of Steel Construction, U.S.A., 2005.

Badie, S.S, Tadros, M.K., Kakish, H.F., Splittgerber, D.L., Baishya, M.C. (2000). "Large Shear Studs for Composite Action in Steel Bridge Girders." Journal of Bridge Engineering, 7(3), 195-203.

Bowen, C.M. and Engelhardt, M.D. (2003). “Analysis, Testing, and Load Rating of Historic Steel Truss Bridge Decks.” Report No. FHWA/TX-03/1741-2, Center for Transportation Research, University of Texas at Austin, Austin, Texas.

Cook, J. P. (1977). “Composite Construction Methods,” New York: John Wiley & Sons.

ENV 1994-1-1: Eurocode 4 (1992). “Design of Composite Steel and Concrete Structures, Part 1-1: General Rules and Rules for Buildings.” Draft. Brussels, Belgium.

Faella, C, Martinelli, E., and Nigro, E. (2003). “Shear Connection Nonlinearity and Deflections of Steel-Concrete Composite Beams: A Simplified Method.” Journal of Structural Engineering. 129(1), 12-20.

Gattesco, N., and Giuriani, E. (1997). “Experimental Study on Stud Shear Connectors Subjected to Cyclic Loading.” Journal of Constructional Steel Research, 38(1), 1-21.

Gattesco, N., Giuriani, E., and Gubana, A. (1997). “Low-Cycle Fatigue Test on Stud Shear Connectors.” Journal of Structural Engineering 123(2), 145-150.

Hilti (2006). “Hilti Anchoring Systems, HIT HY 150/HIT-ICE Injections Adhesive Anchor.” Hilti Product Technical Guide. March 2006 <http://www.hilti.com>.

Hungerford, B.E. (2004). “Methods to Develop Composite Action in Non- Composite Bridge Floor Systems: Part II.” MS Thesis, Department of Civil, Architectural and Environmental Engineering, University of Texas at Austin.

Johnson, R.P. (1999). "Resistance of Stud Shear Connectors to Fatigue." Journal of Constructional Steel Research, (56), 101-116.

Johnson, R.P., May, I.N. (1975). “Partial-Interaction Design of Composite Beams.” The Structural Engineer 53(8), 305-311.

Johnson, R.P., and Molenstra, I.N. (1991). “Partial Shear Connection in Composite Beams for Buildings,” Proc. Instn Civ. Engrs, Part 2, 91, 679-704.

Kayir, H. (2006). “Methods to Develop Composite Action in Non-Composite Bridge Floor Systems: Fatigue Behavior of Post-Installed Shear Connectors.” MS Thesis, Department of Civil, Architectural and Environmental Engineering, University of Texas at Austin.

Kwon, G. (2008). “Strengthening Existing Steel Girder Bridges by the use of Post-Installed Sgear Connectors.” PhD Dissertation, Department of Civil, Architectural and Environmental Engineering, University of Texas at Austin (expected completion in August 2008).

Lehman, H.G., Lew, H.S., Toprac, A.A. (1965). “Fatigue Strength of 3/4 in. Studs in Lightweight Concrete.” Center for Highway Research, The University of Texas at Austin

Mainstone, R.J., Menzies, J.B. (1967). “Shear Connectors in Steel-Concrete Composite Beams for Bridges: part 1: Static and Fatigue Tests on Push-out Specimens.” Concrete, 291-302.

McGarraugh, J.B., Baldwin, J.W. (1971). “Lightweight Concrete-Steel Composite Beams.” Engineering Journal, American Institute of Steel Construction, 8(3), 90-98.

Matus, R.A., Jullien, J.F. (1996). “A New Shear Stud Connector Proposal.” Composite Construction III, 9-14 June. Irsee, Germany: Engineering Foundation Conferences, 70-96.

MTS Systems Division (2000). “Model 407 Controller Product Manual.” Firmware Version 5.3.

Nakajima, A., Saiki, I., Kokai, M., Doi, K., Takabayashi, Y., Ooe, H. (2003). "Cyclic Shear Force-Slip Behavior of Studs under Alternating and Pulsating Load Condition." Engineering Structures, 25(5), 537-545.

National Bridge Inventory (2006). “NBI Report 2003.” February 2006. <http://www.nationalbridgeinventory.com/nbi_report_200322.htm>.

Oehlers, D.J. (1990). “Deterioration in Strength of Stud Connectors in Composite Bridge Beams.” Journal of Structural Engineering, 116(12), 3417-3431.

Oehlers, D. J., Bradford, M.A. (1995). “Composite Steel and Concrete Structural Members (Elementary Behaviour).” Kidlington, Oxford.

Oehlers, D.J., Coughlan, C.G. (1986). “The Shear Stiffness of Stud Shear Connections in Composite Beams.” Journal of Constructional Steel Research, (6), 273-284.

Oehlers, J., Foley, L. (1985). "The Fatigue Strength of Stud Shear Connections in Composite Beams." Institution of Civil Engineers, 79, 349-365.

Oehlers, D.J., Johnson, R.P. (1987). “The Strength of Stud Shear Connections in Composite Beams.” Structural Engineering 65B.2, 44-48.

Oehlers, D.J., Seracino, R., Yeo, M.F. (2000). “Effect of Friction on Shear Connection in Composite Bridge Beams.” Journal of Bridge Engineering 5(2), 91-98..

Oehlers, D.J., Sved, G. (1995) “Composite Beams with Limited-Slip-Capacity Shear Connectors.” Journal of Structural Engineering, 121(6), 932-938.

Ollgaard, J.G., Slutter, R.G., Fisher, J.W. (1971). “Shear Strength of Stud Shear Connectors in Lightweight and Normal-Weight Concrete.” AISC Engineering Journal, 8, 55-64.

Roberts, T. M., Dogan, O. (1998). “Fatigue of Welded Stud Shear Connectors in Steel-Concrete-Steel Sandwich Beams.” Journal of Constructional Steel Research, 45(3), 301-320.

Schaap, B. A. (2004). “Methods to Develop Composite Action in Non-Composite Bridge Floor Systems: Part I.” MS Thesis, Department of Civil, Architectural and Environmental Engineering, University of Texas at Austin.

Slutter, R.G., Fisher, J.W. (1966). “Fatigue Strength of Shear Connectors.” Highway Research Record 147, 65-88.

Thurlimann, B. (1959). "Fatigue and Static Strength of Stud Shear Connectors." Journal of the American Concrete Institute, 1287-1301.

Toprac, A. A. (1965). “Fatigue Strength of ¾-Inch Stud Shear Connectors.” Highway Research Record. 103, 53-77.

Viest, I.M. et al. (1997). “Composite Construction: Design for Buildings.” McGraw--Hill, New York, NY.

Viest, I.M., Fountain, R. S., Siess, C.P. (1958). “Development of the New AASHO Specification for Composite Steel and Concrete Bridges.” HRB Bull. 174, 1-17.

The following references were used for general background but not specifically cited in this report:

3M (2003). “3M Scotch-Weld™ Epoxy Adhesive DP-460 NS, Technical Data.” 3M Engineered Adhesives Division.

AASHO (1961). “AASHO Standard Specifications for Highway Bridges, 7th ed.” Washington, D.C., American Association of State Highway Officials, 1957.

AASHO (1961). "AASHO Standard Specifications for Highway Bridges, 8th ed." Washington, D.C.: American Association of State Highway Officials.

AASHTO (1998). "AASHTO LRFD Bridge Design Specifications, 1998. Customary U.S. Units. 2nd ed." Washington, D.C., American Association of State Highway and Transportation Officials.

AASHTO (1977). "AASHTO Standard Bridge Design Specifications, 11th ed." Washington, D.C., American Association of State Highway and Transportation Officials.

BS 5950. (1990). "Code of Practice for Design of Composite Beams." London: British Standards Institution.

Engelhardt and Klingner. "Summary of project 0-4124 presented by Dr. Engelhardt and Dr. Klingner." 14 pages

Engelhardt, Michael D. (2003) "Composite Beams." Class Notes.

Engelhardt, M. D., Kates, Z. and Beck, H. (2000). "Experiments on the Effects of Power Actuated Fasteners on the Strength of Open Web Steel Joists." AISC Engineering Journal, 37(4), 157-166.

ENR, (1963). "Epoxy Bonds Composite Beams." Engineering News-Record.

Five Star Products Online (2006). "Five Star® Highway Patch Data Sheet". January 2006. < http://www.fivestarproducts.com/html/f1b7e.html>.

Klaiber, F. W., et al. (1983). "Strengthening of Existing Single Span Steel Beam and Concrete Deck Bridges." Final Report, Part I, Engineering Research Institute, Iowa State University.

Klingner, R.E. (2002) "Behavior and Design of Fastening to Concrete." Class Notes.

Powers Fasteners Online (2006). Powers Fasteners Online Product Specifications, Mechanical Anchors, WedgeBolt™. January 2006. <http://www.powers. com/product_07246.html>.